Title
The Differential Role of Mef2c in Modulating Bone Mineral Density

Author
Morfin, Cesar

Publication Date
2023

Peer reviewed|Thesis/dissertation

UNIVERSITY OF CALIFORNIA, MERCED

The Differential Role of Mef2c in Modulating Bone Mineral Density

A dissertation submitted in partial satisfaction of the requirements for the degree Doctor of Philosophy

in

Quantitative and Systems Biology

by

Cesar Morfin

Committee in charge:
Dr. Michael D. Cleary, Chair
Dr. Raman N. Saha
Dr. Katrina K. Hoyer
Dr. Gabriela G. Loots, Graduate Advisor

2023

Signature Page

The Dissertation of Cesar Morfin is approved, and it is acceptable in quality and form for publication on microfilm and electronically:

Michael D. Cleary

Raman N. Saha

Katrina K. Hoyer

Gabriela G. Loots

Date

University of California, Merced

2023

Dedication

To my boys Gabriel and Dominic and, my loving wife, Michelle. You are my reason for getting out of bed everyday and be the best version of myself.

Table of Contents

SIGNATURE PAGE 3

LIST OF ABBREVIATIONS 8

LIST OF FIGURES 10

LIST OF TABLES 12

ACKNOWLEDGEMENTS 13

CURRICULUM VITA 15

ABSTRACT 19

CHAPTER 1. INTRODUCTION 21

1.1 Bone function, development, and homeostasis 21
1.2 Aging and Osteoporosis 24
1.3 Current Osteoporotic therapeutics 26
1.4 Bone cells that mediate bone formation 30
1.5 The osteoclastic lineage and their role in bone resorption 32
1.6 Cellular energy metabolism of bone cell populations 33
1.7 ECM role in maintain bone homeostasis 35
1.8 Gene regulatory networks associated with maintaining bone homeostasis. 36
1.9 Mef2c functional contributions to bone. 38
1.10 Studying bone cell populations involved in bone remodeling 41
1.11 Objective of study 44

CHAPTER 2. CHARACTERIZING FLUORESCENTLY LABELED BONE CELL POPULATIONS USING CLASSICAL BONE MARKERS AT THE SINGLE CELL LEVEL. 46

Abstract 46

INTRODUCTION 47
METHODS 50
RESULTS 56
DISCUSSION 68

CHAPTER 3. MEF2C UTILIZES CELL-TYPE SPECIFIC GENE REGULATORY NETWORKS AMONGST THE OSTEOGENIC LINEAGES TO PROMOTE THE MAINTENANCE OF BONE HOMEOSTASIS 71

ABSTRACT 71
INTRODUCTION 72
METHODS 74
RESULTS 79
DISCUSSION 95

CHAPTER 4. CHARACTERIZING THE *MEF2C*-MEDIATED TRANSCRIPTOME AMONGST OSTEOCLAST POPULATIONS 103

ABSTRACT 103
INTRODUCTION 104
MATERIALS ..... ERROR! BOOKMARK NOT DEFINED.
RESULTS 113
DISCUSSION 121

CHAPTER 5. CONCLUSIONS AND FUTURE DIRECTIONS 125

REFERENCES 128

List of Abbreviations

aCAR – adipo Cxcl12 abundant reticular (CAR) cell

BM – bone marrow

BMD – bone mineral density

BMU – bone multicellular unit

BR - bone remodeling

CB – cortical bone

CH – chondrocyte

ECM – extracellular matrix

EDTA - Ethylenediaminetetraacetic acid

GP – growth plate

GRN – gene regulator network

HBM – high bone mass

HSC – hematopoietic stem cell

KO – knock out

MCSF1 – macrophage colony stimulating factor 1

Mef2c – myocyte enhancer factor 2

MSC – mesenchymal stem cell

MP – mesenchymal progenitor

NCP – non-collagenous proteins

OB - osteoblasts

OCL – osteoclasts

OCP – osteochondro progenitor

OP – osteogenic progenitor

OS – osteocytes

Osx/Sp7- osterix

PTH – parathyroid hormone

PTHrP – PTH related protein

RANKL – receptor activator of nuclear factor kappa-β ligand

ROS – reactive oxygen species

Runx2 – runt-related transcription factor 2

scRNAseq – single cell ribonucleic acid (RNA) sequencing

SERM – selective estrogen receptor modulator

TB – trabecular bone

TF – transcription factor

UMI – unique molecular modifier

UMAP – uniform manifold approximation and projection

List of Figures

Chapter 1. Introduction

Figure 1. Bone cell populations primarily consist of osteogenic and osteoclast populations that function in maintaining bone tissue homeostasis……..……..29

Chapter 2. Characterizing fluorescently labeled bone cell populations using classical bone markers at the single cell level.

Figure 1. Histological analysis of tdTomato expression in lineage tracing mouse strains……56
Figure 2. Single-cell RNA sequencing pipeline and flow cytometric analysis……58
Figure 3. Single-cell transcriptional profiling of cells derived from mature murine long bones……59
Figure 4. Characterization of stromal cell types and enrichment in lineage tracing mouse lines. ……..……..61
Figure 5. Enrichment of bone cell subtypes found amongst Ai9 reporter mice……..63
Figure 6. Enrichment of adipoCAR populations via bone specific marker……..64
Figure 7. Characterization of osteogenic cell types and enrichment in lineage tracing mouse lines..……66

Chapter 3. Mef2c utilizes cell-type specifc gene regulatory networks amongst the osteogenic lineages to promote the maintenance of bone homeostasis.

Figure 1. Comparing skeletal phenotypes of Mef2c conditional knockout mice to Sost-/-……80
Figure 2. Single cell analysis of Mef2c-deficient bone cells. ……..……84
Figure 3. Characterizing Mef2c-deficient mouse phenotype at the single cell level..……85
Figure 4. Differential gene expression analysis of Mef2c-deficient bone cells……...89
Figure 5. Characterization of putative Mef2c target genes in OBs and OSs……..……93

Figure 6. Diminished expression of putative direct targets in the absence of Mef2c.....94

Chapter 4. Characterizing the Mef2c-mediated transcriptome amongst osteoclast populations.

Figure 1. μCT analysis of femora comparing skeletal phenotypes of $Mef2c^{fl/fl}$; Ctsk-Cre mice to $Sost^{-/-}$ and $Mef2c^{fl/fl}$; Ctsk-Cre, $Sost^{-/-}$ mice.....109
Figure 2. Osteoclast differentiation is less efficient in the absence of Mef2c.....111
Figure 3. Decreased number of $TRAP^{+}$ Osteoclast cell populations from the absence of Mef2c.....114
Figure 4. Single cell analysis of Mef2c cKO bone cells.....115
Figure 5. Single cell analysis of differentiating osteoclasts at days 0, 1, and 3.....118

List of Tables

Chapter 2. Characterizing fluorescently labeled bone cell populations using classical bone markers at the single cell level.

Table 1. Percent (%) relative abundance of major bone cell populations amongst Ai9 reporter mice……63
Table 2. Log2 fold change enrichment of bone cell subtypes amongst Ai9 reporter mice vs unlabeled populations……63

Chapter 3. Mef2c utilizes cell-type specifc gene regulatory networks amongst the osteogenic lineages to promote the maintenance of bone homeostasis.

Table 1. Downregulated bone metabolism genes in *Bglap Mef2c* cKO……89
Table 2. Energy metabolism genes harboring Mef2c binding motifs……95
Table 3. Bone metabolism genes harboring Mef2c binding motifs……97

Acknowledgements

This work was conducted under the asupices of the USDOE by LLNL (DE-AC52-07NA27344).

I would like to acknowledge my thesis comittee, Dr. Michael Cleary, Dr. Raman Saha, and Dr. Katrina Hoyer, for the time and effort invested into my doctoral studies at UC Merced. The guidance and critique that you have provide though my doctoral educaton have helped shape me throughout my graduate studies. I am grateful of your thoughtful dedication towards improving my scientific skills and preparation in starting the next chapter of my scientific career.

This document and all the work that it represents would not be possible without the unconditional love, support and motivation provided by Michelle, Gabriel and Dominic. Words can only begin to describe how much you mean to me.

Lastly, I would like to acknowledge the Lawrence Livermore National Laboratory personnel I've had the privilege to work with. There are two individuals that I would like to personally thank for everything they've done to help me become a better scientist. I would like to thank Dr. Nick Hum for your mentorship and guidance throughout my PhD studies. Your experimentalist approach has proven insightful and allowed me to continually expand and develop my practice of doing science.

Last but definitely not least, I would also like to thank my advisor Dr. Gabriela Loots for everthing, starting with the opportunity to join your lab once I was admitted to the PhD program at UC Merced. Your mentorship allowed me to mature as a scientist through providng the space and resources to excel.

Finally, you also served as my north star during the not so easy times that are a part of doing science. Thank you for everything Gaby!

Curriculum Vita

Cesar Morfin
Human Health Sciences Group
Biosciences & Biotechnology Division; Physical and Life Sciences Directorate
Lawrence Livermore National Laboratory
925-216-9837
Morfin2@llnl.gov

Professional Preparation

Los Medanos College, Pittsburg, CA	Biological Sciences	AS, 2012
California State University, San Francisco	Biochemistry	BS, 2015
University of California, Merced	Quantitative & Systems Biology	PhD, 2023

Professional Experience

2017-2022 Graduate Researcher; BBTD/PLS, LLNL, Livermore CA

Research Experience

UC Merced Quantitative & Systems Biology, Merced, CA

Doctoral Graduate Student, January 2017 – March 2023

Research focus: Genetic regulation of Bone Metabolism

Role: Determine transcriptional targets of Mef2c in bone cells using single cell sequencing

San Francisco State University, San Francisco, CA

Master's Research, January 2016 – May 2017

Research Focus: Genetic regulation of pluripotency

Role: Determining genomic localization patterns of Foxd3 during neural crest cell speciation using in vitro stem cells differentiation.

Undergraduate Research, January 2014 – July 2015

- Research focus: MicroRNA regulation of Muscle Development
- Role: Determine in vivo activity of mir206 by micro-injecting a GFP reporter into X. laevis embryos

USDA, Plant Gene Expression Center, Albany, CA

Undergraduate Research, June– July 2011

- Research focus: Genetics of Plant Physiology
- Role: Identify lignin corn mutants via gel electrophoresis

Teaching Experience

Spring 2017-Summer 2022 Teaching assistant, Bio 110 Cell Biology

Presentations

1. C. Morfin, S. Wilson, A. Sebastian, N. R. Hum, D. Murugesh, G. Loots. 2022 Single Cell Transcriptomic Analysis Reveals a Diverse Functional Role for Mef2C Amongst Bone Populations. American Society for Bone and Mineral Research – 2022 Annual Meeting, Austin, Texas; *Oral Presentation*

2. C. Morfin, A. Sebastian, N. Hum, R. D. Murugesh, G. Loots. 2022 Mef2c mediates the transcription of a subnetwork of PTH targets amongst

osteogenic populaitons, independent of Sost. American Society for Bone and Mineral Research – Member Spotlight Series, Webinar; *Oral Presentation*

3. C. Morfin, A. Sebastian, N. Hum, R. D. Murugesh, G. Loots. 2022 Mef2c mediates the transcription of a subnetwork of PTH-signaling targets in osteogenic populations, independent of Sost. Orthopedic Research Society – 2022 Annual Meeting, Tampa, Florida; *Poster Presentation*

4. C. Morfin, A. Sebastian, N. R. Hum, D. Murugesh, G. Loots. 2021 Transcriptomic Analysis Identifies Mef2C as a Regulator of Dystrophin Glycoprotein Complex Genes, in Bone. American Society for Bone and Mineral Research – 2021 Annual Meeting, San Diego, California; *Poster Presentation*

5. C. Morfin, A. Madrigal, J. Ramirez, C. Domingo. 2015 Identification of miR-206 regulated Pathways involved during the formation of skeletal muscle. *Society of Developmental Biology* – 74th Annual Meeting, Snowbird, Utah; *Poster Presentation*

6. C. Morfin, J. Ramirez, C. Domingo. 2014. The role of miR-206 in regulating cytoskeleton dynamics during somite formation. SFSU Summer Research Symposium, San Francisco, CA; *Poster Presentation*

Publications

1. C. Morfin, S. Wilson, A. Sebastian, N. R. Hum, D. Murugesh, G. Loots. Mef2c utilizes cell-type specifc gene regulatory networks amongst the osteogenic lineages to promote the maintenance of bone homeostasis. 2023. (In Preparation; anticipated submission Spring 2023)

2. Sebastian. A, Hum. NR, Morfin. C, Murugesh. DK, Loots. GG. Global gene expression analysis identifies Mef2c as a potential player in Wnt16-mediated transcriptional regulation. Gene. 2018. Epub 2018/07/10. pmid:29981832.

Abstract

The need to treat bone loss disorders, such as osteoporosis, continually compounds as societie's age advances with over 200 million postmenopausal women and elderly men are affected annually. Additionally, the limitions associated with existing therapeautics underscore the need to developed improved osteoanabolic drugs.

The research herein focuses on transcription factor mediated gene regulatory networks (GRN) that govern key bone physiology. Mef2c is a transcription factor that is emerging as a key regulator of bone and endochondral ossification. Given the wide expression profile of Mef2c amongst bone cell populations characterizing the Mef2c GRN could provide incites into novel drug targets or suggest improved strategies in reprogramming MSCs to treat osteoporosis.

Accessility to the underlying bone cell populations is a widely excepted practical limitation associated with bone research. Current bone cell isolation methods are limited and have led to a lack of robust osteocyte-specific data. The development of a improved protocol, adaption of current practices, was used to isolate primary bone cell populations for downstream single cell RNA sequencing (scRNAseq). Additionally, flow cytometry was used to capture floursescent labeling bone cell populations. Transcriptomic analysis revealed that the isolation method was capapble of capturing rare populations such as osteocytes.

The isolation method made it suitable to characterize the Mef2c function in bone. Previous work has shown evidence that Mef2c mediates key cellular behaviors that promote endochondral ossification and bone formation involved

in maintaining bone strength and homeostasis. Such findings underscore the need to uncover the underlying mechaninsm by which *Mef2c* regulates bone cell activity. Here, Mef2c-deficient bone cell populations from *Mef2c$^{fl/fl}$; Bglap-Cre* and *Mef2c$^{fl/fl}$; Dmp1-Cre* mutant mice were isolated to profile the gene expression changes scRNAseq. The work revealed a population level shift towards Lum^{+} mesenchymal progenitor subpopulations. Whereas osteoblasts and osteocytes exhibited defective energy and bone metabolism genes in the absence of *Mef2c*. Taken together, the wide expression amongst bone cell populations exhibits a cell types specific Mef2c function.

Recently, Mef2c function was also found amongst bone resorbing osteoclast populations and was found mediating bone erosion associated with inflammatory arthiritis. Here, we isolated Mef2c-defecient CD11b^{+} osteoclast progenitors from *Mef2c$^{fl/fl}$; Ctsk-Cre* and characterized their ability to differentiate into mature osteoclasts. While *in vitro* studies demonstrated the negative impact the absence of Mef2c has on osteoclast differentiation, transcriptional analysis did not highlight a similar impact. Future studies will have to focus on targeting *Mef2c* at early or the initial stages of osteoclast cell states.

In summary, the current findings illustrate the partial view of how osteogenic cell populations are programmed in order to maintain bone tissues throughout adulthood. By continually characterizing Mef2c will lead to a greater understanding of how cells are programmed and the pathophysiology associated with osteoporosis.

Chapter 1. Introduction

1.1 Bone function, development, and homeostasis

Skeletal system development begins during early embryogenesis arising from 3 different lineages between the sixth and seventh week of embryonic development [1]. The spine and rib cage, key components of the axial skeleton, originate from the structures called somites. The craniofacial bones, on the other hand, originate from the neural crest and the paraxial mesoderm [2-4]. Whereas the appendicular skeleton is derived from the lateral plate mesoderm [2-4]. At each site of future skeletal development, the arrival of migratory mesenchymal stem cells (MSCs) initiates bone development by proceeding toward either the intermembranous or endochondral ossification to form the early skeleton. In the case of endochondral ossification, the formation of these embryonic skeletal tissues is called mesenchymal cell condensation. During the formation of early bone, progenitor cells either differentiate directly into osteoblasts, as is the case during intramembranous ossification, or can differentiate into chondrocytes first, as is the case during endochondral ossification. Such bivalent potential of these mesenchymal progenitors is why they are commonly referred to as osteochondral progenitor cells [5].

Both the axial and the appendicular bones are generated via endochondral ossification. This type of ossification has two phases. During the first phase, the formation of a cartilage template is first formed by chondrocytes. Additionally, surrounding cells define the outside border of the early bone, known as the perichondrium#. During the 2nd phase the ossification of the future bone begins by chondrocytes undergoing hypertrophy and is when the cartilage template starts to become ossified bone. Endochondral ossification is initiated at both primary and secondary ossification sites of developing long

bone and continues postnatally only at the growth plate within the metaphysis Postnatally, the growth plate is responsible for the linear growth of the bones as it serves as a reservoir of proliferating chondrocytes that have now been shown continually mediate the 2nd endochondral ossification phase. Once early bone tissues have been developed, the tissues continue to grow in size and shape, throughout childhood, in a process known as bone modeling. Once in adulthood, bone remodeling is another major key process that serves multiple functions associated with maintaining the health of bone.

The dynamic nature observed in bone development continues well into adulthood as processes such as bone modeling and remodeling are needed to maintain the integrity of bone. Bone growth occurs throughout early childhood and is largely mediated by bone modeling. At which point, formation and shaping of bone are the main processes driving longitudinal and radial bone growth [6]. On the other hand, bone remodeling primarily functions in the replacement of old and broken bone and is the key process occurring throughout adulthood. Specialized bone cells mediate the changes needed in either adding or removing bone. The first type are the bone forming osteoblasts which responsible for adding new bone. [7]. Osteoblasts accomplish this by synthesizing and secreting type 1 collagen, the major bone matrix protein. Next, they locally release phosphates, within the local osteoid, to interact with extracellular Ca^{2+} and form hydroxyapatite crystals and complete the mineralization process of bone tissues. Osteoclasts (OCLs) are the other cell type involved in bone remodeling whose primary function is to remove old and brittle bone during bone resorption [8]. The constant process of renewing bone throughout adulthood is how the accumulation of microdamage in the skeleton is prevented and is why the activity of both resorption and formation must be tightly coupled. In fact, when bone remodeling becomes uncoupled, diseases such as osteoporosis, can begin to develop. During the case of osteoporosis, the

net activity of bone resorption is greater than the activity of bone formation and is a typical an outcome associated with aging or inflammation.

Since the function of bone remodeling (BR) is to maintain bone throughout adulthood, a complex set of steps are in place to ensure that functional demands placed on the skeleton can be met. BR occurs in cycles and can be divided into five stages: activation, resorption, reversal, formation, and termination. During activation, either mechanical or chemical signals initiate the remodeling process. Biological signals are first detected by another bone cell type, the osteocyte, at which point OCL precursors are recruited and are activated [9]. As early OCLs arrive, they begin to differentiate into mature, multinuclear cells that begin to attach to the bone surface. Once attached they become activated and start to secrete acidic hydrogen ions and enzymes to initiate resorption of old and damaged skeletal tissues. The process of resorption typically lasts 2-4 weeks in which pH's as low as 4.5 are used to free old bone mineral. In addition to acids, matrix metalloproteinases and cathepsin K are enzymes that aid resorption by breaking down the organic components of the bone matrix. The resorptive activity results in the formation of cavities that are known as Howship's lacunae. At the completion of the resorption step the short-lived OCLs are removed by undergoing apoptosis.

During the reversal stage, BR coupling signals such as TGF-β, that were previously freed from the bone matrix, promote the recruitment of pre osteoblasts [10]. Simultaneously, TGF-β signaling also inhibits the secretion of pro-OCL factors previously released by osteocytes. Such conditions allow the newly recruited osteoblasts to initiate bone formation that takes between 4-6 months for completion [11, 12]. Here, osteoblasts synthesize new matrix to fill the cavities formed at earlier stages of remodeling by the coordinated secretion of collagen 1 and phosphates needed to promote the formation of mineralized

skeletal tissues. Once bone formation is completed, osteoblasts can either differentiate into bone lining cells or become embedded within the newly formed bone to become osteocytes. Although the newly formed cavities have been filled, the final stage of bone maturation is only accomplished once the process of mineralization is completed past a period of 90-130 days post osteoid deposition [13]. While these cycles continue throughout adulthood, several factors can start to manifest leading to an unbalanced rate between resorption and formation activities. As aging advances, these shifts in BR will often lead to disease states such as osteoporosis.

BR is primarily orchestrated by OCLs, osteoblasts and together form the "Bone Multicellular Units "(BMU). The formation of the BMU involves the OBs, OCL, OS, bone lining cells, and the local vasculature [14]. As such bone tissues are completely renovated after a period of 10 years. BR primarily functions to use bone tissue as a storage unit of calcium and growth factors that can be freed from the mineralized bone matrix and into the blood stream to mediate systemic mineral need. [15]. The secondary function is the maintenance of bone tissue integrity by not allowing microdamage and brittle bone to accumulate.

1.2 Aging and Osteoporosis

As western societies continue to increase human lifespans while also continuing to adopt unhealthy lifestyle practices, there will be a significant need to address late-life chronic diseases such as osteoporosis. As stated by the National institute of Health Consensus Development Panel on osteoporosis is defined as a skeletal disorder having a compromised bone strength that results in severe risks of experiencing a fragility fracture [16]. Postmenopausal women and elderly men make up the majority individuals affected by osteoporosis with approximately 200 million people affected [17-21]. Around 8.9 million fractures are due to fragility fractures annually occurring worldwide [22]. These are

trends that have been observed in amongst various racial and ethnic group and across other western countries [23]. If not addressed, the increasing incidence of osteoporosis will lead to health and social challenges creating a major burden on healthcare systems.

There are two main types of osteoporosis: primary and secondary with the former having two additional subtypes (class I and II). Primary osteoporosis is the most common and is found in 1 in 3 post-menopausal women and older men over the age of 70 [24, 25]. Longitudinal studies, using quantitative computed tomography, have shown lifetime losses of trabecular bone at about 45% in men and 55% in women and cortical bone loss at 18% in men and 25% in women [26]. Amongst women, bone loss is accelerated post menopause throughout the 6-10 year perimenopausal transition [27]. Amongst both sexes, aging leads to shifts in bone remodeling resulting in a net bone loss. Overtime, the thinning or complete removal of trabeculae, cortical thinning, and increase of cortical porosity results in an osteoporotic skeleton [28]. The observed shifts in bone remodeling that occurs as aging advances have been attributed to defective bone formation in which bone researchers have shown a corresponding shift towards increased bone marrow adiposity [29, 30].

On the other hand, secondary osteoporosis is caused by diseases and their associated treatments. Various types of diseases can increase the incidence of osteoporosis. Osteogenesis imperfecta and cystic fibrosis are a few types of genetic diseases that can lead to waning of bone mass and strength. Whereas metabolic disorders serve as another major factor that can promote osteoporotic bone loss including obesity and diabetes mellitus [31]. Glucocorticoid based treatments, such as immunosuppressing or anti-inflammatory drugs, can also lead to net bone loss overtime [32]. Risk factors that promote the incidence of osteoporosis are categorized as either modifiable

or non-modifiable [26]. Some of these risk factors include lifestyle habits such as smoking, alcohol consumption, physical inactivity, dietary calcium deficiency and obesity which are considered modifiable. Conversely, gender, age, race, and genetic characteristics are some of the non-modifiable risk factors for osteoporosis [26]. Osteoporosis is a complex polygenetic disease, with several underlying drivers, and is largely why there hasn't been any developments towards a cure to bring back a normal level of bone mass.

1.3 Current Osteoporotic therapeutics

Several pharmacological drugs are currently available to treat osteoporosis and are classified into one of two types. Anabolic-based treatments can directly stimulate the formation of new bone and anti-resorptive-based treatments can inhibit osteoclast function to prevent resorption of bone. Of these two classes, only the anabolic drugs have the unique ability to build new bone de novo that can result in a net gain in bone mass and lead to improvements of cortical and trabecular mass and microarchitecture. Currently available osteoanabolic drugs include Teriparatide and Abaloparatide which are based on a well-known signaling pathway: parathyroid hormone (PTH) and PTH related protein (PTHrP); respectively.

Teriparatide and Abaloparatide are both based on the first 34 amino acid sequences that have been shown to have biological effects of the native PTH hormone 1-84. Additionally, Abaloparatide also has additional benefits since it employs an 8 amino acid substitution in the 20-34 region of the protein [33-36]. These changes account for the additional benefits of improved skeletal response found between the two drugs. Both agents stimulate the signaling receptor PTH1r to promote bone metabolism such as in increasing the number of OBs, from their osteochondro-progenitors, and also stimulate their bone formation activity at active remodeling sites that can occur in either trabecular

and endocortical bone surfaces [35-38]. Osteoclastic driven bone resorption is subsequently stimulated as a result of prolong use of these PTH based treatment and is believed to be the major contributor of the well-known waning anabolic effect of teriparatide and abaloparatide. Due to waning anabolism overtime and medications are generally limited to prescriptions no longer than 2 years only.

Romosozumab is the most recently developed osteoanabolic pharmacological agent approved by the FDA. It is a humanized monoclonal antibody that inhibits sclerostin, a Wnt signaling antagonist [39, 40]. By doing so Romosozumab can inhibit the effects of sclerostin as a natural inhibitor of bone formation [41]. Romosozumab has an additional benefit over teriparatide and abaloparatide by also inhibiting RANKL signaling. This additional benefit addresses the limitations associated with increased osteoclast activity [42, 43]. Since Romosozumab can also wane over time, treatment is limited to 12 monthly doses but, unlike PTH-based drugs, does not have any lifetime exposure limits in place. BMD can continue to improve after treatment with osteoanabolic based drugs, BMD has been shown to maintain when osteoporotic patients transition by taking anti-resorption based drugs afterwards.

Anti-resorptive based drugs are the other major type of pharmacological treatment available consisting of bisphosphonates, Denosaub, and selective estrogen receptor modulators (SERMs). Bisphosphonates primarily affect OCL survival and activity by inhibiting the mevalonate pathway [44]. Alendronate, risedronate, and ibandronate are the most commonly used bisphosphonates and their administration is not limited as is the case for osteoanabolic agents. Treatment can range from weekly to yearly administration schedules where bone resorption activity can decrease up to

70% depending on the specific type of bisphosphonate used [45]. Increases in BMD were shown after 3-4 years of treatments that successfully led to the reduction of fragility fracture risk. While bisphosphonates are well tolerated, osteonecrosis of the jaw and atypical femoral fractures are rare side effects that are known to occur in less than 0.1% of osteoporotic patients [46-48].

Denosaub is the only currently available RANKL antibody available to treat osteoporosis. Like Romosozumab, Denosaub neutralizes its intended protein target, and in this case is RANKL, thus preventing the recruitment of OCLs. Denosaub treatment was able exhibit improvements in BMD over what was achieved with bisphosphonates-based treatments and a reduction in fracture risk for a period of up to 10 years [49]. The discontinuation of Denosaub results in one of the associated limitations as there is a subsequently return of OCL mediated bone resorption that are at greater levels than found at during pretreatment. Such rapid bone loss leads to the return of increased risk of fragility fractures making such treatment temporary and moderately inefficacious [50, 51]. Necrosis of the jaw and atypical femoral fractures are other rare yet significant side effects. The limitations described amongst the various types of osteoporotic drugs suggest that a much deeper understanding on how to shift bone remodeling activity is required. It is possible that researchers will be able to manipulate bone remodeling to promote bone formation and effectively treat osteoporosis.

MSC based therapies are a non-pharmacological and promising approach to treat osteoporosis. Bone researchers have come to understand that age related development of osteoporosis could be due to the reduction of the number and function of bone and bone marrow derived mesenchymal stromal cells. Populations that include skeletal stem cells, OBs, and fibroblasts that may be a major contributor towards the shift in BR often seen at advanced age [52-55].

Interestingly, stem cell research has pointed towards using MSCs based regenerative therapies to treat various diseases such as osteoporosis. MSC make ideal candidate as a cell therapy due to their ability to remain undifferentiated, self-proliferate, while also having multi-lineage differentiation capacity. Therefore, MSC based regenerative therapies could replace the MSC populations lost throughout the advancing of age [56]. An additional benefit of MSC based therapies is the ability to harvest MSCs from several tissue types such as bone marrow, adipose tissue, umbilical cord, placenta, dental pulp, and tonsil. Additionally, extensive work demonstrating the potential of MSCs to treat osteoporosis after transplantation. regardless of MSC subtype transplantation into osteoporotic rodent models all showed improved bone density parameters [57-60].

Bone marrow MSCs are the most extensively studies across several OVX animal models [57-60]. While regenerative medicine has shown great promise, only a few MSC transplantation clinical trials have been conducted but have not reported their findings (NCT02566655, NCT01532076). Several limitations first must be addressed for MSC based therapies to be successful. Limitations need to be addressed for MSC bases therapies to be successful. The self-renewal capacity of MSCs poses a major risk in tumor progression and metastasis. A meta-analysis revealed an increased incidence of tumor metastasis post MSC transplantation [61]. The formation of a thrombus is another well known limitation that has proven fatal [62]. Addressing the limitations associated with MSC based therapies would make stem cell transplantation a feasible strategy to prevent or treat osteoporosis.

1.4 Bone cells that mediate bone formation

The OB and OCL cell populations are two key cell types that are involved in maintaining homeostasis through the process of bone remodeling. While the cellular behaviors of these bone cells are spatially and temporally coordinated, they have very different characteristics starting with how they are derived. Bone-forming osteoblasts originally develop from mesenchymal stem cells residing in the bone marrow. These multipotent populations have the potential to differentiate towards adipo-, myo, chondro-, and osteo-genic lineages depending on which regulatory transcription factors activity is prompted. Both Bmp1 and Wnt signaling promote differentiation into osteoblasts [63]. At which point osteoblast progenitors progress from the precursor stage and into functional mineralizing osteoblasts (Figure 1). As the end of a bone remodeling cycle approaches, mature osteoblasts undergo apoptosis while smaller proportion become bone lining cells or osteocytes [64-66]. About 50- 70% osteoblasts undergo apoptosis with the remainder differentiating into bone lining or osteocytes (Figure 1). Bone lining cells can go on to redifferentiate into osteoblasts as needed [67, 68]. On the other hand, embedded osteocytes become part of the extensive lacuno-canalicular network that connects the bone lining, osteoblasts, and other osteocytes.

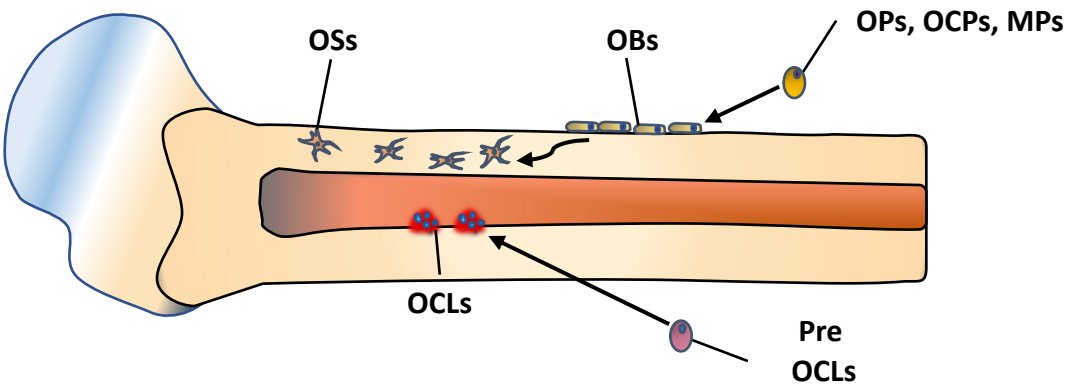

Figure 1. Bone cell populations primarily consist of osteogenic and osteoclast populations that function in maintaining bone tissue homeostasis. *A) Osteogenic populations are the bone cells that promote bone growth via a process of mineralization and consisting of 3 subtypes of cells: mesenchymal (MPs), osteogenic (OPs) and osteochondro progenitors (OCPs), osteoblast (OBs), and osteocytes (OSs). Conversely, osteoclasts (OCLs) are the bone cell populations that remove old and damaged bone throughout adulthood.*

Osteocytes are the most abundant and longest-lived specialized cell type found in bone. These terminally differentiated cells form a lacuna shortly after they are engulfed into the newly formed bone. Once fully differentiated, their cellular morphology changes and acquires dendritic-like processes while also losing over 70% of their organelles and cytoplasm [69]. The star-like cell shape aids becoming part of the lacunar-canalicular network needed to maintain contact with neighboring bone cells needed to maintaining bone homeostasis [70]. As previously mentioned, biological stimuli initiate bone remodeling where signals are detected and relayed by osteocytes [9]. Typically, physical forces that result in mechanical strain and microdamage to the skeleton serve as the biological stimuli that lead to the activation of osteocytes.

Mesenchymal stromal cells play a crucial role in maintaining a constant supply of osteogenic precursors that is required for the formation of new bone (Figure 1). Recent advancements in our understanding of MSC osteogenic differentiation and associated mechanisms have expanded. For example, long bones have been found to house various stem cell niches with unique properties yet contribute towards maintaining bone homeostasis. These niches house skeletal stem cells and have been found in various bone compartments such as the superficial zone of articular cartilage, epiphyseal growth plate, periosteum, and the perivascular niche in the BM. All of which share the capacity to become osteogenic populations that can go on to maintain bone formation activity [71-79]. Underlying mechanisms such as MSC migratory behaviors have shown to influence the microstructures of bone tissues that could promote appropriate bone formation [80]. Additionally, the MSC cytoskeleton has been found to play a role in mediating adhesion with ECM and promote differentiation by altering cell shape [81, 82]. As mentioned previously, disruption in the MSC supply towards providing osteogenic precursors is what researchers now understand how BR shifts towards an osteoporotic skeleton state.

1.5 The osteoclastic lineage and their role in bone resorption

OCLs are the other key cell type involved in maintaining homeostasis through its role in bone resorption. Unlike the cells of the osteogenic lineage, OCLs are derived from the hematopoietic lineage [83]. OCLs are the other key cell type involved in maintaining homeostasis through its role in bone resorption (Figure 1). During development, OCLs derived from embryonic erythro-myeloid progenitors to aid in the formation of the bone marrow compartment. Here, hematopoietic stem cel (HSCs) and their immune progenitors can be

maintained [84, 85]. Postnatally, HSC derived monocyte/macrophage precursors can become mature OCLs. [86-88]

Macrophage colony-stimulating factor 1 (MCSF-1) and receptor activator of NF-κB ligand (RANKL) are key cytokines that are secreted by osteoblast, osteocytes and stromal populations in response to PTH signaling [89]. Together, CSF-1 and RANKL promote the differentiation of precursor cells into mature OCLs by proliferating, undergo cellular fusion, and become large multinuclear cells [90-92]. Resorption begins once mature OCLs attach to the local bone matrix and become polarized. At which point, specialized membranes form such as the sealing zone, the ruffled border, and the functional secretory domain to contain secreted vesicles containing H^+ ions, metalloproteinases, and cathepsin K. At which point collagen is degraded and calcium and phosphate is released from bone [93]. After about 2-4 weeks, resorption is completed and the multinucleated OCLs undergo apoptosis.

1.6 Cellular energy metabolism of bone cell populations

Recently, bone researchers have begun to appreciate the complex mechanisms the various cell subpopulations use to generate cellular energy to meet the demands of BR. The dynamic nature of bone energy metabolism has garnered much more appreciation to that of other more well studied fields such as in neuroscience and cardiovascular biology. As is the case with other tissue types, cellular energy metabolism has been shown to play an integral part amongst the various types of bone cell populations. For example, bone tissues were understood to have mostly a hypoxic microenvironment that is very low in oxygen. Oxygen being a key player as the final electron accepter of oxidative phosphorylation; a major pathway to generate cellular energy ATP. Under these hypoxic conditions osteoblasts and their MSC derived progenitors were

found generating energy primarily through the glycolytic pathway in early studies [94, 95].

Interestingly, new technologies have enabled improved measurements of oxygenation and vascularization *in vivo* of bone tissues [96]. These recent studies have demonstrated that while bone marrow remains to be a hypoxic microenvironment, bone tissues have instead found having a vascular network consisting of capillaries with a pO_2 of about 4%. Only osteogenic progenitors are now believed to generate ATP via glycolysis while having low oxidative phosphorylation activity [97-100] and is a common characteristic of other stem like cell populations [98, 101, 102]. In their undifferentiated state, osteoprogenitors are able to preserve low levels of reactive oxygen species (ROS) and maintain an overall reduced cell state. Conditions that are key for maintaining stem cell like cell populations by keeping genomic and mitochondrial DNA damage at minimal levels.

Differentiated osteoblasts and osteocytes, conversely, have been found to exhibit higher rates of oxidative phosphorylation. As osteoprogenitors undergo differentiation a metabolic shift occurs towards oxidative phosphorylation as it is upregulated and oxygen consumption increases, mitochondrial fusion and enlargement occurs during osteoblast commitment [98]. The complex functions of osteoblasts and osteocytes require oxidative phosphorylation for the generation of sufficient ATP levels. Like other highly specialized cells, osteoblasts require metabolite precursors and molecular intermediates for the building blocks of extracellular matrix deposition and mineralization. With collagen type 1 being the about 90% of the organic matrix of bone self-assembly of mature collagen requires oxygen and α-ketoglutarate [103]. Such osteoblast related functions support the need for increase oxidative phosphorylation activity. Ldha is a glycolytic enzyme involved in fermentation that primarily

functions during anaerobic glycolysis which is pivotal in maintaining the pool of NAD^+ under hypoxic conditions [104].

1.7 ECM role in maintain bone homeostasis

The loss of bone strength is a major health challenge for postmenopausal women and elderly men as over 50% women and 20% men will experience a fracture within their lifetime [17, 18, 22]. Typically, BMD measurements have been the most widespread tool to assess fracture risk but has recently been found to be only one of many indicators of bone health (89). Researchers have come to appreciate the composition of the bone tissues and their role in influencing bone quality such as the proportion of hydroxyapatite, type I collagen and other non-collagenous proteins (NCPs). Biophysical properties such as the type of collagen crosslinking and its effect on hydroxyapatite crystal formation are also critical for bone strength [105]. Additionally, the ECM structure can influence bone quality. All of which can independently contribute to the increased risk of fractures while not meaningfully decreasing BMD.

The study of osteoporosis in animal models and human patients has highlighted alterations to bone microarchitecture in addition to reductions in bone mass. Both, cortical and trabecular bone types accumulate changes to their microstructures overtime. In cortical bone, reductions in bone tissue density, along with a corresponding increase in cortical porosity, is a trend that continues to worsen throughout age [106]. Trabecular bone shares a similar trend as reductions in number, thickness, and degree of trabecular connectivity are also observed. All of which become increasingly severe throughout the progression of osteoporosis [107]. As these alterations to the microarchitecture continue to accumulate, the bone's ability to translate mechanical stimuli into

biological signals continually dampens, compounding the acceleration of osteoporosis.

Collagen crosslinking are changes to the ECM that cause loss of bone quality and represent post translational modification involved in modulating tensile strength and elasticity of bone tissues [108]. There are two major types of modifications: enzymatic and non-enzymatic that occur during the collagen maturation process. Enzymatic crosslinking occurs at the ends of two adjacent collagen molecules resulting in the stable and non-reducible conformation. Such stable conformation is understood to have a beneficial impact on bone strength [108, 109]. On the other hand, non-enzymatic crosslinks are detrimental to bone strength and can form within and across neighboring collagen fibers in a semi random pattern. These are called advanced glycation end products that accumulate with age and disease [108]. The resulting sporadic pattern in an altered spatial distribution and is why bone quality and strength are negatively impacted.

1.8 Gene regulatory networks associated with maintaining bone homeostasis.

The coordination amongst the various types of bone cells is a requirement for the maintenance of bone mineral density that is accomplished through complex gene regulatory networks (GRN). GRNs consist of key transcription factors and the network of genes they regulate. These GRNs are responsible for the spatiotemporal coordination of the cellular behaviors involved in building functional bone during development and in the maintenance of bone tissue in adults. TFs are regulatory proteins that mediate developmental, cell renewal, and differentiation processes involved in maintaining tissue homeostasis through direct DNA binding interactions. TFs can be regulated at multiple

levels and that include interacting with binding partners to fine tune expression by either activating or repressing target genes. Typically, TFs respond to intrinsic cues, such as development and differentiation, and extrinsic cues, such as environmental signals [110]. Any alteration to TF expression can lead to overall dysregulation of a given cellular process and lead to the deterioration of tissues such as the case for osteoporosis. Understanding how the changes in TF expression can alter throughout aging should shed light on the underlying gene regulatory mechanisms that occur as bone remodeling shifts towards overactive bone resorption.

Runt-related transcription factor 2 (Runx2) is a key TF that has been shown to be a "master" regulator of osteogenesis [111]. Expression is found in both the osteoblast lineage cells and chondrocytes and is essential for chondrocyte maturation and osteoblast differentiation [4]. Such functions suggest that Runx2 coordinates the cellular behaviors associated with the endochondral ossification process needed to build and maintain bone. *Runx2* knockout studies highlighted mice lacking *Runx2* in osteoblast populations display lower body weight, and unmineralized calvaria [112-115]. Additionally, key ECM proteins such as Col1a1, Col1a2, Spp1, Ibsp, and Bglap/Bglap2 were reduced when *Runx2* was absent. *Runx2* also indirectly mediated OCL activity by up regulating the expression of RANKL [116, 117]. Additionally, absence of *Runx2,* also affected chondrocytes maturation at the growth plate as there were no hypertrophic populations found [118, 119]. Whereas overexpression had the opposite affect leading to accelerated chondrocyte maturation and endochondral ossification. The overexpression even led to the articular cartilage to undergo endochondral ossification [120, 121].

Transdifferentiation of hypertrophic chondrocytes was also affected when Runx2 was absent. Hypertrophic chondrocytes were once believed to be

terminally differentiated but have recently been shown to be a source of osteogenic cell populations that contribute to endochondral ossification [122-124]. In *Runx2*$^{fl/fl}$; *Col10a1-Cre* mice, transdifferention was disrupted as an increased number of hypertrophic chondrocytes was found to undergo apoptosis instead. The finding suggests a role for *Runx2* in mediating the transdifferentiation of hypertrophic chondrocyte into osteoblasts [125].

Another key TF that regulates key aspects of the osteogenic lineage is *Osterix* (*Osx/Sp7*). *Osx* shares a similar expression pattern as *Runx2* and is found amongst the various bone compartments. Interestingly, knockout studies, using *Sp7*$^{-/-}$ mice, determined that *Runx2* expression was unaffected indicating that *Runx2* transcription is not directly or indirectly dependent on *Osx*. However, *Runx2*$^{-/-}$ mice lacked *Osx* expression suggesting that *Runx2* is upstream of *Osx* [126]. *Sp7*$^{-/-}$ mutants died at birth and lacked any formation of embryonic bone. Whereas conditional deletion led to a reduced number of OBs and affected OS cell shape by resulting in fewer dendrites [127]. Additionally, the lack of *Osx* greatly reduced key bone metabolism genes among OBs and OS populations [127]. Taken together, research has demonstrated the importance of TFs Sp7 and Runx2 in regulating the cells that underpin endochondral ossification from both chondrogenic and osteogenic lineages.

1.9 Mef2c functional contributions to bone.

Myocyte enhancer factor 2 C (*Mef2c*) is part of the MADS family of proteins and is one of four members of the MEF2 family that include *Mef2a, Mef2b, and Mef2d*. During embryogenesis, *Mef2C* expression is found in many different cell types such as cardiac muscle, skeletal muscle, neural, chondroid, immune, endothelial, and bone cells to regulate tissue specific gene expression. Global

deletion of *Mef2c* is lethal due to improper looping morphogenesis of the heart tube and abnormal right ventricle development [128]. *Mef2c* deficient mice also exhibited reduced brain sizes with neurons that were found not able to mature [129]. A similar expression trend was found postnatally and was best characterized in skeletal muscles [130-132]. Condition deletion studies, using a skeletal muscle specific Cre-recombinase, suggested that *Mef2c* was needed for muscle tissue homeostasis. The KO mutant skeletal muscles were able to differentiate normally during embryogenesis but subsequently deteriorated and the sarcomere fiber organization became disorganized [133]. More recently, *Mef2c* was recognized as a key cardiogenic transcription factor, along with *Gata4* and *Tbx5*, by work done by Yamanaka [134]. These reprogramming factors were shown to be able to directly reprogram fibroblast cells into cardiomyocytes. Such work highlights the importance of *Mef2c* in establishing cell fates in stem like populations.

In bone tissues, *Mef2c* has been shown to mediate key physiological processes that resemble the function of key osteogenic master regulators *Runx2* and *Sp7*. Bone-specific Cre recombinase studies have shown developmental and postnatal affects that impacted overall bone tissue quality and strength. Such work has resulted into two major functions that appear to be mediated by *Mef2c* expression. Expression that is found amongst osteogenic populations and their MSC derived progenitors. Conditional knockout studies shared a similar skeletal phenotype when targeting OBs (*Col1*) and OSs (*Dmp1*) populations [135, 136]. Both of the adult *Mef2c* mutant genotypes had increased bone mass that later was shown to be a direct result of downregulating *Sost*, a key regulator of bone formation [137]. Mef2c functions as transcriptional activator that is needed to maintain bone mass and later shown to be upstream of the Wnt amongst OS populations [135]. In vitro

studies also demonstrated Mef2c function in OB populations that were sensitive to anabolic pathways such as PTH [138].

Another line of evidence/research hase uncovered Mef2c function in MSC populations that has been shown to impact bone tissue homeostasis. Early work showed *Twist1* specific deletion of *Mef2c* in osteogenic precursors resulted in mice exhibiting shorted long bones due to impaired endochondral ossification and delayed ossification of bone [139]. Additional cell cultures studies shed light on how Mef2c may be functioning in specifying the osteogenic lineage in mesenchymal progenitors [140]. Researchers found that hypertrophic gene (*Col10a1, Ihh, and Ibsp*) expression changed in response to modulating *Mef2c* levels in cultured human MPC [140]. Similarly, *Mef2c* levels diminished in response to hypoxia that also attenuated hypertrophy in ATDC5 cells; a chondrogenic cell line that originated from mouse teratomcarcinoma cell populations. [141]. Such findings suggest Mef2c is playing a key role during transdifferentiation and is involved in mediating transcriptional changes that are needed to switch between osteo- and chondro-lineages.

Mef2c function was most recently described in the bone resorbing OCLs. An earlier study unexpectedly revealed that *Dmp1* mediated *Mef2c* deletion resulted in decreased OCL resorption surface area but was not made clear if the observed phenotype was a direct effect of *Mef2c* deletion [136]. Very recently, *Mef2c* function in OCLs was confirmed in both *in vitro* and *vivo* experiments. Mx1-mediated deletion led to mutants exhibiting HBM phenotype in a similar trend as found in osteogenic studies [142]. The *Mef2c* deficiency in OCL precursors showed a reduced differentiation capacity to become actively resorbing cell types. Interestingly, monocyte precursors isolated from the synovial fluid of rheumatoid arthritis patients had increased MEF2C expression levels [142]. A disease characterized by pathogenic bone

loss due to overactive OCL activity. This work points to another mechanism by which Mef2c coordinates the cellular behaviors needed to maintain bone mineral density.

1.10 Studying bone cell populations involved in bone remodeling

Isolating bone cell populations of interest is a key requirement involved in understanding the cellular behaviors associated with bone remodeling. Due to the inherent qualities of bone tissue, isolation procedures need to be capable of digesting and removing mineralized bone thus presenting a widely accepted limitation of bone research. Current experimental approaches to isolate primary bone cell populations have been hampered in their ability to identify, isolate, and study specific/discrete cells due to capturing heterogenous progenitors populations of the MSC lineage. [143]. The various gaps that exist in our understanding of the MSC-derived osteogenic lineages are due to the unique practical issue associated with studying adult bone tissues. Researchers are still not sure to what extent discrete cell subpopulations exist within bone nor is the hierarchy among these MSC-derived lineages exhaustively delineated. Additionally, the differentiation trajectory is not yet understood to be linear or, instead, transdifferentiation and plasticity between cell states of the osteogenic lineages further increases the complexity of relationships among different cell types. Out of all the cells that make up the osteogenic lineage, OSs are the most difficult to isolate given their entombed locations within the lacunar-canicular network found throughout mature bone tissues.

On the other hand, MSC are the most understood population associated with the osteogenic lineage and is due to their relatively accessible location within

the bone marrow compartment. The accessibility of MSCs has led to their study as early as 1968 when researchers first reported that cells residing in the BM could become cells of the osteogenic lineage [73]. Later, MSCs were also found in other somatic tissues including, dental pulp, synovium tissues, and adipose tissues all of which were shown to be able to differentiate into cells of the mesenchymal lineage [144-146]. These are populations that have specific features, as defined by the International Society for Cell Therapy, to include: adhesion to plastic surfaces, expression of surface markers: CD44, CD90, CD105, and CD73, lack expression of hematopoietic markers, and can differentiate into OBs, CHs, and adipocytes [147]. The plastic nature of MSCs has led towards their use in regenerative medicine and is currently an active field of research to understand the endogenous mechanisms to aid in making them suitable for transplantation-based therapies to treat diseases caused by chronic inflammation [148, 149]. Single cell sequencing technologies will be pivotal in uncovering key mechanisms amongst the relatively heterogenous populations.

OBs and OS are osteogenic cells that are not as comparatively understood due to their native locations within bone tissue. Traditionally, primary OBs have been isolated from neonatal rodents as these tissues have yet to mineralize [150, 151]. Subsequently, additional isolation methods were developed to study primary OBs from aged samples to more accurately capture the conditions that causes osteoporosis that is not possible using neonatal calvariae. Explant culture methods, using 1-2mm bone pieces, enabled OB cell outgrowth in cultures but was limited due to cell contamination form other bone residing cell types [152, 153]. Enzymatic isolation methods have, more recently, been adapted and is the preferred methods in obtaining homogeneous bone cell populations [150, 151, 154]. Similar enzyme-based methods have been utilized to isolate primary OS populations from neonatal calvaria and adult murine

long bone but exhibit about 70% cell purity and is considered suboptimal [155]. Most recent isolation methods have incorporated flow cytometry in conjunction with fluorescently labeled OS populations using Cre recombinase mixed with the DMP1 or other bone cell specific promoter [156-158].

The difficulty in identifying and isolating skeletal bone cells has impacted bone researchers in their ability to confidently interpret experimental results. For example, assigning phenotypes to cell subpopulations is not clear due to current isolation methods resulting in heterogenous cell populations. The issue is due to our limited understanding of bone cell subpopulations and the limited selection of available bone cell markers that are adequately specific. The circumstance has led to the inability to identify single populations of interest as current markers typically target more than one subpopulation using currently available markers [159, 160]. Cell culture experiments using isolated primary bone cell populations further highlight the issues with accessing these skeletal bone cells. The cellular composition of isolated bone cells is understood to be inconsistent between experimental and control groups are believed to influence the experimental results. A major factor to this observation is attributed to the high degree of plasticity of MSCs and their progenitors particularly in culture conditions. Such aforementioned factors are largely believed to be a major contributor to the problem of experimental reproducibility amongst bone researchers [161].

OCLs are the other major bone cell type involved in bone remodeling and functions in the resorption of bone. These HSC-derived cell populations are distinct from the cells of the osteogenic lineage and is reflected in the experimental methods used to isolate and study primary OCLs. OCLs are large, multinucleated cells that differentiate from myeloid precursors that along with environmental cues and as result can be functionally heterogenous

[162]. Unlike cells of the osteogenic lineage, primary OCLs cannot be isolated from mice or humans and must be generated *in vitro* from precursor populations [163-165]. To isolate the OCL precursor populations, bone marrow is isolated from murine hindlimbs and then $Cd11b^+$ populations are selected to enrich for monocyte populations. Once done, $Cd11b^+$ OCL precursors are cultured using media contianing OCL factors M-CSF and RANKL to induce differentiation into multinuclear osteoclast populations after 5-7 days in culture. The isolation and differentiation procedure does exhibit associated limitations as there is a consensus that only a small percentage, at around 20%, of the populations are fully differentiated OCLs [162]. Factors that researchersk need to consider when drawing conclusions using data collected from using this method as it could lead to inconsistent and biased results.

1.11 Objective of study

Bone mass is maintained throughout life by a highly orchestrated process called bone remodeling. The process is mediated by the cellular behaviors of several bone cell types through the action TFs and their associated GRNs. By understanding the GRN of key bone TFs, such as *Mef2c*, will shed light on how BR-related cellular behaviors are genetically programmed/regulated. Thus, my objective is to characterize the Mef2c mediated transcriptome across bone cell subpopulations to understand how *Mef2c* contributes to bone tissue homeostasis

In this dissertation, my aim is to study how Mef2c programs the cellular behaviors involved in maintaining BR by completing the following objectives.

1. Develop a bone cell isolation method for downstream scRNAseq experiments. Current bone cell isolations methods used in scRNAseq show insufficient accessibility to OS in murine adult long bone-based studies. Here, we develop an updated isolation protocol that successfully obtains OS populations for using in scRNAseq experiments. The isolation method incorporated several advantages such as using fluorescent lineage reporters, optimized digestion steps, and flow cytometry. These results are detailed in Chapter 2.
2. Characterize the Mef2c mediated transcriptome across different osteogenic subpopulations involved in maintaining bone homeostasis. I characterize genes that are affected in the absence of *Mef2c* and generate new hypotheses about how lack of Mef2c results in a HBM phenotype, independent of Sost. *Mef2c* deficient bone cell subpopulations were isolated and used in scRNAseq studies to understand molecular changes that shifts BR at the single cell level. These results are discussed in Chapter 3.
3. Characterize the *Mef2c* mediated transcriptome amongst osteoclast precursors during differentiation that are involved in functionally resorbing bone during BR. *Mef2c*-deficient OCL precursors were differentiated in culture and subsequently used in RNA sequencing studies. These results are discussed in Chapter 4.

Chapter 2. Characterizing fluorescently labeled bone cell populations using classical bone markers at the single cell level.

Cesar Morfin[1,2], Nicholas R Hum[2], Deepa K Murugesh[2], Aimy Sebastian[2], Gabriela G Loots[1,2]

[1]Molecular Cell Biology Unit, School of Natural Sciences, University of California, Merced. CA USA
[2]Physical and Life Sciences Directorate, Lawrence Livermore, National Laboratories, Livermore, CA, USA

Abstract

Efforts to study primary bone cell populations have been hampered due to the inaccessibility associated with skeletal tissues. These practical issues have limited our understanding of rare or inaccessible osteogenic populations such as osteocytes (OS). Our understanding of OS biology has been primarily expanded through the development and use of various OS cell lines such as IDG SW3s. Whereas primary OS populations have not been intensively studied since obtaining primary bone cells is a key requirement for understanding how they function in maintaining bone homeostasis throughout adulthood. Such inaccessibility has resulted in gaps of knowledge amongst osteogenic cell populations such as how they function during endochondral ossification. OS are terminally differentiated osteogenic cells that are believed to arise from osteoblasts (OB) populations during the bone formation where they serve multiple bone and non-bone functions and are one of the most inaccessible bone cell type. Robust OS transcriptomic data needs to be generated to understand how these cells function and yet there is minimal data available using the latest single cell RNA sequencing (scRNAseq technologies). Here, we present a method to isolate primary osteogenic populations from adult murine long bones using bone specific fluorescent reporters *Dmp1-Cre;* Ai9, *Bglap-Cre; Ai9*, *Ctsk-Cre; Ai9,* and *Col2-Cre; Ai9* for downstream scRNAseq analysis. The present

protocol is adapted from serial digestion methods that was optimized to increase efficiency of capturing a sufficient number of osteogenic populations for downstream scRNAseq *via* fluorescently labeling specific bone subtypes. Successful scRNAseq of captured osteogenic populations identified various bone cell populations such as: mesenchymal progenitors (MP), osteoprogenitors (OP), osteochondro progenitors (OCP), adipo Cxcl12 abundant reticular (aCAR) cells, OB, OS, and chondrocytes (CH) with some populations exhibiting several subtypes. A preliminary examination of single cell transcriptional signatures shed some light on the lineage of OS populations. Namely, OB differentiation may not be the primary method of deriving OS populations which serves as an example of the promise from successfully obtaining single cell data from rare osteogenic populations. In summary, the present protocol is suitable for obtaining osteogenic populations, including rare subtypes, for scRNAseq based experiments and will be pivotal in understanding the discrete molecular mechanisms each respective bone cell employs to maintain bone homeostasis and under disease states such as osteoporosis.

Introduction

Single cell RNA sequencing (scRNAseq) is one of the latest technologies that has provided extensive information towards understanding the complex and heterogenous cellular behaviors that underpin tissue development and homeostasis. Such expansion was possible as researchers are capable of determining the diversity of cell types [166-169], identify novel cell types [160, 170] and understand the different stages of differentiation for a given cell type [171-173] by employing scRNAseq-based approaches. Additionally, single cell approaches can be complemented by supporting in vivo and ex vivo functional

studies to aid in understanding of the cellular compartment of an any organ of interest. In employing scRNAseq technologies, there is a key consideration for the success of such experiments such as the cell isolation method of choice. Isolation methods are selected based on the ability to capture viable cell populations of interest. Typically, cell isolation is done by tissue dissociation-based methods that release cells of interest from their endogenous locations but also in cellular debris, doublets, and non-viable cells that subsequently need to be removed via flow cytometry. That is why scRNAseq based methods will be pivotal in the field of bone research by expanding our understand how various bone cell populations behave during homeostasis and in disease.

Bone is a mineralized tissue that is constantly undergoing renewal in order to maintain homeostasis and strength in a process called bone remodeling. Amongst post-menopausal women and older men, bone remodeling becomes less efficient at replacing bone and results in the accumulation of old and brittle bone. Overtime, these conditions lead to the development and progression of an osteoporotic skeleton. A skeletal disease that is characterized by compromised bone strength and is accompanied with increased risk of fracture as defined by the National Institutes of Health Consensus Development Panel on osteoporosis [16]. While several therapeutics have been developed to treat osteoporosis, there currently is no cure to stop the overall deterioration of the skeletal system in aging individuals. Efforts to understand the underlying conditions that cause the loss of bone strength are not well understood as various gaps of knowledge exists amongst the bone cells that function in maintaining bone tissue homeostasis.

The incorporation of scRNAseq approaches to the field of bone biology will lead to an expanded understanding of the underling cellular behaviors involved in maintaining bone tissue homeostasis. Early scRNAseq studies have

demonstrated the strength of the approach in bone such as identifying mesenchymal progenitors that potentially support bone tissues. Chan and colleagues described skeletal stems cells found at the perinatal growth plate in both murine and human [174, 175]. Another scRNAseq study identified a novel population of chondrocytes that behave as a transient mesenchymal precursor population [176]. A stem cell population was also found on the periosteum of bone that had both chondrogenic and osteogenic potential ath [160]. Such studies suggest that skeletal bone maintenance is mediated by the existence of separate and anatomically distinct pools of stem cell populations. Novel subtypes are not limited to only mesenchymal progenitors but also adipo progenitors as well. Zhong found a unique progenitor that expressed adipocyte markers but was phenotypically distinct from other early adipocyte progenitors. These populations were shown to be critical in regulating the bone marrow environment and bone formation [177].

A few other scRNAseq based studies focused on osteoblast heterogeneity known to exist within the osteogenic lineage. Primary bone cells were isolated from neonatal calvaria via selection of 2.3kb Col1a1-labeled populations and found subpopulations representing the various osteoblast maturation stages, and different functional states [178]. While the continued efforts to study bone, at the single cell level will provide key insights of the underlying cellular biology, the success of these studies rely on existing primary bone cell isolation methods. To date, there have been no successful reports profiling osteocyte populations from adult long bone using scRNAseq. Osteocytes represent the most common cell type found in bone and yet their isolation has proven troublesome.

In the present study, we report on an isolation method to obtain primary osteogenic cell populations from adult murine long bones using several bone

specific tdTomato reporter mice. tdTomato reporter mice were bred with *Dmp1-cre* (*Dmp1* tdTomato), *Bglap-cre* (*Bglap tdTomato*), *Ctsk-cre* (*Ctsk tdTomato*), and *Col2-cre* (*Col2 tdTomato*) to label and enrich various types of bone cell subpopulations during primary bone cell isolation. The various fluorescent reporters were utilized to aid in selecting the different bone cell subpopulations. Dmp1 Cre expression is limited to osteocytes and mature osteoblasts and is why it's often used as an osteocyte marker [179]. Bglap Cre has been recently adopted to target osteoblast populations [179-181]. Ctsk Cre have been commonly used to conditionally target the osteoclast populations that mediate bone resorption [182, 183]. The last marker used was *Col2 Cre* has been extensively used to study chondrocytes, another key bone cell type [139, 184, 185]. To obtain primary osteogenic populations, a modified digestion protocol was developed specifically for downstream scRNAseq experiments. Successful isolation of primary bone cells for subsequent scRNAseq studies will be pivotal in understanding the complex nature of osteogenic lineage and their ability to mediate bone formation needed to maintain bone homeostasis.

Methods

Reagents

1. Collagenase solution I: 7.5 mg/ml Collagenase I (Worthington) dissolved in α-MEM + 100 ug/mL DNase I (Roche, catalog no. 11284932001). (2 ml/pair of femur or tibias)
2. Collagenase solution II: 3.75 mg/ml Collagenase I (Worthington) dissolved in α-MEM + 100 ug/mL DNase I (Roche, catalog no. 11284932001). (2 ml/pair of femur or tibias)
3. EDTA solution: 100mM dissolved 1x PBS (Ca^{2+} & Mg^{2+} free) containing 0.1% bovine serum albumin (BSA). (2 ml/pair of femur or tibias)
4. 1x PBS (Ca^{2+} & Mg^{2+} free) containing 1% FBS.

Reporter Mice

All animal experimental procedures were completed in accordance with guidelines under the institutional animal care and use committees at Lawrence Livermore National Laboratory under an approved protocol by the IACUC committee and conform to the Guide for the care and use of Laboratory animals. *Dmp1-Cre* (The Jackson Laboratory, BarHarbor, ME; B6N.FVB-Tg(Dmp1-cre)1Jqfe/BwdJ; stock number: 023047), *Bglap-Cre* (The Jackson Laboratory, BarHarbor, ME; Tg(BGLAP-cre)1Clem; stock number: 019509), *Ctsk Cre* [182], and *Col2a1-CreER* [184] mice were bred with *Ai9* reporter mice (The Jackson Laboratory, BarHarbor, ME; Gt(ROSA)26Sor(tdTomato-WPRE) stock number: 007909) for fluorescent labeling of bone cell populations [186, 187]. Genotyping was carried out by PCR. All mice were born at expected Mendelian rations and animal experiments were carried out in accordance with set by the Institutional Animal Care and Use Committees at University of California, Merced, and Lawrence Livermore National Laboratory.

Single-cell RNA sequencing

16-week-old male *Bglap Ai9*, *Dmp1 Ai9, Ctsk Ai9,* and *Col2 Ai9 reporter* mice (N=3/genotype) were used to isolate primary bone cell populations by isolating hindlimbs via dissection. Tissues were thoroughly cleaned of extraneous tissue. Thoroughly clean femurs and were next processed by opening the bone marrow cavity to remove the bone marrow followed by 2x PBS washes. Bones were next minced into 1-2mm fragments using surgical scissors and placed into 8ml of 7.5mg/ml Collagenase (Worthington Biochemical, Lakewood, NJ; CLS-1) digestion solution and 100 µg/mL DNase I (Roche, Basel, Switzerland; 11284932001) in DMEM/F12 for 30 min at 37°C on a shaker at 150 rpm. Next, the digestion solution was transferred to a 50ml conical tube and washed with

1x PBS. Add 8ml of 100mM EDTA and incubate for 30 min at 37°C on a shaker at 150 rpm. Transfer digestion solution to 50 ml collection tube. Repeat alternating digestion steps using Collagenase and EDTA solutions for a total of 9 digestion incubations. Contaminating red blood cells were lysed by adding ACK (ThermoFisher Scientific, Waltham, MA, USA; A1049201) to collection tube containing isolated bone cells followed filtering out cellular debris using a 100µm nylon cell strainer. Further enrichment of bone cell populations was carried out by flow cytometry. Bone cell suspensions were incubated in Biolegend antibodies APC/Cyanine7 anti-mouse CD45 Antibody (Clone: 30-F11) and anti-mouse APC Ter119 at a 1:100 dilution in PBS+1%FBS. Dapi was used for viability staining. Viable CD45/Ter119$^{-/-}$ populations were sorted from unlabeled cell captured from b6 mice and CD45^{-}/Ter119^{-}/tdTomato^{+} sorted from each respective *Ai9* reporter mice with flow cytometric analysis performed on a BD FACSMelody system. Isolated CD45^{-}/Ter119^{-}/tdTomato^{+} bone cell populations were sequenced using Chromium Single Cell 3' Reagent Kit and Chromium instrument (10x Genomics, Pleasanton, CA). Library preparation was performed according to manufacturer's protocol and sequence on an Illumina NextSeq 500 (Illumina, San Diego, CA, USA).

scRNAseq data analysis

Generated scRNAseq data was processed as per 10x Genomics Cell Ranger software (version 6.0.0) manufacturer's recommended protocols (10x Genomics, Pleasnaton, CA, USA). Once biological samples were sequenced by the Illumina NextSeq 500 sequencer, and the base call files (BCL) were demultiplexed into FASTQ files using the Cell Ranger 'mkfastq' command. Data was aligned to the mouse reference genome (mm10) barcoding counted, and unique molecular identifier (UMI) counted performed using the 'count' command.

The remainder of the analysis was performed using the R package Seurat to perform quality control and subsequent analysis on the feature-barcode matrices produced by Cell Ranger (version 6.0.0;10x Genomics, Pleasnaton, CA, USA). Resulting output file were read into Seurat v3 and cells with less than 500 detected genes/cell and genes that expressed in less than 5 cells were filtered out. Both dead cells and doublets were also filtered out from further analysis. Afterwards, the data was normalized by employing a global-scaling normalization methods 'LogNormalize' and a set of highly variable genes were identified. Next, the data was scaled and dimensionality of the data was reduced by principal component analysis (PCA) with cells grouped into an optimal number of clusters for de novo cell type discovery using Seurat's 'FindNeighbors' and 'FindClusters' functions. At which point a non-linear dimensional reduction was performed via uniform manifold approximation and projection (UMAP) and various clusters were identified and visualized. Seurat's 'FindAllMarkers' function was used to identify marker genes per cluster. The various immune and osteogenic cell types were characterized in detail by their respective cell type-specific markers to identify population subtypes.

Statistical analysis

R statistical software and Graphpad Prism were used for statistical analysis. One-way ANOVA and student's t test were used to determine statistically significant differences of mean values. *P*-value of ≤ 0.05 were considered statistically significant.

Protocol

1. **Harvest and processing of *Ai9*-reporter mouse long bones**
    a. *Ai9* reporter mice were obtained and euthanized at 16 weeks of age.
    b. Leg bones (femora and tibiae) were isolated from each mouse and thoroughly cleaned to remove muscle and connective tissues from skeletal tissues.
    c. Transfer prepared bones to biosafety hood and place into a 6 well (1 replicate per well containing 10ml of 1x PBS (1% FBS). *Sets of bone were processed individually then combine for thorough processing of each bone.
    d. Gently crush bone to open marrow cavity and thoroughly wash bone fragments with 1x PBS solution (BM fraction).
    e. Marrow depleted bone fragments are next minced with surgical scissors to yield ~1-2mm fragments.

2. **Serial digestion and fractionation of adult mouse long bone**
    a. Wash and transfer bone fragments to a 15 ml conical tube containing collagenase I solution and incubate for 30 min @ 37^{o}C on a shaker (150rpm).
    b. Collect collagenase solution from 15 ml conical tube and wash bone fragments with 1x PBS to collect remaining residual cells. Combine digestion and wash solutions into a separate 15 ml conical tube and centrifuge @ 500 x G for minutes at 4^{o}C to pellet cells then resuspend in 2ml of complete media and store on ice until bone digest is completed. (Fraction 1).
    c. Add 100 mM EDTA solution to 15 ml conical tube containing bone fragments and incubate for 30 min @ 37^{o}C on a shaker (150rpm).

d. Remove EDTA solution and wash residual cells released with 1x PBS. Combine digestion solution and wash solution. Centrifuge @ 500 x G for minutes at 4°C to pellet cells then resuspend in 2ml of complete media and store on ice until bone digest is completed. (Fraction 2).
e. Repeat steps 5-8 to collect fraction 3 using collagenase I solution and for fractions 5, 7, and 9 with collagenase solution II.

*Note: a gentler collagenase digest is used for the subsequent collagenase digestions. This was found to yield comparable cell yields and minimized the consumption of reagents.

f. Repeat steps 5-8 to collect fractions: 4, 6, 8 with 100mM EDTA digest solution.
g. Following the completion of fraction 9, pellet all cells and pass through a 100μm cell strainer, then perform a red blood cell lysis using ACK lysis buffer.

3. **Enrichment of osteocyte populations from total cell populations collected**
    a. Resulting pooled cells from serial bone digestion and further enriched as follows via subsequent MACS and FACS steps.
    b. MACS separation using anti-Ter119 and anti-CD45 magnetic microbeads to deplete erythroid and immune cells depletion using LS columns.
    c. Stain resulting cell populations, from MACS step, with anti-Ter119 APC and anti-CD45 PE-Cy7 antibodies and sort flow through for CD45/Ter119$^-$ populations.

Results

Bone-specific Ai9 reporter mice suitable for characterization of bone cell subpopulations using scRNAseq

The tdTomato fluorescent reporters were utilized to aid in selecting the different bone cell subpopulations by isolating cells from *Dmp1* tdTomato, *Bglap tdTomato*, *Ctsk tdTomato*, and *Col2 tdTomato* murine long bones. To determine the expression pattern of each tdTomato reporter line, we examined tdTomato expression in femoral sections of *Dmp1 tdTomato, Bglap tdTomato, Ctsk tdTomato, and Col2 tdTomato* samples (Figure 1 A-D). Consistent with prior reports [188], only *Col2 tdTomato* femurs had labeled cells within the articular cartilage of the knee joint while the other Ai9 reporters remained unlabeled (Figure 1A-D). Interestingly, *Col2* expression also led to the labeling of cells within the cortical and trabecular bones such as osteocytes. Suggesting that Col2 positive progenitors could have gone on to differentiate into osteocytes.

On the other hand, finding *Bglap Ai9* samples having a similar tdTomato$^+$ labeling at the growth plate was an unexpected finding (Figure 2aa-dd). Interestingly, all *Ai9* reporter examined displayed dtomato$^+$ cells found within cortical and trabecular bone albeit with some slight variation (Figure 1aaa, aaaa-bbb, bbbb). Only the *Bglap Ai9* and *Ctsk Ai9* samples exhibited labeling on the bone surfaces (endosteum and periosteum). In all, the *Ai9* reporter mice appeared suitable for investigating bone cell biology using scRNAseq based experiments (Figure 1E).

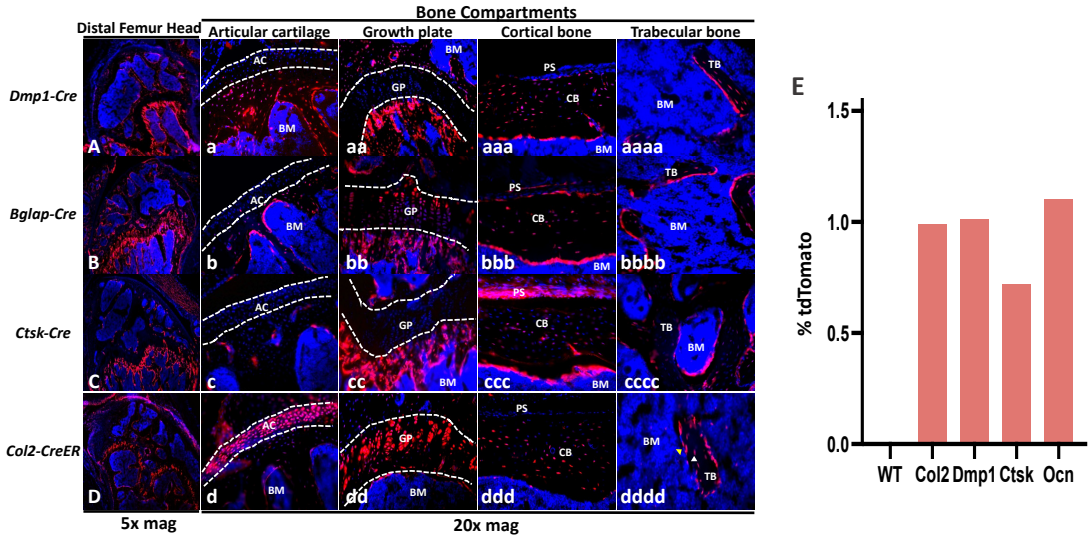

Figure 1. Histological analysis of tdTomato expression in lineage tracing mouse strains. *A-D) Distal femur from each lineage tracing mouse lines denoting localization of Ai9 expression in long bones. Articular cartilage (a-d), growth plate (aa-dd), cortical bone (aaa-ddd), and trabecular bone (aaaa-dddd) bone compartments shown. E) Expression of tdTomato across all genotypes identifies specific expression of the Ai9 cassette. (N=3/genotype)*

Isolation method to capture fluorescently labeled bone cell populations for scRNAseq

To determine the extent of cellular heterogeneity in the adult bone and define all the subpopulations associated with each cell type known to reside in mineralized bone we developed a protocol to isolate rare or hard to access populations for downstream scRNAseq analysis. The method incorporated optimized digestion cocktail concentrations for both collagenase and EDTA solutions that are typically used to break down the mineralized tissues of bone. At 16 weeks of age the bone *Ai9 reporter* mice were sacrificed and isolated their hindlimbs. Once isolated, bone marrow was removed from both femurs and tibiae long bones and minced into 1-2mm^3 fragments. Fragments were

transferred to the 50 ml conical tubes to begin the digestion process consisting of 9 alternating steps between collagenase and EDTA. Bone cells captured from tissue digestion were sorted using flow cytometry by sorting tdTomato^{+} populations. tdTomato^{+} bone cells were then processed for scRNAseq using the 10x Genomics Chromium pipeline (Figure 2A, B). Maintaining cell viability throughout the tissue dissociation stage is a critical requirement ensure preserving data quality and found that the present method exhibited 96% viability (Figure 2B). As expected, a large portion of captured cell populations contained mostly immune populations at 94.5% of the total cells captured. The observation underscores the need for incorporating selection steps for successful isolation of bone cell populations (Figure 2C, D).

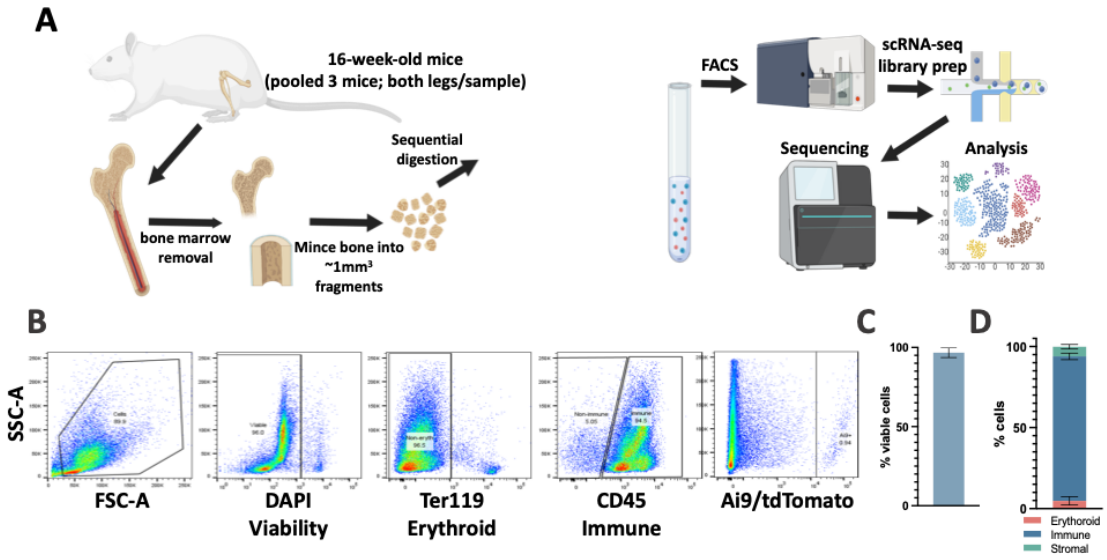

Figure 2. Single-cell RNA sequencing pipeline and flow cytometric analysis. *A) Femurs and tibias are dissected from adult mice then bone marrow is removed and bones are minced into small pieces for enzymatic digestion to release bone cells. B) Next, flow cytometry is used to identify viable, erythroid, immune, or tdTomato^{+} cells for cell sorting. Cells from this approach yield highly viable (C) predominately immune cells but also contain minor erythroid or stromal cells.*

Fluorescent labeling of bone cell populations drastically reduce number of captured immune populations

Isolated dtTomato$^+$ bone cell populations were further processed into single cell containing droplets using the 10x chromium single cell analyzer. Followed by library preparation and sequencing using Illumina standard protocol. A total of 14,287 bone cells derived from all *Ai9* Cre lines (*Bglap Ai9:* 2,848 cells*, Dmp1 Ai9:* 4846 cells, *Ctsk Ai9:* 2,116 cells, and *Col2 Ai9:* 4,477 cells) led to the identification of 9 total clusters (Figure 3A). Both immune and stromal cell types were present, and gene expression signatures of immune markers indicated the presence of neutrophils, myeloid, T cells, B cells and NK cell populations within cluster 6 (Figure 3A). Capturing tdTomato$^+$ population via flow cytometry demonstrated the beneficial enrichment of bone cells of interest as the relative abundance of captured populations was drastically enriched for bone cells. Enrichment of stromal cells eliminated about 90% of immune populations that were present in unfiltered bone digests (Figure 3B).

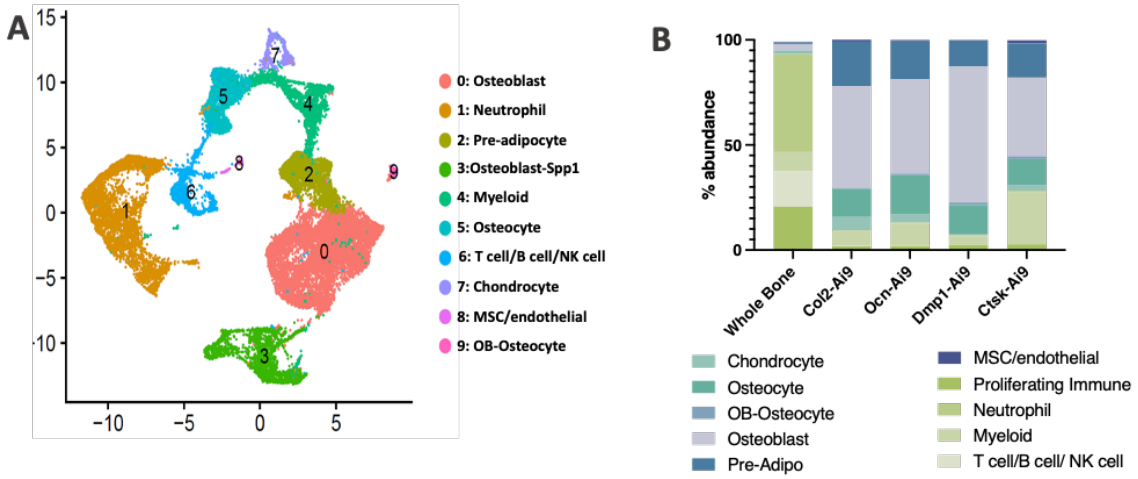

Figure 3. Single-cell transcriptional profiling of cells derived from mature murine long bones. *A) UMAP projection of 21,065 bone cells identifying 9 clusters of immune and stromal cell types based on transcriptional profiles. B) Relative abundance of cell types from whole bone or Ai9⁺ lineage tracing populations reveals selective enrichment in target populations largely in stromal populations.*

Captured flourescently-labeled cells include major bone cell subpopulations

Since the focus of the study was on characterizing OB and OS subpopulations, all immune cells (2,202 cells) were removed computationally, and the remaining 18,863 tdTomato⁺ were reanalyzed. Subsequently, we identified 10 distinct clusters using only the cells captured from the Ai9 reporters used. The relative abundance of the stromal populations was significantly greater in Ai9 mice. As expected, the proportion of osteoblast and osteocyte populations both increased over 1000% due to selecting for tdTomato⁺ cells whereas immune populations experienced a drastic decrease as both neutrophil and T cell/B cell/ NK cell populations dropped to 1% or less (Figure 3B).

The fluorescent selection of bone cell populations led to an increase amongst of the stromal fractions when comparing against the unlabeled populations isolated from C57BL/6 wildtype populations. Cells in clusters 0 expressed *Lifr* and *Vldlr* and were labeled osteoprogenitors (OP) as both are involved in inducing the osteogenic fate [189, 190]. Cells in clusters 1 expressed high levels of *Cxcl12* and *Adipoq*, two markers associated with adipogenic progenitors so were labeled adiopCAR (aCAR) [177]. Clusters 2 and 3 were labeled OB 1 and 2, respectively as they both expressed *Col1a1* and *Mmp13*; respectively. Clusters 4 exhibited Omd and *Prg4* expression and were labeled osteochondro progenitors (OCP). Cluster 5 cells were labeled osteocyte 1 (OS 1) since they expressed *Ank* and *Tnfrsf11b*, clusters 6 and 8 were two subsets of chondrocytes (CH) as both expressed *Col2a1. Whereas cluster 8 also expressed Col10a1* so were labeled hypertrophic chondrocytes (HCs). Cluster 7 expressed *Sost* and *Mepe* and labeled OS 2, cluster 9 expressed *Col3a1* and Ly6a so were labeled mesenchymal progenitors (MP). Cluster 10 expressed a combination of OB and OS markers such as *Phex, Dmp1*, and *Col1a1*, so were labeled OC-OBs (Figure 4 A-C).

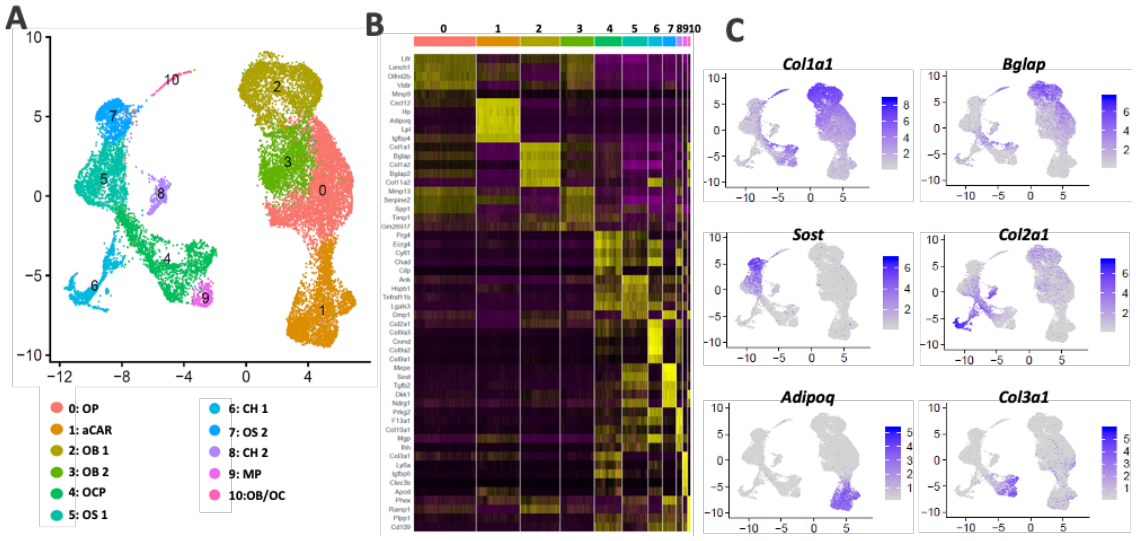

Figure 4. Characterization of stromal cell types and enrichment in lineage tracing mouse lines. *A) UMAP projection of 18,863 stromal cells identifying 9 clusters of cells from all genotypes. B) Heat map of differentially expressed genes from each cluster. C) Feature plots of various bone markers used to denote each cell subtype.*

With the captured populations defined, we next sought to compare whether any of the bone specific *Ai9* reporters were capable of enriching for specific bone cell subpopulations. Interestingly, each of the respective Ai9 reporters all were capable of enriching for 2 major bone cell populations such as OBs and OS (Figure 5A, B). There were some mild enrichments amongst individual Ai9 reporters. *Ctsk Ai9* cells had a slightly increased of MSC populations *Dmp1 Ai9* based labeling showed specific decreased ability to capture aCARs and CHs (Tables 1 and 2; Figure 5A, B). The data appears to suggest that bone cell markers are not as exclusive in their specificity within the MSC-derived cell lineages found within mature long bones. The present method is suitable for isolating and studying primary osteogenic cell populations, such as OS, from adult murine long bones for use in single cell sequencing-based technologies.

Table 1. Percent (%) relative abundance of major bone cell populations amongst Ai9 reporter mice.

Genotype:	AdipoCAR	Osteoblast	OS-OB	MSC	Osteocyte	Chondrocyte
Stromal	15	37	1	17	13	17
Col2	21	52	0	7	14	7
Ocn	18	47	1	11	19	4
Dmp1	12	68	1	4	14	1
Ctsk	17	40	1	25	13	3

Table 2. Log2 fold change enrichment of bone cell subtypes amongst Ai9 reporter mice vs unlabeled populations.

Cell type:	*Col2*	*Ocn*	*Dmp1*	*Ctsk*
AdipoCAR	0.48	0.24	-0.33	0.17
Osteoblast	0.46	0.34	0.86	0.10
OS-OB	-0.92	-0.27	0.45	0.54
MSC	-1.36	-0.67	-2.02	0.56
Osteocyte	0.08	0.56	0.12	0.05
Chondrocyte	-1.28	-1.93	-4.74	-2.52

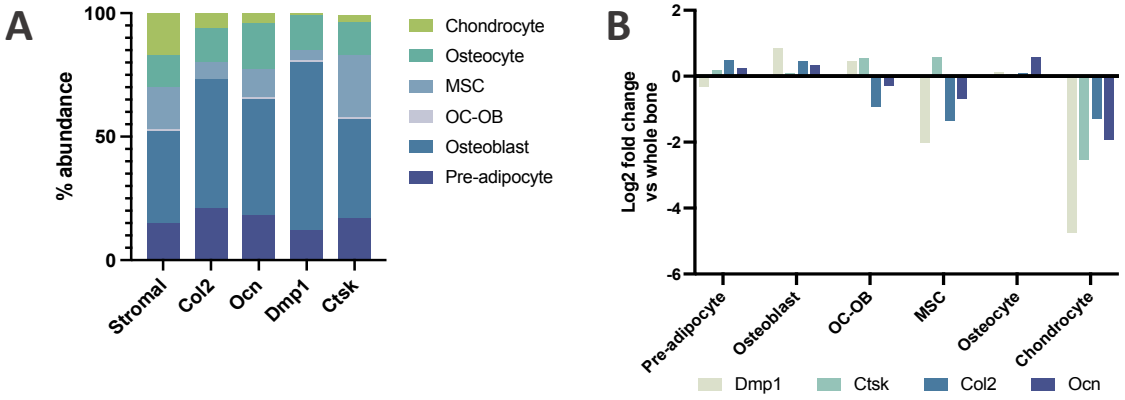

Figure 5. Enrichment of bone cell subtypes found amongst Ai9 reporter mice. A) Relative cell type abundance of each bone cell subtype as compared to the other bone reporters. B) Heat map of differentially expressed genes from each cluster. B) Relative enrichment from each mouse line relative to WT stromal abundance.

Classic bone markers label adipoCAR populations involved in maintaining bone homeostasis

Next, we focused on identifying bone cell subpopulations amongst the MSC, OB, and OS populations isolated using the present method. The characterization of the MSC, OB, and OS populations was conducted using dtTomato$^+$ populations from each respective *Ai9* reporter mouse. Captured bone cell populations (Figure 5A) contained early progenitors of the adipocyte lineage aCARs and express early mesenchymal/osteoprogenitors markers *Lepr* and *Kitl* (Figure 6A). Interestingly, these early adipocyte progenitors also expressed various modulators of bone formation such as stimulators*: Ccl2, Igf1, Bmp6* and inhibitors *Grem1* and *Sfrp1* (Figure 6B) [191-195]. Of note, MP 2 populations were shown to express moderate levels of *Igf1*. aCAR populations also expressed *Vegfc,* a known stimulator of lymphangiogenesis, and was shown to promote bone homeostasis (Figure 6C) [196, 197]. Taken together, the present protocol used was able to isolate aCAR populations that are involved in maintaining bone homeostasis as there is transcriptional evidence of being able to modulate bone formation.

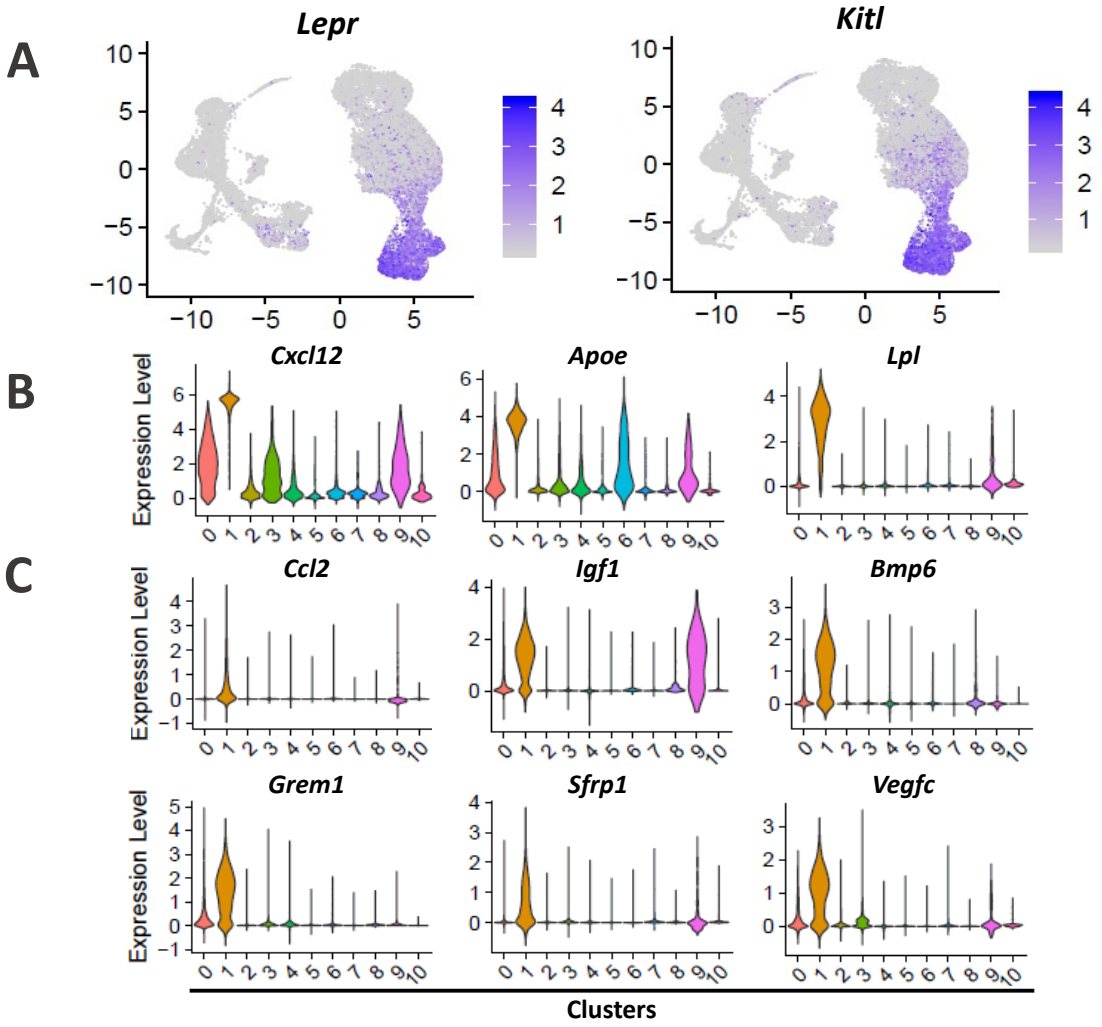

Figure 6. Enrichment of adipCAR populations via bonespecific marker. *A) Feature plots of OP markers. Violin plots of adipocyte progenitor markers (B) and modulators of bone metabolism (C).*

scRNAseq of osteogenic subpopulations suggest multiple cell types are the cellular source for osteocytes

Afterwards, we further investigated captured OB and OS populations along with their relevant progenitors. This was accomplished by reanalyzing clusters

0 (cell #: 5719), 2 (cell #: 2330), 3 (cell #: 2317), 4 (cell #: 2196), 5 (cell #: 1643), 7 (cell #: 720), and 10 (cell #: 114) using cells captured from each *Ai9* reporter mice and unlabeled samples as was done earlier (Figure 7A). UMAP projection of osteogenic populations led to 9 clusters generated with two major groups formed that were distinctly either OB or OS populations (Figure 7B). Cells in clusters 0 expressed *Cxcl12* and *Igfbp4* and were labeled OPs, cluster 1 was labeled pre-OBs (POB) due to expression of *Spp1* and *Mmp13*, clusters 2 and 4 were labeled OB 1 and 2 respectively, since they expressed *Col1a1* and *Bglap*. With OB 2 exhibiting a greater expression of these ECM related genes, they were considered mature OBs while cluster 2 likely representing inactive OBs. Cluster 3 and 6 expressed *Sost* and *Dmp1* so were labeled OS 1 and 2 respectively, with OS 2 populations robustly expressing osteocyte markers in respect to the OS 1 cluster. As such OS 2 were thought to be more mature osteocyte population. Clusters 5 was labeled MP due to their expression of *Ly6a* and *Col3a1*, clusters 7 was labeled OCP as these expressed *Prg4.* Cluster 8 were labeled proliferating since they had high levels of *Mki67; a* classical cell cycle marker [198]. Cluster 9 was labeled OB/OS since expression of OB markers *Col1a1* and *Col1a2* were found as were OS markers *Dkk1* and *Phex* was similarly expressed unlike the clusters representing individual OB or OS cell types (Figure 7B, C). The arrangement between these two major cluster grouping was not expected as OSs were spatially located closer to OCP clusters whereas OBs were spatially located closer to OP clusters. As it was previously understood that OS arise from OB populations that are embedding during the bone formation process [64-66].

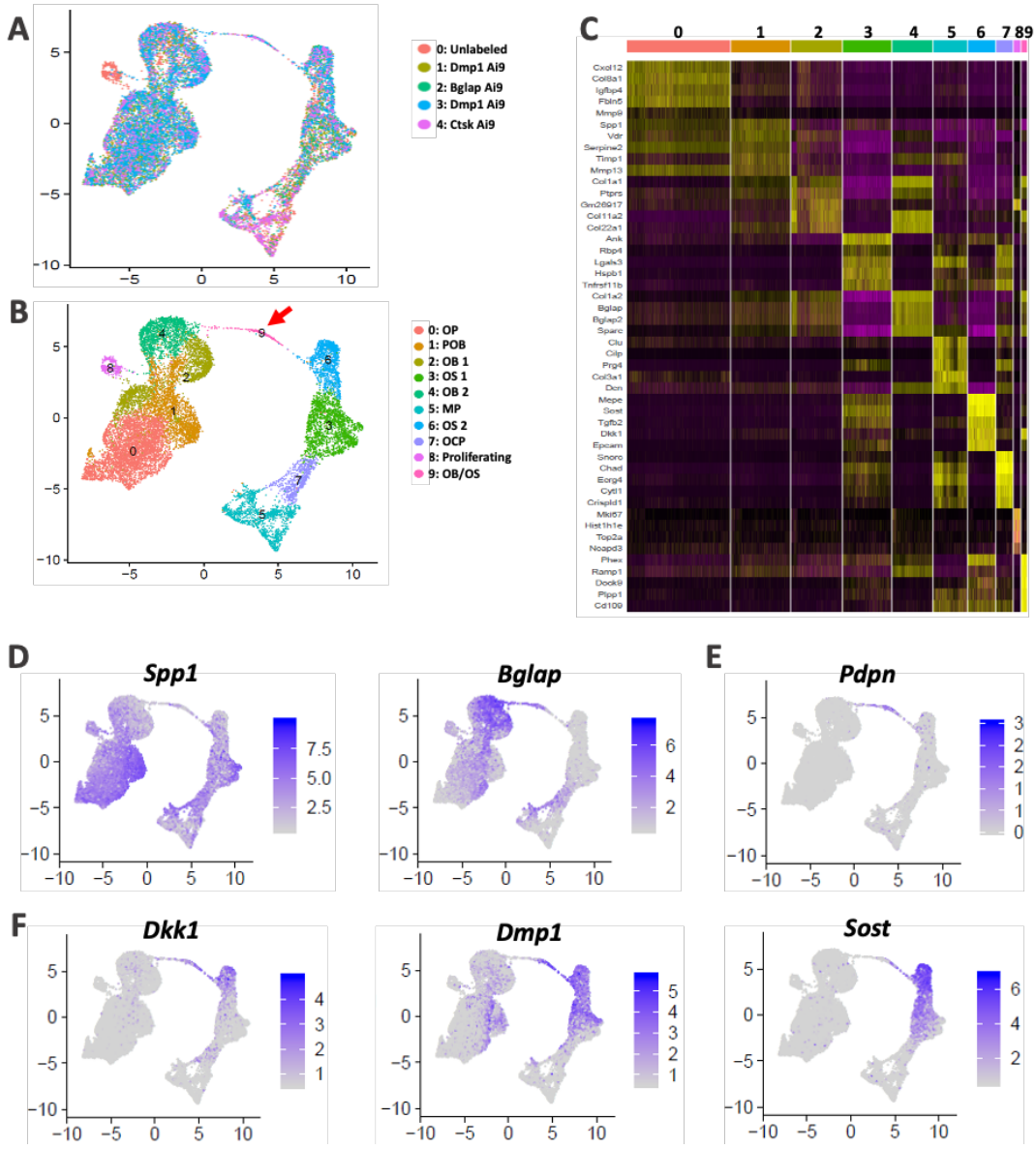

Figure 7. Characterization of oteogenic cell types and enrichment in lineage tracing mouse lines. *A) UMAP projection of x cell populations from unlabeled and Ai9 reporter mice. B) UMAP projection of 9 clusters of identified osteogenic populations. Colors indicate clusters of various cell types. C) Heat map of differentially expressed genes from each cluster. Feature plots of OB (D), OS differentiation (E), and mature OS (F) markers.*

Interestingly, a closer examination of OB and OS marker expression revealed that cluster 9 had contained cells expressing OB 2 marker *Bglap* that was spatially located within the closer half of the linearly shaped group (Figure 7B, D; red arrow). *Pdpn*, which is a known marker of osteocytogenesis, expression was also found but instead amongst cells centrally located within the OB/OS cluster (Figure 7E) [199]. In a corresponding fashion, OS markers *Dkk1, Dmp1*, and *Sost* were then found in the half of the OB/OS cluster that is spatially located closer to the OS clusters (Figure 7F). These trends in OB and OS marker expression suggests cells from cluster 4 become OS populations which has been understood as the major osteogenic lineage trajectory. Successful scRNAseq of isolated primary adult murine osteogenic populations suggests that the well-known pathway responsible for the generation of OS populations may be only one route as the present data shows additional populations that can also be a source of OSs.

Discussion

Previously developed methods used to isolate and study osteocyte populations were limited by prolonged isolation times and by the contamination of immune cell populations. While there have been successful reporting of osteogenic populations using scRNAseq, none of the methods used have been capable of capturing rare or hard to access populations such as OS populations [200]. Additionally, the use single cell-based technologies for the continued examination of bone cell populations will be pivotal in our understanding of key molecular mechanisms used by the various cell populations that mediate bone homeostasis. The availability of osteogenic transcriptomes corresponding to each type of bone cell will be vastly informative by shedding light on fundamental aspects of the osteogenic lineage that is responsible for the development and maintenance of bone. Such as informing our understanding

of the cellular hierarchy associated with endochondral ossification. To date, successful isolation of primary osteogenic populations, including OS, have been from using neonatal calvaria tissues obtained from mouse pups [155]. Here, we show an isolation method to obtain primary osteogenic populations, including osteocytes, from adult murine long bones for use in scRNAseq-based studies.

The availability of cre/lox mouse models have allowed researchers to study discrete cell populations more accurately when used in conjunction with cell type specific markers. Here, *Ai9* reporter mice were bred with several bone specific markers to isolate various types of osteogenic populations for downstream scRNAseq and analysis. Isolation of primary osteogenic cell populations was performed using the protocol listed in an earlier section of the present report (see methods). We were able to obtain enough tdTomato$^+$ cells, from each respective *Ai9* reporter, for use in scRNAseq experiments. An additional benefit is only requiring a minimal number of mice (N=3). This feature can allow for decreasing the amount of time needed to collect dtomato$^+$ cells by using more experimental mice that can result a significant reduction in total digestion time.

Primary osteogenic single cell transcriptional signatures generated by scRNAseq reveals the benefit of using tdTomato$^+$ labeling to enrich for bone cells of interest when compared to using non labeled methods. Enriching for primary bone cells populations sequencing depth is not consumed by the presence of contaminating cell populations. The use of *Ai9* reporter led to a significant reduction in contaminating immune and erythrocyte populations (Figure 5D). An additional benefit stems from having the capacity to isolate primary bone cell populations from aged bones as this ability allows bone researchers to examine correspondingly aged transcriptomes of relevant bone cell populations. An early look of scRNAseq data generated from primary

osteogenic populations supports an emerging theory related to poorly understood aspects of endochondral ossification. To date, how the transdifferentiation of chondro lineage populations towards osteogenic lineages is not fully resolved. The present data suggests that a large portion of OS arise from OCP lineages and not OB populations. OCPs give rise to chondrocyte populations and was shown to also possibly be a source of OS to a much greater extent according to the captured single cell transcriptional signatures. In fact, of the OB populations that are believed to be the primary source of OS cells, only a comparative minority appeared to become OSs. By incorporating the present isolation method, future studies will be able to continually unveil novel aspects of the osteogenic lineage such as whether the major source of OS populations is through the transdifferentiation of OCP lineage populations.

Finally, the present protocol is not without limitations. For example, the bone specific markers used to label bone cell populations demonstrated a wide range of leakiness. A major contributing reason bone markers label additional populations stem from the limited availability of accurate bone cell markers that can target discrete populations. Continued single cell characterization of bone populations will lead to improved candidate bone markers so that bone researchers can sufficiently study genes of interest amongst discrete cell populations. Recently, *Sost creER* mice has been developed with early studies suggesting improvements over *Dmp1* in targeting primary osteocytes [201].

Chapter 3. Mef2c utilizes cell-type specific gene regulatory networks amongst the osteogenic lineages to promote the maintenance of bone homeostasis

Cesar Morfin[1,2], Aimy Sebastian[2], Stephen Wilson[2], Beheshta Amiri[2], Deepa K. Murugesh[2], Nicholas R. Hum[2], Gabriela G. Loots[1, 3]

[1]Molecular Cell Biology Unit, School of Natural Sciences, University of California, Merced. CA USA
[2]Physical and Life Sciences Directorate, Lawrence Livermore, National Laboratories, Livermore, CA, USA
[3]Comprehensive Cancer Center, University of California, Davis. CA USA

Abstract

Mef2c has been shown to mediate key cellular behaviors that promote endochondral ossification and bone formation associated with maintaining bone strength and homeostasis. Previous work has shown how *Mef2c* function is associated with the osteogenic switch amongst MSC precursors while also having a role in regulating osteoblasts activity. However, the underlying mechanisms in which *Mef2c* regulates bone cell activity is not fully understood. To gain a better understanding of *Mef2c* function in regulating the cellular behaviors associated with supporting bone formation, we isolated Mef2c-deficient bone cell populations from *Mef2c$^{fl/fl}$; Bglap-Cre* (*Bglap Mef2c cKO*) and *Mef2c$^{fl/fl}$; Dmp1-Cre* (*Dmp1 Mef2c cKO*) mutant mice and profiled the gene expression changes by scRNAseq. *Bglap Mef2c cKO* and *Dmp1 Mef2c cKO* mutant mice exhibited a HBM skeletal phenotype, so were interested in characterizing the underlying GRN supporting bone formation. Differential gene expression analysis found a total of 96 up- and 2434 down-regulated genes in *Bglap Mef2c cKO* mutant bone cells and 176 up- and 1041 down-regulated

genes in *Dmp1 Mef2c cKO* mutant bone cell subpopulations. *Mef2c* deletion affected the transcriptomes across the osteogenic cell lineage including mesenchymal progenitors (MP), osteoprogenitors (OP), osteoblasts (OB), osteocytes (OS)- subpopulations. Single cell transcriptional signatures suggest Mef2c deficiency resulted to shifts in relative osteogenic populations and enriched Lum^{+} MP subpopulations. On the other hand, OBs and OSs experienced defective bone and energy metabolism. Energy metabolism genes such as *Uqcrb, Ndufv2, Ndufs3, Ndufa13, Ndufb9, Ndufb5, Cox6a1, Cox5a, Atp5o, Atp5g2, Atp5b, Atp5* were all down regulated in the absence of *Mef2c*. Binding motif analysis of promoter regions of identified amongst *Bglap Mef2c cKO* and *Dmp1 Mef2c cKO* mutants and found evidence of Mef2c binding in several bone and energy metabolism such as *Col10a1* and *Ibsp* Taken together, the present data suggest Mef2c transcriptional function by inducing suffecient bone and energy metabolism genes expression associated with proper bone formation in a cell type specific manner.

Introduction

Osteoporosis is a highly prevalent bone disorder characterized by low bone mass and a compromised bone microstructure. [19]. As this bone disorder progresses so does bone fragility and is accompanied by the increased risk of fractures. Worldwide, osteoporosis causes more than 9 million fractures annually. Although various lifestyle risk factors exist, the weakening of bones is generally caused by aging where the bone loss that occurs is due to the uncoupling of bone remodeling. Aging causes activity of bone-forming osteoblasts to decrease leaving the relative activity of bone resorbing osteoclasts remaining leads to increased bone loss overtime. While there is no known cure to osteoporosis, there are some available disease-modifying

treatments. Most of the available therapeutics such as bisphosphonates are anti-resorptive in nature, which slow down bone resorption by osteoclasts. Parathyroid hormone (PTH) based drugs such as Teriparatide and Abaloparatide are two osteoanabolic treatments currently available and are able to stimulate bone formation by activating PTH signaling [202-204]. But these drugs may contribute to adverse events such as dose dependent risk of osteosarcomas [205]. The Sost antibody-based drug, Romosozumab was recently developed and has been shown to be more effective in treating osteoporosis by having a dual effect on building bone [43, 206]. The mode of action can simultaneously stimulate bone formation while also inhibiting bone resorption. Romosozumab has shown promise but also has side effects such as the increased risk of cardiovascular events [207]. Taken together, there is an urgent need to develop better anabolic therapeutics that can be used for long term care.

Mef2c is a transcription factor (TF) with several roles in different tissues such as muscle [208, 209], neurons [210], immune [211], endothelial [212, 213], cartilage [139] and bone [135, 142]. In the context of bone, Mef2c has garnered much interest due to the associations with BMD, bone metabolism, and in establishing the osteogenic cell fate [140-142]. Such lines of evidence include epigenomic studies highlighting Mef2c genomic binding trends found near genes related to BMD and inflammation [214]. Another study found that single nucleotide polymorphisms (SNPs) at the *Mef2c* locus were associated with increased risk of osteoporosis and fragility fractures [215]. Additionally, bone specific conditional deletion of Mef2c resulted in mutant mice exhibiting high bone mass (HBM) compared to their Cre negative littermates [135, 136]. During bone development, mice with a chondrocyte specific *Mef2c* deletion (*Col2-Cre*) reach birth but exhibited poorly ossified axial and appendicular bone at postnatal day 1 [139]. The accruing evidence suggests a more complex

role in bone than previously understood and yet, only a small number of Mef2c target genes have been characterized. These targets include *Sost* in osteocytes [136], *Mmp13* and *Runx2* in osteoblasts [138, 216], and *Col10a1* in chondrocytes [139]. Our prior studies have suggested that Mef2c may target additional genes in osteoblasts/osteocytes [217]. An in-depth characterization of Mef2c-regulated transcriptome in osteogenic lineage could reveal additional, and potentially novel, mechanisms that can be therapeutically targeted to treat metabolic bone disorders such as osteoporosis.

To identify potential Mef2c target genes in bone, we utilized *Bglap Cre* and *Dmp1 Cre* to delete *Mef2c* in osteoblasts and osteocytes, respectively. These mutant mice were used to isolate and transcriptionally profile *Mef2c*-deficient bone cell populations using single-cell RNAseq (scRNAseq). Differentially expressed genes (DEGs) in *Mef2c$^{fl/fl}$; Bglap-Cre* and *Mef2c$^{fl/fl}$; Dmp1-Cre* compared to *wildtype* cell populations were further analyzed to understand potential functions of *Mef2c* in osteogenic cells. Common DEGs highlighted between *Mef2c$^{fl/fl}$ Bglap-Cre and Mef2c$^{fl/fl}$ Dmp1-Cre* mice suggested that, in addition to regulating bone development and metabolism, *Mef2c* may play a major role in regulating energy metabolic pathways in bone.

Methods

Generation of knockout animals

All animal experimental procedures were completed in accordance with guidelines under the institutional animal care and use committees at Lawrence Livermore National Laboratory under an approved protocol by the IACUC committee and conform to the Guide for the care and use of Laboratory

animals. *Mef2c$^{fl/fl}$; Bglap-Cre* mice (*Bglap Mef2c cKO), Mef2c$^{fl/fl}$; Dmp1-Cre* mice (*Dmp1 Mef2c cKO), and Mef2c$^{fl/fl}$; Col1-Cre* mice were generated by breeding *Mef2c$^{fl/fl}$* with either *Bglap-Cre* (The Jackson Laboratory, BarHarbor, ME; stock number: *019509*), *Dmp1-Cre* (The Jackson Laboratory, BarHarbor, ME; stock number: 023047), *and Col1 Cre* mice [186, 187]. *Sost$^{-/-}$* mice were subsequently bred with *Dmp1 Mef2c cKO* mice to generate *Sost$^{-/-}$*; *Dmp1 Mef2c cKO* mice [218]. Ai9 reporter mice (The Jackson Laboratory, BarHarbor, ME; stock number: 007909) were also bred with *Bglap-Cre* and *Dmp1-Cre* mice for fluorescent labeling of bone cell populations. Genotyping was carried out by PCR.

Single-cell RNA sequencing

Femurs and tibia of 16-week-old male *Bglap Mef2c cKO* and *Dmp1 Mef2c cKO* mutant and *wildtype* mice (N=2/genotype) were were harvested, cleared of soft tissues, depleted of bone marrow, then underwent 2x PBS washes. Bones were next minced into fragments and placed into 8ml of 7.5mg/ml Collagenase (Worthington Biochemical, Lakewood, NJ; CLS-1) digestion solution with 100 µg/mL DNase I (Roche, Basel, Switzerland; 11284932001) in DMEM/F12 for 30 min at 37^{o}C on a shaker at 150 rpm. After 30 min, the resulting digestion solution was transferred into a 50ml conical tube and washed with 1x PBS.This process was repeated for a total of 9 incubations with each respective digestion mix collected in between washes. Next, red blood cells were lysed by adding ACK (ThermoFisher Scientific, Waltham, MA, USA; A1049201) followed by removal of cellular debris using a 100µm nylon cell strainer. Further enrichment of bone cell populations was completed using flow cytometry. Bone cell suspensions were made from using the primary bone cells collected and were incubated in Biolegend antibodies APC/Cyanine7 anti-mouse CD45 Antibody (Biolegend, San Diego, CA; Clone: 30-F11) and anti-mouse APC

Ter119 (Biolegend, San Diego, CA; Clone: TER-119) at a 1:100 dilution in PBS+1%FBS. Dapi was used for viability staining. Viable CD45/Ter119$^{-/-}$ populations were sorted with flow cytometric analysis performed on a BD FACSMelody system.

Isolated CD45/Ter119$^{-/-}$ bone cell populations were sequenced using Chromium Single Cell 3' Reagent Kit and Chromium instrument (10x Genomics, Pleasanton, CA) as previously described [219, 220]. Library preparation was performed according to manufacturer's protocol and sequence on an Illumina NextSeq 500 (Illumina, San Diego, CA, USA).

scRNAseq data analysis

Raw scRNAseq data was processed with 10x Genomics Cell Ranger software (version 6.0.0;10x Genomics, Pleasanton, CA, USA) as was done previously [219]. The resulting output was then exported into the R package Seurat where quality control steps and additional analysis were performed [221]. Data filtering criteria included: cells with less than 500 detected gene per cell, genes that were expressed by fewer than 5 cells, had mitochondrial greater than 15%, or had aberrantly high gene count all of which were removed. Data was normalized using the global-scaling method known as 'LogNormalize' to find highly variable genes at which point the data from the male *Bglap Mef2c cKO* and *Dmp1 Mef2c cKO and WT* experimental data was integrated, scaled, and reduced by principal component analysis (PCA). Cells were grouped into clusters for cell type discovery using Seurat's 'FindNeighbors', and 'FindClusters' commands. Followed by the visualization of the produced clusters using the non-linear dimensional reduction via uniform manifold approximation and projection (UMAP). Cluster marker genes were determined using Seurat's 'FindAllMarkers' command. Next, Seurat's 'FeaturePlot',

'DotPlot', 'VlnPlot', and 'Heatmap' commands were used to graphically plot the cell type specific gene expression measurements amongst the datasets. To determine the differentially expressed genes between conditions, A pseudo-bulk RNAseq approach was used where each cell's gene expression was treated as a sample. Cell clusters were isolated by dataset and their counts extracted. The experimental metadata was generated by matching the cell's barcodes with their respective annotation. The resulting information was input into Deseq2 package for statistical analysis [222]. Enrichr provided the ontology enrichment analysis on the differentially expressed genes [223].

Binding motif analysis

Predicted Mef2c binding sites on differentially expressed genes were determined via query of the respective promoters, defined as 2kb upstream of coding regions, of genes using ensembl's biomaRt package, followed by a transcription factor binding prediction tool Ciiider to determine the frequency of Mef2c binding [224, 225]. Mef2c PWM (MA0947.1) was obtained from the Jaspar online database [226].

μCT scanning

Hindlimbs of 16-week-old Mef2c cKO and $Sost^{-/-}$ mutant mice (n of 5 or more per gentoype) were dissected, and fixed and dehydrated in 70% ethanol prior to scanning on a μCT instrument (SCANCO μCT 35, Brüttisellen, Switzerland) according to the rodent bone structure analysis guidelines (X-ray tube potential = 55kVp, intensity -114 μA, 10 μm isotropic nominal voxel size, integration time = 900ms). Trabecular bone in the distal femoral epiphysis was analyzed by manually drawing contours on 2D transverse slides. The distal femoral epiphysis was designated as the region of trabecular bone enclosed by

the growth plate and subchondral cortical bone plate. Epiphyseal trabecular bone volume fraction was determined by quantifying trabecular bone volume fraction was by quantifying trabecular bone volume per total volume (BV/TV). Trabecular thickness (TB.Th, mm), trabecular number (TB.N, mm), trabecular thickness (Tb.Sp, mm), connective density (Conn.D, 1/mm^3), and structure model index (SMI) were also quantified. Statistical analysis was performed by comparing *dKO, Mef2c cKO, Sost*$^{-/-}$ mutants and *wildtype*.

Histology and Immunohistochemistry

Knee joints were collected from 16-week-old from *Bglap cKO Mef2c* and *Dmp1 Mef2c cKO* mice for histological evaluation as mentioned previously [227]. Whole hindlimbs were fixed in 10% NBF and decalcified using 500 mM EDTA. Samples were embedded in OCT and cryosectioned in the sagittal plane at 10µm. Sections were stained on glass slides using 0.1% Safranin-O (Sigma, St. Louis, MO, USA; S8884) and 0.05% Fast Green (Sigma, St. Louis, MO, USA; F7252) using standard procedures (IHC World, Woodstock, MD, USA), then imaged using a Leica DM5000 microscope.

Sagittal sections of knee joints from *Bglap Mef2c cKO* and *Dmp1 Mef2c cKO* mice were used for IHC. Primary antibodies were incubated at 4^{o}C overnight after antigen retrieval. Secondary antibodies were incubated for 2 hr at room temperature. Negative control slides had only secondary antibody stains. Prolong Gold with DAPI (Molecular Probes, Eugene, OR, USA). Imaging software included ImagePro Plust V7.0 Software, aQIClick CCD camera (QImaging, Surrery, BC, Canada), and ImageV1.53 Software were used to image or edit photos. Primary antibodies used: Mef2c (Abcam, Cambridge, UK; Ab64644), Lum (Abcam, Cambridge, UK; Ab168348), Dmp1 (ThermoFisher,Waltha m, MA. USA ; PA5-47621), Alpl (Abcam, Cambridge,

UK; Ab97384), Col10a1 (Abcam, Cambridge, UK; Ab260040), and Smpd3 (Abcam, Cambridge, UK; Ab85017). Secondary antibodies used: Donkey anti-rabbit 594 (Thermofisher, Waltham, MA, USA; A-21207)

Statistical Analysis

R statistical software and Graphpad Prism were used for statistical analysis. One-way ANOVA and student's t test were used to determine statistically significant differences of mean values. *P*-value of ≤ 0.05 were considered statistically significant.

Results

Combined Mef2c and Sost deficiency in bone causes significantly higher bone mass than in Sost deficiency alone

Bglap and *Dmp1 Mef2c* cKO mutant mice were born at normal mendelian rates and were indistinguishable from their control littermates. MicroCT analyses of femora determined that *Bglap* mediated deletion of *Mef2c* promoted a high bone mass phenotype (HBM) consistent with previously described *Dmp1 Mef2c cKO* mutant mice (Figure 1A-C). BV/TV was significantly increased in both *Bglap Mef2c cKO* mice and *Dmp1 Mef2c cKO* mutant mice. Connectivity density was also significantly increased in both mutants indicating increased interconnectivity of the trabecular network (Figure 1B, C). However, only *Dmp1 Mef2c cKO* mutant mice had significantly increased trabecular number and a decreased trabecular separation (Figure 1C).

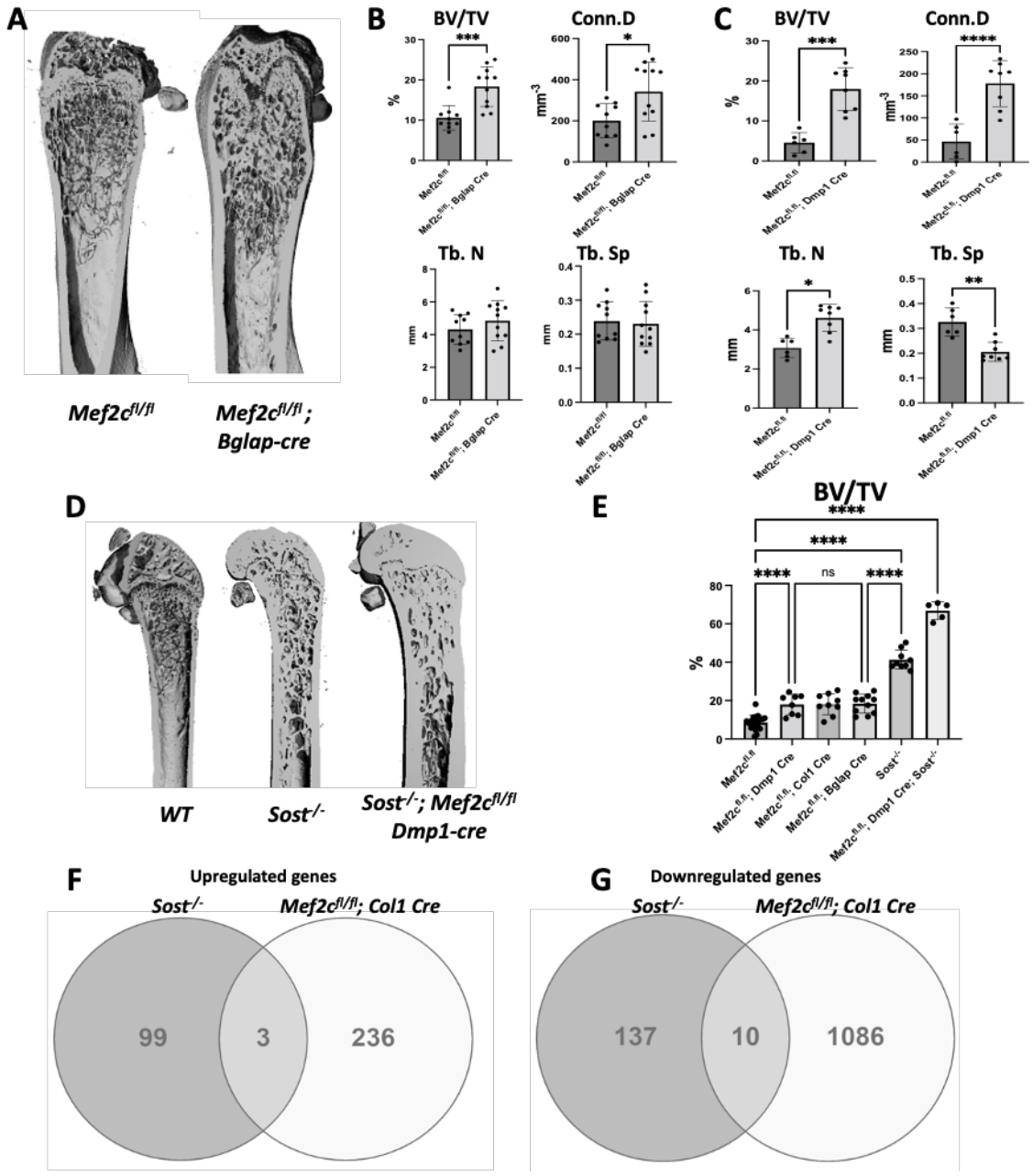

Figure 1. Comparing skeletal phenotypes of Mef2c conditional knockout mice to Sost$^{-/-}$. *MicroCT analysis of femora of Bglap Mef2c cKO, Dmp1 Mef2c cKO, and Sost$^{-/-}$ (A, D) 3D representation of Bglap Mef2c cKO, Dmp1 Mef2c cKO, and Sost$^{-/-}$ highlighting changes in bone mass in femora. Quantification of trabecular bone vouge/total volume (BV/TV) in Bglap Mef2c cKO, Dmp1 Mef2c*

cKO, and Sost$^{-/-}$ (B, C, and E), connective density (Conn.D), trabecular number (Tb.N), trabecular spacing (Tb. S) in Bglap Mef2c cKO and Dmp1 Mef2c cKO mice (B, C). Overlap between up- (F) and down-regulated genes (G) in Sost$^{-/-}$ mice and Mef2c$^{fl/fl}$; Col1 Cre mice compared to their respective controls. p<0.05, both by ANOVA and t test compared to own Cre negative controls.

Furthermore, analysis of *Sost$^{-/-}$; Mef2c$^{fl/fl}$ Dmp1-cre* femora revealed an even greater increase in bone mass than *Sost$^{-/-}$* alone, suggesting that Mef2C may contribute to HBM phenotypes through multiple pathways (Figure 1D, E). To identify gene targets of transcriptional regulation, bulk RNA sequencing (RNAseq) analysis was compared between wildtype, *Sost$^{-/-}$ and Mef2c$^{fl/fl}$; Col1-cre mouse*. Bulk RNA seq analysis revealed transcriptional changes due to the absence of either *Sost* or *Mef2c*. *Sost$^{-/-}$* had 102 genes up- and 147 genes down-regulated while *Mef2c$^{fl/fl}$; Col1-cre* had 239 gene up- and 1096 genes down-regulated. Of the differentially expressed genes, only 3 up- and 10 down-regulated genes were found to overlap between *Sost$^{-/-}$ and Mef2c$^{fl/fl}$; Col1-cre* datasets (Figure 1F, G), in support of additional Mef2c targets contributing to bone mass independent of Sost.

scRNAseq analysis reveals Mef2c expression amongst various bone cell subpopulations

ScRNA-seq analysis of 3334 CD45^{-}/Ter119^{-} bone cells sequenced from *Mef2c$^{fl/fl}$* (1076), *Bglap Mef2c cKO* (704) and *Dmp1 Mef2c cKO* (865) femurs were further analyzed to identify differences among bone cell subpopulations in these genotypes. Ten distinct cell clusters were identified with unique transcriptional profiles (Figure 1B)[221]. Cells in cluster 1 expressed high levels of *Lifr, Postn, and Vdr* and were labeled osteoprogenitors/pre-osteoblasts (OP/pOB) (Figure 1B-D). Cells in cluster 2 expressed high levels of *Col1a1,*

Bglap, and Col1a2 and were labeled osteoblasts (OB) (Figure 1B-D). Clusters 3 included cells expressing high levels of *Adipoq, Lepr* and *Cxcl12* were labeled adipoCAR (aCAR)(Figure 1B-D). The cells found in cluster 4 all expressed *Dmp1, Mepe, and Sost* so were labeled osteocytes (OS) (Figure 1B-D). Cluster 5 contained chondrocytes (CH) as this cluster had cells expressing high levels of *Acan, Col9a1, and Col2a1* (Figure 1C, D). Clusters 6, 7 and 8 were labeled mesenchymal progenitors/fibroblasts (MP) 1-3 respectively. These cluster had similar gene expression pattern *for Col3a1,* a collagen highly expressed in fibroblasts/MSCs (Figure 1D) but also had unique markers (Figure 1C). The cells found in cluster 9 expressed *Omd, Cytl1,* and *Chad* which were identified as osteochondro progenitors (OCP). Cluster 10 contained cells that expressed a mix of osteoblast and osteocyte markers such as *Col1a1, Bglap and Dmp1* and *Phex* and *Pdpn*, genes upregulated during osteoblast to osteocyte transition [157]. However, this cluster had extremely low levels of *Sost* expression. Therefore, this cluster was identified as an intermediate cell type between osteoblasts and osteocytes (OB/OS) (Figure 1C). *Mef2c* expression was found at significant levels in clusters 1 (OP/pOB), 2 (OB), 4 (OS), 5 (CH), 8 (MP-3), 9 (OCP) and 10 (OB/OS) (Figure 1D). Therefore primary Mef2C gene targets were presumed to be harbored in these subpopulations, while transcriptional changes in other clusters were likely due to indirect effects.

Growth plate structure impacted amongst Bglap Mef2c cKO long bones

The proportion of MP2 and MP3 clusters were significantly increased in *Bglap Mef2c cKO* and *Dmp1 Mef2c cKO* mutant mice compared to *wildtype* (Figure 3A). Cluster MP 1 also had a similar increase in the number of sequenced cells compared to those from wildtype but at a lesser level than MP2/3. In contrast, we observed a decrease in the number of chondrocytes and osteocytes sequenced in the mutants relative to wildtype (Figure 3A). The expansion of

clusters MP 2 and 3 in *Bglap Mef2c cKO* and *Dmp1 Mef2c cKO* also correlated with an increased expression of *Lum,* a marker of MP 3 (Figure 3B-C). We also observed that *Bglap Mef2c cKO* has significantly elevated *Lum* expression in MP3 compared to *Dmp1 Mef2c cKO* (Figure 3B). *Lum* has been shown to be expressed in bone and cartilage matrix and may promote bone formation [228]. It has also been shown to play a key role in fibrosis [229-231]. Protein levels of *Lum* was also up regulated in the mutants and was spatially found within the growth plate (Figure 3D). We also observed a wider expression pattern of *Lum* in *Bglap Mef2c cKO mice* compared to the other two conditions *(Figure 3D).*

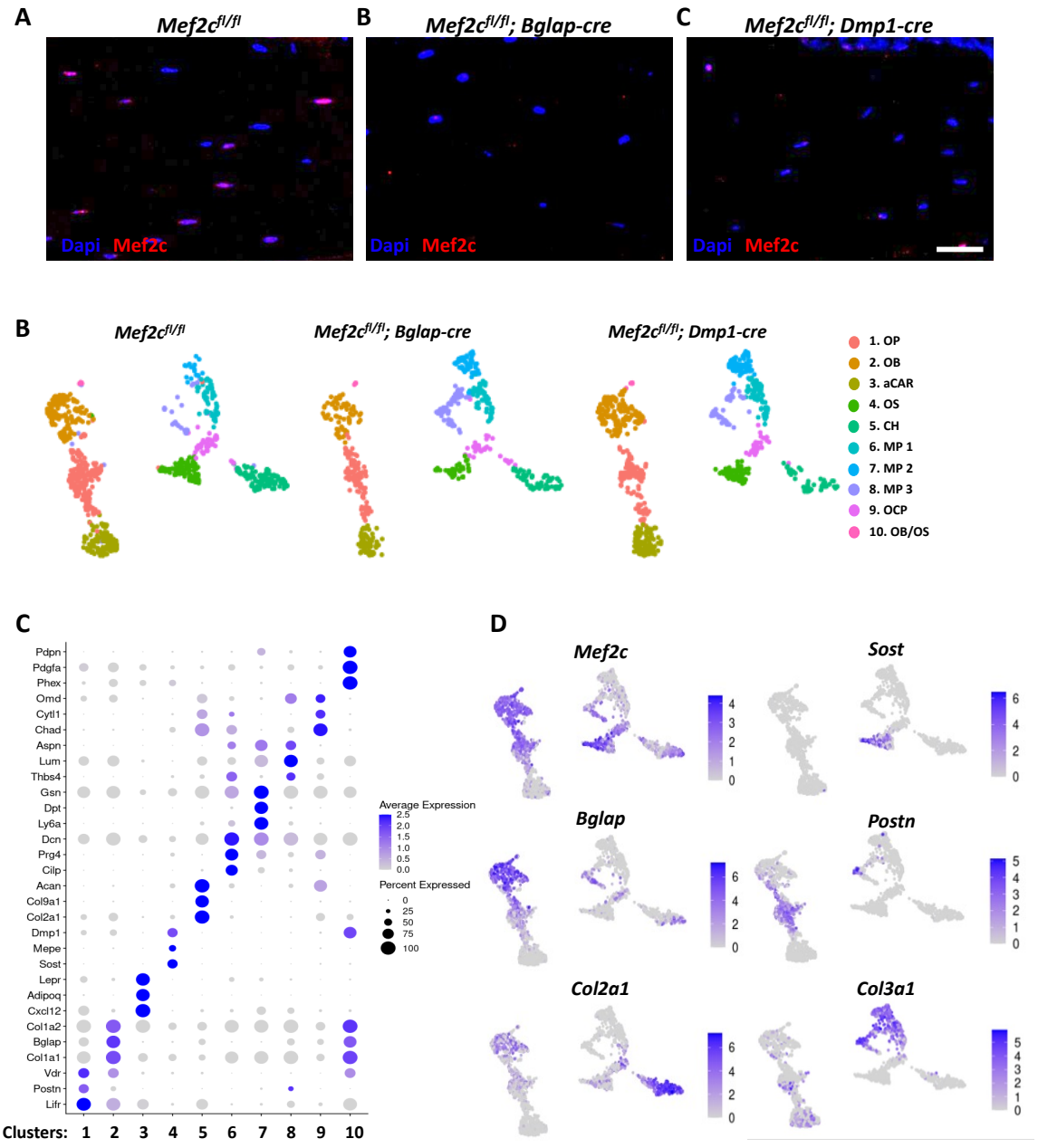

Figure 2. Single cell analysis of Mef2c-deficient bone cells. Mef2c-deficient bone cells were isolated for scRNA-seq from Mef2c$^{fl/fl}$ *(A), Bglap Mef2c cKO (B), and Dmp1 Mef2c cKO (C) (scale bar = 50μm). (D) Cell clusters from 10x Genomics scRNA-seq analysis visualized by Uniform Manifold Approximation and Projection (UMAP) in Mef2c$^{fl/fl}$, Bglap Mef2c cKO, and Dmp1 Mef2c cKO.*

Colors indicated clusters of various cell types. (E) Dot plot showing the expression of selected markers of various cell types. Dot size represent the fraction of cells expressing a specific marker in a particular clusters and intensity of color indicates average expression level in that cluster. (F) Markers of various bone cell subtypes that were used to denote each subtype.

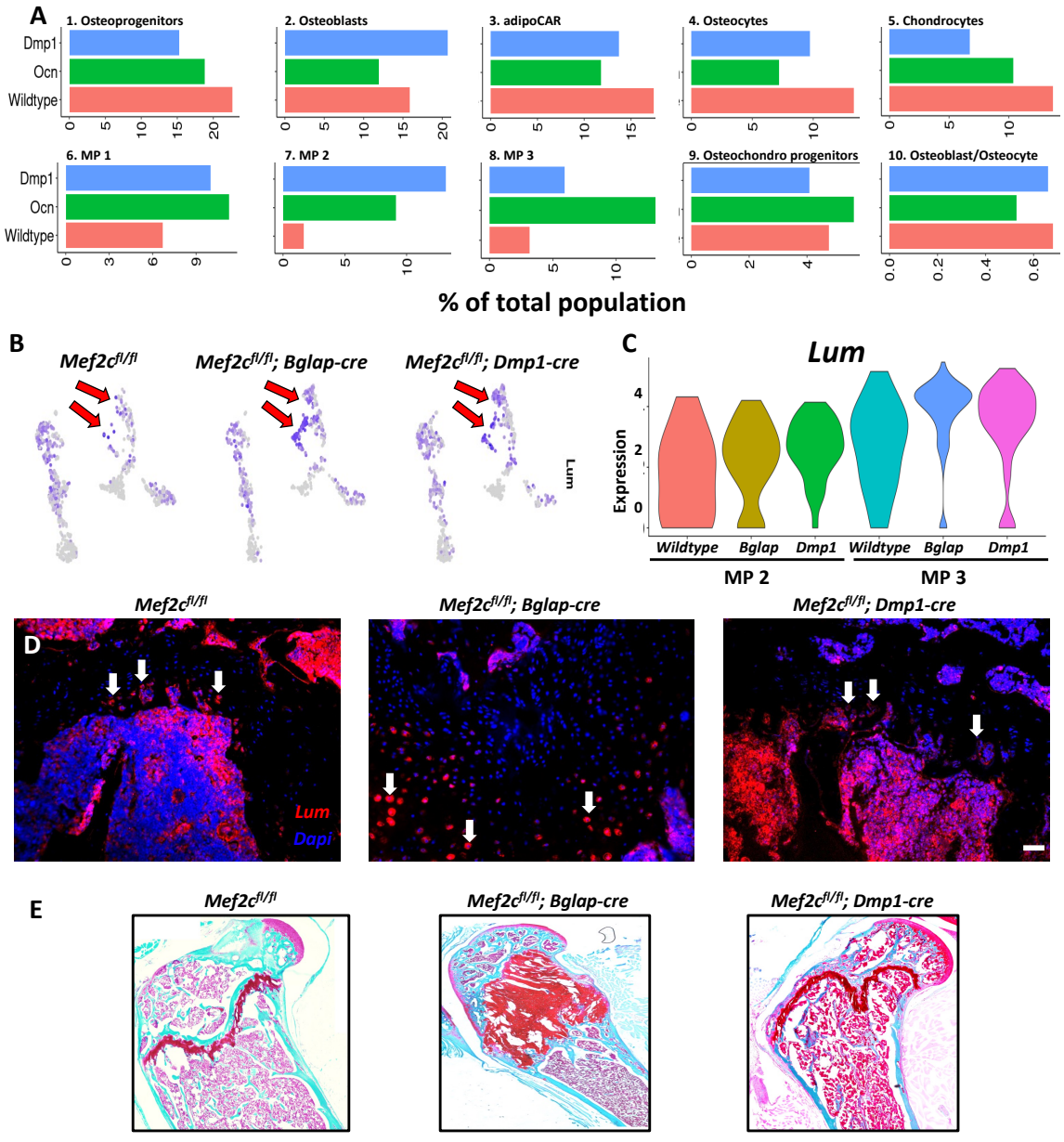

Figure 3. Characterizing Mef2c-deficient mouse phenotype at the single cell level. *(A) Changes in the proportion of various cell types amongst Mef2c$^{fl/fl}$, Bglap Mef2c cKO, and Dmp1 Mef2c cKO. (B) Feature plots showing the expression of Lum amongst Mef2c$^{fl/fl}$, Bglap Mef2c cKO, and Dmp1 Mef2c cKO. Red arrows highlight MP 1 and 2 clusters. (C) Violin plot showing the expression of Lum in MCP 1 and 2 subtypes. (D) IHC showing Lum expression within the growth plate (20x magnification; scale bar = 50µm). White arrows highlight Lumican+ populations. (C) Violin plot showing the expression of Lum in MCP 1 and 2 subtypes (E) Safranin-O histological stained sections of 16-week-old Mef2c$^{fl/fl}$, Bglap Mef2c cKO, and Dmp1 Mef2c cKO femurs.*

Histological evaluation of the femurs, also revealed significant differences between *Bglap Mef2c cKO* and *Dmp1 Mef2c cKO* growth plate morphology, where a significantly expansion was observed in *Bglap-Cre* mutants only (Figure 3D). To further characterize cellular changes associated with this phenotype, we next examined *Dmp1-cre; Ai9* and *Bglap-Cre; Ai9* mice. In *Bglap-Cre; Ai9* mice, we observed robust dTomato expression in the growth plate region which was absent in *Dmp1-cre; Ai9* mice. This suggest that Bglap-mediated targeting of cells in the growth plate region in *Bglap Mef2c cKO* mice may have contributed to expanded growth plate observed in this mutant (Supp. Figure 1). *Dmp1 Mef2c cKO* mutant femora did not exhibit a similar morphological change possibly due to the inactivity of the Dmp1 promoter at the growth plate (Chapter 2. Figure 1). Such growth plate phenotype supports the *Mef2c* function in early osteogenic lineages in inducing the osteogenic differentiation of early progenitor cell populations.

Energy metabolism and bone metabolism genes make up the Mef2c-regulated transcriptome in the osteogenic lineage

To gain a better understanding of the Mef2c-mediated transcriptome, a differential expression analysis was performed between both *Bglap Mef2c cKO* and *Dmp1 Mef2c cKO* mutant cells in comparison to the *wildtype* cells. The analysis identified a total of 96 up- and 2434 down-regulated genes in *Bglap Mef2c cKO mutant bone cells* and 176 up- and 1041 down-regulated genes in *Dmp1 Mef2c cKO* mutant bone cells (Figure 4A). Figure 4B and C show genes differentially expressed in individual bone cell subpopulations derived from *Bglap Mef2c cKO* and *Dmp1 Mef2c cKO* mice, respectively (Figure 4B, C). Amongst the bone cell subpopulations, OBs and CHs had the most significant number of differentially expressed genes. CHs having 1701 genes affected (21 up- and 1680 down-regulated) in *Bglap cKO* mutant cells and 411 genes affected (37 up- and 374-downregulated) in *Dmp1 cKO* mutant cells (Figure 4B, C). OBs had 1479 genes affected (15 up- and 1479 down-regulated) in *Bglap Mef2c cKO* mutant cells and 604 genes affected (16 up- and 588-downregulated) in *Dmp1 Mef2c cKO* mutant cells. (Figure 4B, C). Interestingly, *Bglap Mef2c cKO* cells had a much higher number of differentially expressed genes compared to *Dmp1 Mef2c cKO* amongst the bone cell subpopulations. We next examined differentially expressed genes amongst subpopulations that may play a direct role in bone metabolism, OP/pOBss, OCPs, OBs and OS [7, 9, 63, 70, 77]. OB/OS cluster was not included in this analysis as this cluster represented less than 1% (3-5 cells total) of the cells sequenced in the mutants. When looking at the overlap of differentially expressed genes amongst these subpopulations in each mutant we found that *Dmp1 Mef2c cKO* only had 4 up-regulated genes in common amongst the osteogenic clusters (Figure 4 D, E). Amongst the down-regulated genes, *Bglap Mef2c cKO* had 19 genes in common whereas *Dmp1 Mef2c cKO* had 3 common

genes amongst the osteogenic populations (Figure 4 F, G). OBs and OPs had the highest number of shared downregulated genes; 118 genes in Bglap *Mef2c* cKO and 40 genes in *Dmp1 Mef2c cKO*. OBs and OS shared 87 and 15 downregulated genes in *Bglap Mef2c cKO* and *Dmp1 Mef2c cKO,* respectively. A significant majority of differentially expressed genes amongst OPs, OCPs, OBs and OSs were unique suggesting Mef2c functions in a cell type specific manner.

Table 1. Downregulated bone metabolism genes in Bglap Mef2c cKO.

Genes:	*Actb, Camp, Cfl1, Chchd2, Dap, Ftl1, Id3, Itm2b, Ldha, mt-Atp6, mt-Cytb, Ppia, Rpl2, Rpl29, Rps2, S100a8, S100a9, Spp1, Ubb*

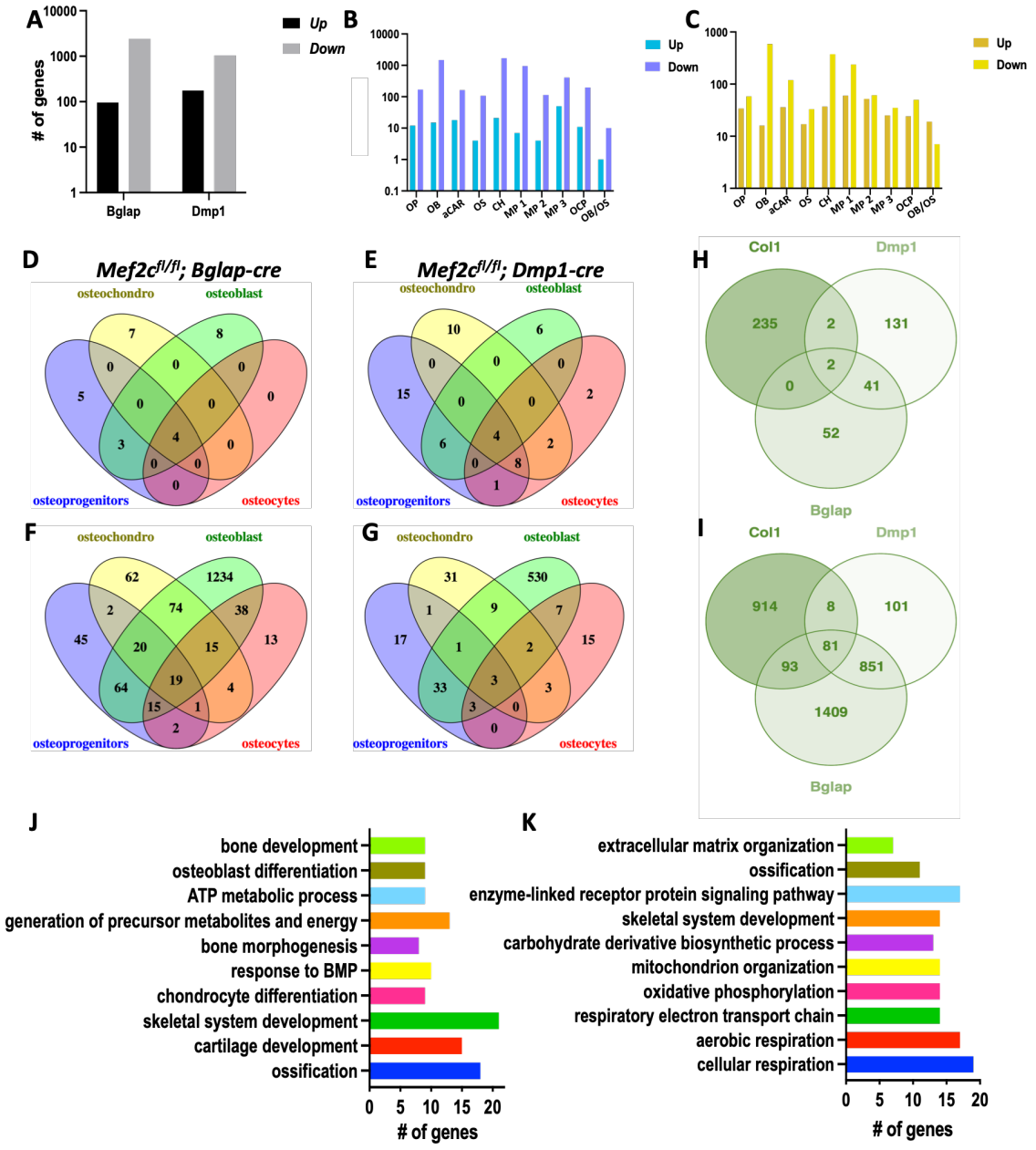

Figure 4. Differential gene expression analysis of Mef2c-deficient bone cells. *(A) Total number of genes up- and down-regulated amongst Bglap Mef2c cKO and Dmp1 Mef2c cKO mutants. Number of genes up- and down-regulated amongst bone cell subpopulations in amongst Bglap Mef2c cKO (B) and Dmp1 Mef2c cKO mutants (C). Overlap of genes up-regulated by OPs, OBs, OSs, and*

OCPs amongst Bglap Mef2c cKO (D) and Dmp1 Mef2c cKO mutants (E). Overlap of genes down-regulated by OPs, OBs, OSs, and OCPs amongst Bglap Mef2c cKO (F) and Dmp1 Mef2c cKO mutants (G). Overlap of genes up- (H) and down-regulated (I) amongst Col1 Mef2c cKO, Bglap Mef2c cKO and Dmp1 Mef2c cKO. Enriched ontology terms associated with overlapping genes amongst Col1 Mef2c cKO, Bglap Mef2c cKO and Dmp1 Mef2c cKO (J) and Bglap Mef2c cKO and Dmp1 Mef2c cKO (K).

A HBM phenotype is commonly observed trait when *Mef2c* is conditionally deleted in bone tissues [135, 136, 142]. To explore the possible underlying molecular mechanisms that underpin the HBM, we compared *Bglap Mef2c cKO* and *Dmp1 Mef2c cKO* transcriptome datasets with a bulk RNAseq dataset generated from *Mef2c$^{fl/fl}$; Col1 Cre (Col1 Mef2c cKO)* murine long bones. Up-regulated genes in common between the 3 transcriptomes highlighted only 2 genes whereas 81 down-regulated genes were found in common (Figure 4 H, I). Given the small overlap amongst the up-regulated genes we focused primarily on down-regulated gene that overlapped between *Bgla Mef2c cKO*, *Dmp1 Mef2c cKO* and *Col1 Mef2c cKO*. A gene ontology analysis identified 'ossification', 'cartilage development', 'skeletal system development', 'response to BMP', 'bone morphogenesis', 'generation of precursor metabolites and energy', 'ATP metabolic process', 'osteoblast differentiation', and 'bone development' as some of the most significantly enriched biological processes associated with overlapping down-regulated genes (Figure 4J). A comparison between DEGs downregulated only in *Col1 Mef2c cKO* and *Bglap Mef2c cKO* conditions yielded 93 common genes (Figure 4I) and were associated with biological process 'cellular respiration', aerobic respiration', 'respiratory electron transport chain', 'oxidative phosphorylation', 'mitochondrion organization', 'carbohydrate derivative biosynthetic process', 'skeletal system', enzyme-linked receptor protein signaling pathway',

'ossification', and extracellular matrix organization'. Eight genes downregulated in *Col1 Mef2c* cKO including: *Bmp7, Dst, Fbn2, Fermt2, Pdha1, Rgs7bp, Slc41a1, Synm* overlapped with *Dmp1 Mef2c* cKO but not with *Bglap Mef2c* cKO. We also identified 851 downregulated genes shared only between *Bglap Mef2c cKO* and *Dmp1 Mef2c cKO* with many of them playing a role in bone and energy metabolic pathways. The highlighted gene set from the absence of *Mef2c* across bone cell subpopulations suggests that *Mef2c* regulates a large number of genes associated with bone metabolism and energy metabolism.

Bone and energy metabolism-associated genes harbor Mef2c binding motifs

In order to find putative direct gene targets of Mef2c, the promoter regions of the total DEGs identified amongst *Bglap Mef2c cKO* and *Dmp1 Mef2c cKO* (Figure 4A, Supp. Table 1) were analyzed using the binding motif analysis tool Ciiider and putative Mef2c binding sites were determined [225]. This analysis identified 81 and 149 upregulated and 2099 and 891 downregulated genes in *Bglap Mef2c cKO* and *Dmp1 Mef2c cKO* respectively as putative Mef2c targets. Amongst DEGs harboring Mef2c binding motifs in promoters, 1 up- and 66 down-regulated genes were common to *Bglap Mef2c cKO, Dmp1 Mef2c cKO, and Col1 Mef2c cKO* (Figure 5 A, B) suggesting that Mef2C may normally function to activate gene expression. A significant number of genes harboring Mef2c motifs were associated with energy metabolism and were key enzymes found in either glycolysis, TCA cycle, or oxidative phosphorylation pathways (Figure 5C). Additionally, OBs had the highest expression and most significant down regulation of the energy metabolism genes identified in the study including several mediators of oxidative phosphorylation such as *Uqcrb, Ndufv2, Ndufs3, Ndufa13, Ndufb9, Ndufb5, Cox6a1, Cox5a, Atp5o, Atp5g2, Atp5b, Atp5j* (Figure 5C). OS are a terminally differentiated osteogenic cell

type and are believed to derive their energy through oxidative phosphorylation [232]. Interestingly, we found enrichment for transcripts of glycolytic enzymes in the OS clusters. *Ldha, Pkm, Tpi*, and *Aldoa* expression was enriched in OS compared to OB and was subsequently down-regulated in the absence of Mef2c (Figure 5C, D). *Oxct1* is a key catabolic enzyme that is involved in the generation of acetyl-CoA from ketone bodies and was down regulated in OPs, OBs, Oss, and in OCPs in *Bglap Mef2c cKO* and *Dmp1 Mef2c cKO* mutant cells (Figure 5F). Collectively, our analysis suggest that *Mef2c* plays a major role in regulating energy metabolism in osteogenic cells.

Mef2c regulates multiple bone metabolism genes

Several genes previously identified as key regulators of bone metabolism including 158 genes had putative Mef2c binding motifs in their promoter region (Table 3). Among these genes, 14 genes including *Col10a1, Col11a1, Ibsp, Ifitm5, Smpd3, and Wwtr1* were downregulated in *Col1 Mef2c cKO, Bglap Mef2c cKO* and *Dmp1 Mef2c cKO*. Eleven downregulated bone metabolism genes including *Nog, Tob1, Mepe, Thbs3, and Sost* were specific to *Col1 Mef2c cKO* and *Bglap Mef2c cKO* while 89 downregulated genes were specific to *Bglap Mef2c cKO and Dmp1 Mef2c cKO* (Table 2). IHC analysis revealed that protein expression corresponded with the single cell transcriptional data. *Col10a1* has been previously described as a Mef2c target gene and was similarly found to harbor Mef2c binding motifs in the present study (Figure 6A) [139]. Additionally, Col10a1 protein expression was diminished at the growth plate in both *Bglap Mef2c cKO* and *Dmp1 Mef2c cKO in a similar trend revealed transcriptionally (Figure 6B, C, c). Ibsp* was another downregulated bone metabolism gene predicted to harbor Mef2c binding motifs within the promoter region (Figure 6D*).* Interestingly, Ibsp protein expression was also diminished but only in *Bglap Mef2c cKO at the*

growth plate and in cortical bone reflecting the same transcriptional changes amongst OCP, OB2, and CHs (Figure 6D,d,E,e).

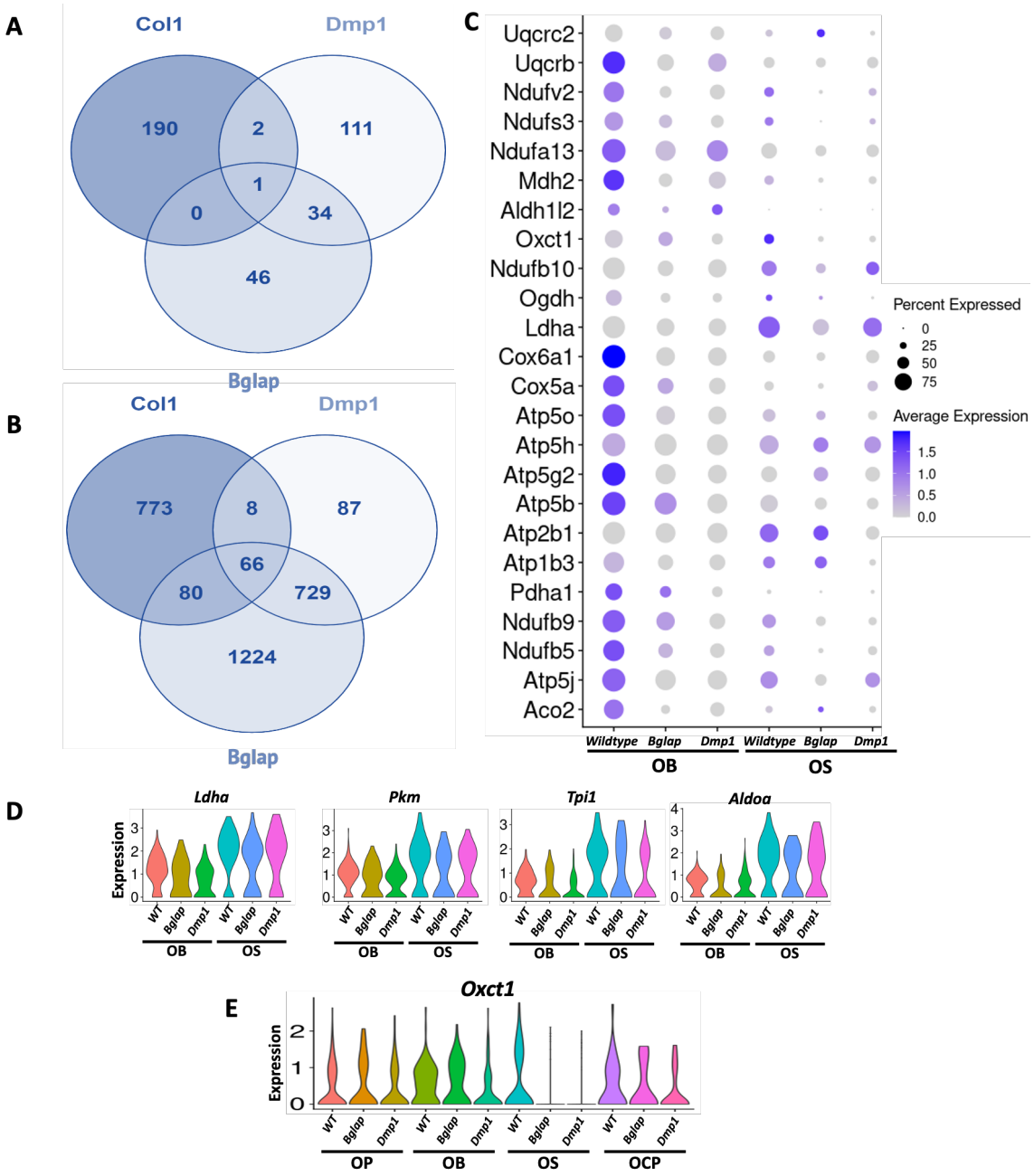

Figure 5. Characterization of putative Mef2c target genes in OBs and OSs. *Overlap of genes up- (A) and down-regulated (B) amongst Col1 Mef2c cKO, Bglap Mef2c cKO and Dmp1 Mef2c cKO found harboring mef2c binding motifs. (C) Dot plot showing down-regulation of glycolytic and oxidative phosphorylation genes amongst OBs and OSs. (D) Violin plots showing expression of Ldha, Pkm, Tpi, and Aldoa in OS subtypes. Violin plots showing expression of Oxct1 (E) amongst OP, OB, OS, and OCP subpopulations.*

Table 2. Energy metabolism genes harboring Mef2c binding motifs. 'X' indicating gene was differentially expressed in the absence of Mef2c.

Gene	*Mef2c$^{fl/fl}$; Col1-cre*	Mef2c$^{fl/fl}$; *Bglap-Cre*	*Mef2c$^{fl/fl}$; Dmp1-Cre*
Aco2	X	X	X
Atp5j	X	X	X
Cox4i2	X	X	X
Ndufb5	X	X	X
Ndufb9	X	X	X
Tpi1	X	X	X
Aldh1l2	X	X	
Idh3a	X	X	
Mdh2	X	X	
Ndufa12	X	X	
Ndufa13	X	X	
Ndufa5	X	X	
Ndufb4	X	X	
Ndufc1	X	X	
Ndufs3	X	X	
Ndufv2	X	X	
Uqcrb	X	X	
Uqcrc2	X	X	
Pdha1		X	X
Atp1b3		X	X
Atp2b1		X	X

Atp5b	X	X
Atp5c1	X	X
Atp5g2	X	X
Atp5h	X	X
Atp5o	X	X
Cox5a	X	X
Cox6a1	X	X
Enpp1	X	X
Ldha	X	X
Ndufa8	X	X
Ndufb10	X	X
Nt5e	X	X
Ogdh	X	X
Oxct1	X	X
P4ha2	X	X
Pfkp	X	X
Pgam1	X	X
Steap4	X	X
Suclg1	X	X
Tkt	X	X
Vcp	X	X

Discussion

While significant prior work has highlighted the direct relationship between Mef2C and Sclerostin, here we show evidence in support of Mef2c having a larger role in regulates bone metabolism through both Sost-dependent and independent mechanisms. μCT analysis of *Bglap Mef2c cKO* and *Dmp1 Mef2c cKO* mutant long bones exhibited a HBM phenotype that is characteristic of bone-specific Mef2c deletion [135, 136]. Interestingly, a dKO (*Sost*$^{-/-}$*; Mef2c*$^{fl/fl}$ *Dmp1-cre)* had an even greater HBM phenotype that was significantly greater than individual *Sost*$^{-/-}$ or *Mef2c cKO* mutant mice. A finding that was

supported by a comparison between *Sost*$^{-/-}$ and *Mef2c*$^{fl/fl}$ *Col1-cre* mutant bone where bulk transcriptomic data highlighted minimal overlap between differently expressed genes.

Table 3. Bone metabolism genes harboring Mef2c binding motifs. 'X' indicating gene was differentially expressed in the absence of Mef2c.

Gene	*Mef2c*$^{fl/fl}$*; Col1-cre*	*Mef2c*$^{fl/fl}$*; Bglap-Cre*	*Mef2c*$^{fl/fl}$*; Dmp1-Cre*
Ifitm5	X	X	X
Col10a1	X	X	X
Wwtr1	X	X	X
Col11a1	X	X	X
Smpd3	X	X	X
Ibsp	X	X	X
Nog	X	X	
Tob1	X	X	
Mepe	X	X	
Thbs3	X	X	
Sost	X	X	
Bmp7	X		X
Sbno2		X	X
Id4		X	X
Dmp1		X	X
Runx2		X	X
Cbfb		X	X
Vdr		X	X
Ank		X	X
Ccn2		X	X
Hspg2		X	X
Csf1		X	X
Xylt1		X	X
Nipbl		X	X
Creb3l1		X	X

Spp1	X	X
Mmp9	X	X
Fndc3b	X	X
Fgfr3	X	X
Fgfr1	X	X
Sfrp4	X	X
Mmp13	X	X
Bgn	X	X
Sox9	X	X
Col1a2	X	X
Mia3	X	X
Ptch1	X	X
Alpl	X	X
Pth1r	X	X
Bmp6	X	X
Egr2	X	X
Enpp1	X	X
Slc26a2	X	X
Satb2	X	X
Dlx5	X	X

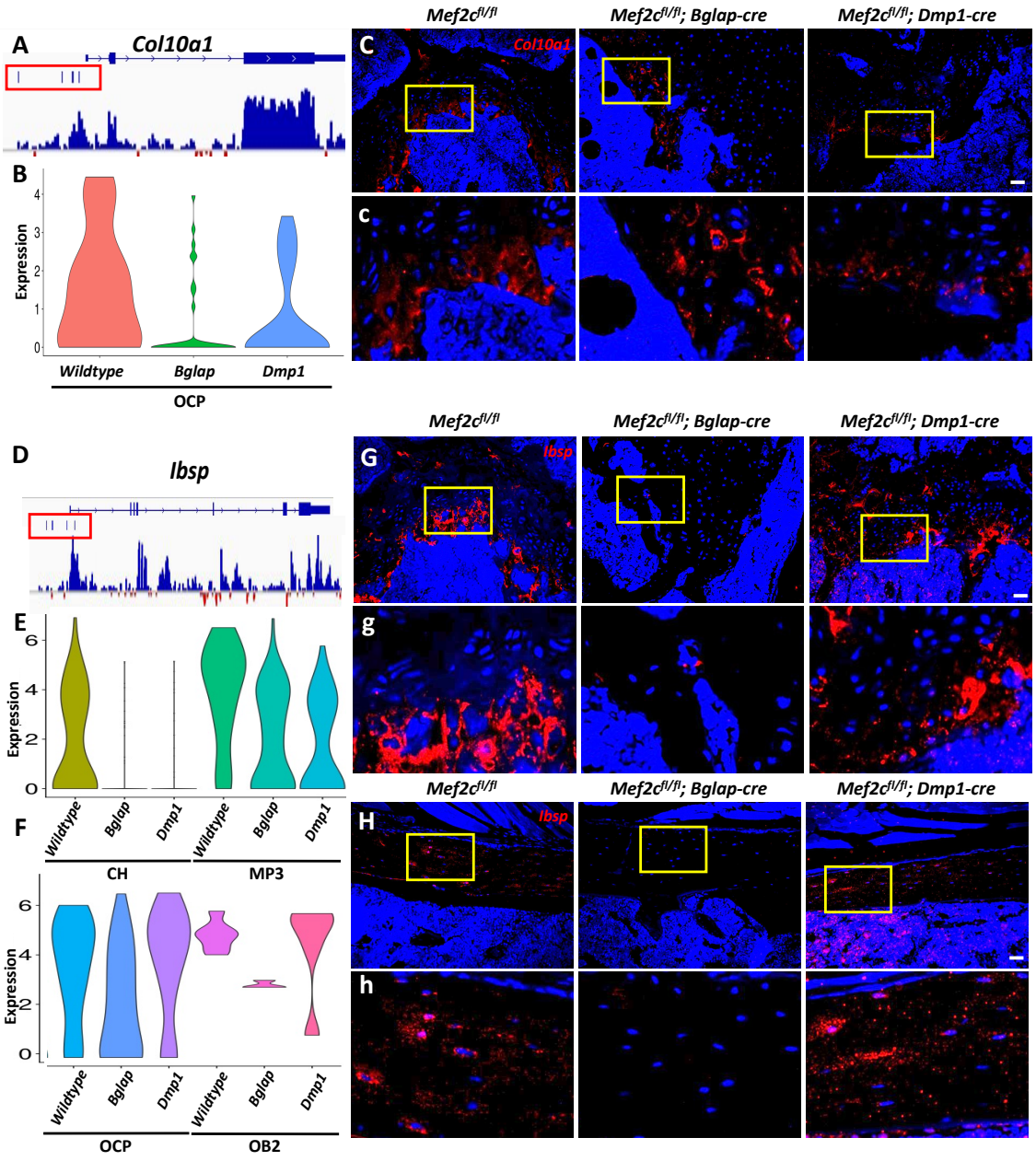

Figure 6. Diminished expression of putative direct targets in the absence of Mef2c. *Mef2c binding motifs predicted within the promoter regions of Col10a1 (A) and Ibsp (D). Average transcriptional expression of Col10a1 in chondrocytes and osteochondro progenitors (B). Average transcriptional expression of Ibsp in chondrocytes, osteochondro progenitors, osteoblast (E) and mesenchymal progenitors 1-3 (F). Protein level expression of Col10a1 (C,*

c) and Ibsp at the the growth plate (G, g) and cortical bone (H, h) (20x magnification; scale bar =50μm).

Single cell level analysis of primary bone cells from *Bglap Mef2c cKO* and *Dmp1 Mef2c cKO* mutant mice unveiled a greater network of genes associated with the Mef2c-regulated transcriptome. All major bone cell subpopulations including MPs, OPs, OBs, OSs, and OCPs were affected by the absence of *Mef2c*. In fact, there was a marked increase of MP subpopulations exhibited by the *Mef2c*-deficient mice. While not as dramatic, cell clusters associated with the MSC lineages had corresponding decreases. Indicating potential lineage-wide shifts that may have been caused by the absence of *Mef2c.* Future work could unveil how *Mef2c* potentiates the osteogenic program amongst mesenchymal populations and whether *Lum* expression mediates key cellular behaviors found at the growth plate.

In all, the absence of *Mef2c* led to a significant number of DEGs across the osteogenic-type cell populations. Each bone cell subcluster identified in the present study experienced perturbed transcriptomic profiles. Both OBs and CHs were impacted most significantly when *Mef2c* was deleted. Interestingly, affected genes amongst OPs, OBs, OSs, and OCPs populations had minimal overlap supporting the notion that Mef2c can mediate unique cell-type specific transcriptomes amongst the osteogenic lineages. This study unveiled several indirect and direct target genes mediate the characteristic HBM phenotype of *Mef2c cKO* mutant mice [16, 22]. Additionally, gene ontology of affected genes was associated with bone and energy metabolism.

According to the scRNAseq data collected from *Bglap Mef2c cKO*, *Dmp1 Mef2c cKO, and Col1 Mef2c cKO* mutants point to a larger *Mef2c* gene target network in bone. A subset of putative gene targets harbored *Mef2c* motifs including

bone and energy metabolism genes suggesting *Mef2c* mediates the generation of cellular energy to meet the demands associated with building and maintaining bone. Energy metabolism plays a central role on maintaining bone homeostasis. Early osteoprogenitors primarily derive ATP through glycolysis and is understood to mediate the 'stemness' of mesenchymal progenitors under proliferative conditions with relatively low oxidative phosphorylation energy production [97, 98, 233, 234]. In OBs and OSs, oxidative phosphorylation is the predominant method of generating ATP [235, 236]. The data suggest *Mef2c* supports bone homeostasis by programing the energetic metabolism in OBs and OSs while also programming their respective precursor populations. Follow up studies are needed to understand changes in cellular behaviors occurring within the growth plate of *Bglap Mef2c cKO* mutant mice. Previous studies have shown high expression Mef2c levels associated in response to osteogenic induction of mesenchymal progenitors [11, 23, 24]. Determining whether similar mechansims play a role in determining cell fate in other progenitors could reveal a similar underlying mechanism associated with the general function of Mef2c as shown in tissue types such as cardiovascular studies.

A few direct Mef2c target genes have been shown to be involved in bone metabolism such as functioning in endochondral ossification. *Col10a1* is a classical hypertrophic chondrocyte marker found at the growth plate [237-239] . We found that *Col10a1* is downregulated in mice lacking *Mef2c*. The mechanism in which Col10a1 functions during endochondral ossification is not well understood. Several proposed mechanisms include facilitating cartilage matrix removal to permit mineralization [240-242], directly organize the calcification of the cartilage matrix [243], or by acting as a boundary to protect regions from mineralization such as the growth plate [244]. *Col10a1 KO* mice phenocopied the skeletal dyspalsisa disorder known as Schmid metaphyseal

chondrodysplasia [245-247] characterize by a short stature and an irregular growth plate [248, 249]. We also identified *Ibsp* as a potential direct Mef2c target which was significantly downregulated in response to Mef2c deletion. *Ibsp* is a non-collagenous protein that also exhibited evidence of direct Mef2c binding. Additionally, *Ibsp* is part of the SIBLING family of proteins that have been shown to regulate ECM properties, cell-matrix interactions, and responses to environmental stimuli [250]. *Ibsp* was found to initiate hydroxyapatite crystal formation *in vitro* suggesting a function in initiating mineralization [251]. In fact, additional studies demonstrated that Ibsp protein structure was capable of concentrating calcium ions that initiated ossification. Interestingly, *Ibsp* KO mice displayed a growth plate phenotype with an increased hypertrophic zone and an increased trabecular bone region [252, 253].

The highlighted Mef2c-mediated transcriptome is highly complex and remains to be mechanisitically understood how the HBM phenotype results from osteogenic populations exhibiting perturbed energy and bone metabolism. Insights could be provided by examining how diabetes mellitus affects bone overtime. Diabetes is a metabolic disorder associated with mitochondrial dysfunction [254, 255]. Such dysfunction, in part, is due to decreased mitochondrial content and biogenesis leading to perturbed cellular energy production [256]. Interestingly, the bones of diabetic patients have increased bone mineral density as shown by high resolution peripheral quantitative computer tomography [257] and yet these changes to bone negatively impact bone strength. In fact, having diabetes increases the incidence of having a fracture [258] since the underlying microarchitecture of bone undergoes deterioration over time.

Recently, the use of bone mass as a predictor of bone strength has been updated to include additional criterion. The relative composition, organization, and maturation of the bone microstructures are additional characteristics that are now considered when accessing fracture risk [105]. *Mef2c* deletion appears to impact bone properties that lead to increases in bone mass but is not clear of whether bone strength has correspondingly increased as well. Future functional studies will reveal the impact on mechanical strength and whether the relative composition, organization, or the maturation of the bone microstructures could be negatively altered in *Mef2c cKO* mutant mice.

In summary, the present study identified Mef2c gene regulatary function amongst various osteogenic cell populations, in part, to support bone formation and homeostasis throughout adulthood.

Chapter 4. Characterizing the *Mef2c*-mediated transcriptome amongst osteoclast populations

Cesar Morfin[1,2], Aimy Sebastian [2], Deepa K Murugesh[2], Nicholas R Hum[2], Gabriela G Loots[1,2]

[1]Molecular Cell Biology Unit, School of Natural Sciences, University of California, Merced. CA USA
[2]Physical and Life Sciences Directorate, Lawrence Livermore, National Laboratories, Livermore, CA, USA

Abstract

Mef2c is a transcription factor that is emerging as a key regulator of bone. Various lines of evidence have been reported indicating the importance of *Mef2c* amongst osteogenic populations. Bone researchers have shown *Mef2c* function regulating mechanisms that mediate bone formation as part of maintaining tissue homeostasis. Recently, *Mef2c* has been shown to also function in osteoclasts (OCLs) populations another key bone cell type involved in bone remodeling. *Mef2c* function was found to be involved in mediating bone erosion when deleted in the murine model of inflammatory arthritis. While *c-Fos* identified as a direct gene target, the Mef2c-mediated transcriptome remains to be fully characterized amongst OCL populations. To gain a better understanding of Mef2c function in regulating the cellular behaviors associated with supporting bone resorption, we isolated Mef2c-defecient CD11b^{+} OCL progenitors from *Mef2c$^{fl/fl}$; Ctsk-Cre* (*Mef2c cKO*) and characterized their ability to differentiate into mature OCLs. While we could determine that the absence of *Mef2c* negatively impacted osteoclastgenesis, these changes could not be observed transcriptionally. Interestingly, scRNAseq of primary bone cell populations revealed *Ctsk* expression amongst captured osteogenic populations suggesting that the observed HBM phenotype could be mediated by previously documented *Mef2c* function. Examination of publicly available single cell transcriptomic data was referenced to shed light on how

to sufficiently target *Mef2c* amongst OCL populations. The approach highlighted the OCL marker *Cx3cr1* to appropriately target *Mef2c* amongst OCL populations. In summary, the present data supports Mef2c function in OCL populations in which the incorporation of *Cx3cr-Cre* mice should aid in further characterizing how this key regulator of bone mediates the cellular behaviors associated with bone resorption.

Introduction

Osteoporosis is a bone disease that develops amongst aging individuals that is primarily characterized by a significant loss of bone. As bone loss continues there is an accompanying increased risk of experiencing a fragility fracture. Around 200 million people are affected by osteoporosis that is primarily found amongst postmenopausal women and elderly men [16]. U.S. Census Bureau projections highlight an increasing average age of the population showing the greatest percentage increases in the 65 and older age group [259]. Overtime, the thinning of trabecular bone and increasing cortical porosity leads to the development of the osteoporotic skeleton [28]. Typically, bone strength and homeostasis are maintained by the constant renewal of skeletal tissues that ensures minimal accumulation of old and damaged bone [260]. The incidence of osteoporosis is an increasing trend observed amongst various racial and ethnic group and across other western countries [23]. An effect of severe osteoporosis relates to the compounding incidence of chronic disease, such as cardiovascular disease and obesity, as these individuals are required to adopt a sedentary lifestyle to avoid the risks of experiencing a fragility fracture [261]. The situation points to a growing need to address the significant public health threat associated with the advancing age of society and the need to develop improved bone therapeutics by understanding the complex behaviors of bone cell populations such as osteoclasts (OCL).

Bone remodeling (BR) is the key physiological process that maintains homeostasis throughout adulthood. A major function of BR is the constant replacement of the underlying mineralized tissues to prevent the accumulation of old and brittle bone and is mediated by key bone cell populations. OCLs are a HSC-derived bone cell type that are recruited towards various sites to remove old and damaged bone via the secretion of digestive acids and enzymes such as matrix metalloproteinases and cathepsin K [93]. The bone resorptive function of OCLs results in the formation of cavities called Howship's lacunae that are subsequently filled upon the arrival of bone-forming osteoblasts (OB). In aging individuals, the coordinated activity of OCLs and OBs begins to shift towards a net decrease in bone formation that is largely been attributed to the decreasing size of MSC populations that serve as a cellular source of OBs needed to maintain adequate levels of bone formation [71, 73, 78]. In fact, various therapeutics have been developed to treat osteoporosis that function by targeting the OB cell lineages such as PTH-based agents Teriparatide and Abaloparatide and Sclerostin based agents Romosozumab [33-36]. Additional therapeutics have been designed to target OCL populations as well and are called anti-resorptive. Anti-resorptive treatments consist of bisphosphonates (such as: Alendronate, Risedronate, and Ibandronate) and are designed to reduce OCL survival and activity [44, 45]. While these treatments have proven to be effective, they are not without their limitations. For example, the waning effectiveness of Teriparatide, Abaloparatide and Romosozumab is well documented whereas antiresorptive based treatments carry with it the rare side effect of osteonecrosis of the jaw and atypical femoral fractures [46, 47, 262]. Such limitations suggest that a deeper understanding of bone remodeling is required to understand how to develop better osteoporotic therapeutics that can potentially target both OB and OCL populations.

Transcription factors (TF), and their target gene regulatory networks, are key regulators that are responsible for the spatial-temporal coordination of key cellular behaviors associated with physiological processes such as BR. Various lines of evidence suggests *Mef2c* being a key TF in both OB and OCL populations. Genome-wide association studies (GWASs) identified single polymorphisms (SNPs) surrounding the *Mef2c* locus was associated with adult osteoporosis and related fragility fractures [215]. Additionally, a genome-wide map of Mef2c binding points to a function in bone as genes highlighted were associated with 'RANK Signaling in Osteoclasts' and other inflammatory related pathways [214]. A few murine knock out studies demonstrated the importance of *Mef2c* function in bone. During bone development, *Mef2c* deletion in chondrocytes led to delayed ossification in mutant mice [139]. Whereas OB- (*Col1)* and OS- (*Dmp1*) deletion led to mutant mice displaying a high bone mass (HBM) phenotype [135, 136]. Interestingly, the Kramer group also reported that OCL activity was negatively impacted by the *Dmp1*-mediated deletion of *Mef2*c [136]. Mef2c function amongst OCL populations was later confirmed as mice with a *Mx1*-mediated Mef2c deletion similarly exhibited a HBM phenotype that was a result of targeting osteoclast precursors [142]. Here, OCLs showed reduced differentiation capacity to become actively resorbing cell types. Interestingly, Mef2c levels were increased under the inflammatory conditions found amongst rheumatoid arthritis patients; a disease that is characterized by pathogenic bone loss from overactive OCL activity. Taken together, Mef2c function is found amongst OB and OCL cell populations that are function in maintaining bone homeostasis possibly by utilizing similar gene regulatory mechanisms to ensure their cellular behaviors remain closely coordinated.

The present work sought to expand on the function of *Mef2c* by characterizing the GRN amongst OCLs. An accruing level of evidence suggest that *Mef2c*

function is more complex in bone than previously appreciated and yet a minimal number of *Mef2c* target genes have been described. Gene targets such as *Sost*, *Mmp13*, *Runx2* and *Col10a1* have been reported amongst bone cell populations that support bone formation [137-139, 216]. Gene targets amongst OCL populations is comparatively much less understood as *c-Fos* is the only direct gene target described to date [142]. An in-depth characterization of Mef2c-regulated transcriptome amongst OCL populations could reveal novel mechanisms that can be therapeutically targeted to treat osteoporosis. Here, *Ctsk-cre* mice were used to target OCL populations as has been done previously [263-265]. We found that *Ctsk-cre* mice were bred with *Mef2c$^{fl/fl}$ mice* (*Ctsk Mef2c cKO*) exhibited the characteristic HBM phenotype as shown in other Mef2c bone mutants [135, 136, 142]. Culture based experiments demonstrated that OCL differentiation was negatively impacted in the absence of *Mef2c*. Interestingly, scRNAseq revealed changes in osteogenic populations isolated from *Ctsk Mef2c cKO* mutants and were associated with previously described roles suggesting *Ctsk* promoter leakiness amongst additional bone cell populations and is supported by recent studies [160]. Future studies utilizing *Cx3cr1-Cre* transgenic mice is expected to provide additional insights into the functional role of *Mef2c* in OCL populations to gain a better understanding of the *Mef2c* GRN associated with bone resorption.

Methods

Experimental mice

Animal experimental procedures were completed in accordance with guidelines under the institutional animal care and use committees at Lawrence Livermore National Laboratory under an approved protocol by the IACUC committee and conform to the Guide for the care and use of Laboratory

animals. *Mef2c$^{fl/fl}$; Ctsk-Cre* mice (*Mef2c cKO)* were generated by breeding *Mef2c$^{fl/fl}$* with *Ctsk Cre* mice [182, 266]. The resulting mutant mice were genotyped by PCR.

μCT scanning

Hindlimbs of *Mef2c cKO* mice were dissected and dehydrated using 70% ethanol in preparation to scanning on a μCT instrument (SCANCO μCT 35, Brüttisellen, Switzerland) using 60kVp, 180 mA, 750-ms integration time with an isotropic voxel size at 10 μm. To measure the metaphysic trabecular bone in the distal femur, a 2 mm region of secondary spongiosa was isolated by manual analysis. The region of interest began 1mm proximal to the distal growth plate and extended proximally for 2 mm. Prior to scanning, the total length of each femur was measured with the digital calipers; these measurements were used to identify the mid-diaphysis in each femur CT scan by considering slice thickness (10μm) and counting slices from the distal tip of the condyles until the calculated midshaft was reached. The central 20 slices at the midshaft were analyzed for cortical properties. Trabecular bone volume fraction was determined by quantifying trabecular bone volume fraction via trabecular bone volume fraction (BV/TV, %), trabecular thickness (TB.Th, mm), trabecular number (TB.N, mm), trabecular thickness (Tb.Sp, mm), connective density (Conn.D, 1/mm^3), and structure model index (SMI).

In vitro osteoclast differentiation

Femurs and tibia of 16-week-old *Mef2c cKO* mutant mice were harvested. Bone marrow was obtained from femurs and tibia by centrifugation as previously described [267]. Briefly, proximal ends of long bones were removed and placed into 1.5 ml microfuge tubes with plastic inserts cut from 0.5 ml microfuge

tubes. Samples were centrifuged at 2000 rpm for 30 seconds to move bone marrow into 1.5 ml microfuge tubes and resuspended in culture medium after red blood cells were lysed with ACK solution (Sigma-Aldrich). Murine $CD11b^+$ monocytes were isolated from the bone marrow isolates using microbeads for magnetic separation according to the manufacturer's protocol (Miltenyl Biotec). $CD11b^+$ monocytes were cultured in 24-well using a seeding density of 2×10^5 cells/well in 500 μL OCL differentiation medium (DMEM/F12 supplemented 10% FBS (Thermo Fisher), 1% penicillin-streptomycin (Thermo Fisher, 15140122), 50 μM β-mercaptoethanol, 25 ng/mL M-CSF (Invitrogen) and 25ng/mL RANKL (R&D systems) at 37°C, 5% CO_2 for six days. Medium was changed every 2 days as was done previously [162].

Visualization of mature osteoclasts generated ex-vivo

Mature *Mef2c cKO* OCLs generated, as previously mentioned, were washed with PBS and fixed using 4% paraformaldehyde (Thermo Fisher, J19943.K2) for 10 min. To detect TRAP amongst OCLs, staining was performed using the TRAP staining kit from Sigma Aldrich (387A-1KT) following the manufacturer's protocol. Quantifying total TRAP area by imaging 5-6 fields of view for each well examined (n=3/group). To visualize F-actin ring structures in differentiating and mature OCLs, cells were permeabilized with 0.1% Triton™ X-100 for 10 min and washed with PBS. Next, OCLs were incubated with phalloidin (594nm, 1:600) for 15 min. After three washes with PBS, 200μL PBS was added to each well to image OCL populations using a Leica DM5000 microscope.

Single-cell RNA sequencing

16-week-old male *Mef2c cKO* mutant mice (N=2/genotype) were used to isolate primary bone cell populations. To isolate primary bone cell populations, an isolation protocol was used for downstream scRNAseq. Briefly, hindlimbs were isolated and thoroughly cleaned of any contaminating tissues from bone. Once bones were ready, femurs and tibiae were depleted of bone marrow after opening marrow cavity followed by 2x PBS washes. Bones were then processed into 1-2mm fragments and placed into 8ml of 7.5mg/ml Collagenase (Worthington Biochemical, Lakewood, NJ; CLS-1) digestion solution and 100 µg/mL DNase I (Roche, Basel, Switzerland; 11284932001) in DMEM/F12 for 30 min at 37^{o}C on a shaker at 150 rpm. After 30 min, the resulting digestion solution was transferred into a 50ml conical tube and washed with 1x PBS.

Next, 8ml of 100mM EDTA was added to tube containing bone pieces and incubated for 30 min at 37^{o}C on a shaker at 150 rpm followed by transferring the 2nd digestion solution to the 50 ml collection tube containing the digestion solution from the earlier digestion step. These alternating digestion steps were repeated for a total of 9 incubations with each respective digestion mix collected in between washes. Once collection of primary bone cells is completed, contaminating red blood cells were then lysed by adding ACK (ThermoFisher Scientific, Waltham, MA, USA; A1049201) followed by removal of cellular debris using a 100µm nylon cell strainer. Further enrichment of bone cell populations was completed using flow cytometry. Bone cell suspensions were made from using the primary bone cells collected and were incubated in Biolegend antibodies APC/Cyanine7 anti-mouse CD45 Antibody (Clone: 30-F11) and anti-mouse APC Ter119 at a 1:100 dilution in PBS+1%FBS. Dapi was used for viability staining. Viable CD45/Ter119$^{-/-}$ populations were sorted with flow cytometric analysis performed on a BD FACSMelody system.

Isolated CD45/Ter119$^{-/-}$ bone cell populations were sequenced using Chromium Single Cell 3' Reagent Kit and Chromium instrument (10x Genomics, Pleasanton, CA). Library preparation was performed according to manufacturer's protocol and sequence on an Illumina NextSeq 500 (Illumina, San Diego, CA, USA).

scRNAseq data analysis

Generated scRNAseq data was processed with 10x Genomics Cell Ranger software (version 6.0.0;10x Genomics, Pleasanton, CA, USA). Once biological samples were sequenced by the Illumina NextSeq 500 sequencer, and the base call files (BCL) were demultiplexed into FASTQ files using the Cell Ranger 'mkfastq' command. Data was aligned to the mouse reference genome (mm10), barcoding counted, and unique molecular identifier (UMI) counted performed using the 'count' command. The resulting output was then exported into the R package Seurat where quality control steps and additional analysis were performed [221]. Data filtering criteria included: cells with less than 500 detected gene per cell, genes that were expressed by fewer than 5 cells, had mitochondrial greater than 15%, or had aberrantly high gene count all of which were removed. Data was normalized using the global-scaling method known as 'LogNormalize' to find highly variable genes at which point the data from *Mef2c cKO* and *WT* experimental data was integrated, scaled, and reduced by principal component analysis (PCA). Cells were grouped into clusters for cell type discovery using Seurat's 'FindNeighbors', and 'FindClusters' commands. Followed by the visualization of the produced clusters using the non-linear dimensional reduction via uniform manifold approximation and projection (UMAP). Cluster marker genes were determined using Seurat's 'FindAllMarkers' command. Next, Seurat's 'FeaturePlot', 'DotPlot', 'VlnPlot',

and 'Heatmap' commands were used to graphically plot the cell type specific gene expression measurements amongst the datasets. Cell clusters were isolated by dataset and their counts extracted. The experimental metadata was generated by matching the cell's barcodes with their respective annotation. The resulting information was input into Deseq2 package for statistical analysis [222].

Analysis of osteoclast scRNA-seq data

A publicly available dataset was utilized that was generated from murine monocyte/macrophage progenitors and differentiated into osteoclast after endogenous M-CSF and RANKL treatment. RNA was collected on day of treatment (D0), 24hrs (D1) and 72hrs (D3) post treatment. scRNAseq data was processed similarly done in the *scRNAseq data analysis* section using Cell Ranger and transferred output was subsequently analyzed using 10x Genomics Loupe Browser 6.4.1.

Statisical Anaylysis

R statistical software and Graphpad Prism were used for statistical analysis. Student's t test were used to determine statistically significant differences of mean values. P-value of ≤ 0.05 were considered statistically significant.

Results

Mef2c deficiency in Ctsk-expressing cells results in significantly greater bone mass

To characterize how Mef2c functions in OCL biology, $Mef2c^{fl/fl}$ mice were bred with Ctsk-Cre transgenic mice to generate $Mef2c^{fl/fl}$; Ctsk-Cre mutant mice (Mef2c cKO) [182, 266]. Mef2c cKO mice reveal no obvious defect at birth and during aging or changes in size and weight. At peak skeletal bone mass (16 weeks), μCT analysis was used to assess changes to bone mass (Figure 1). Mef2c cKO mice femurs have a significant increase in bone mass compared to Cre-negative controls. Although not significant, Mef2c cKO bones show increases in various μCT parameters such as bone volume (BV/TV), trabecular number (TB. N) and connective density (Conn.D; Figure 1A, B). Additionally, examination of $Sost^{-/-}$; $Mef2c^{fl/fl}$ Ctsk-Cre (dKO) femora reveal a greater increase in bone mass than observed in $Sost^{-/-}$ alone (Figure 1A, C). These results suggest the observe increase in bone mass is driven by a potential novel Mef2c function independent of the characterized role associated with Sost-expressing osteogenic populations.

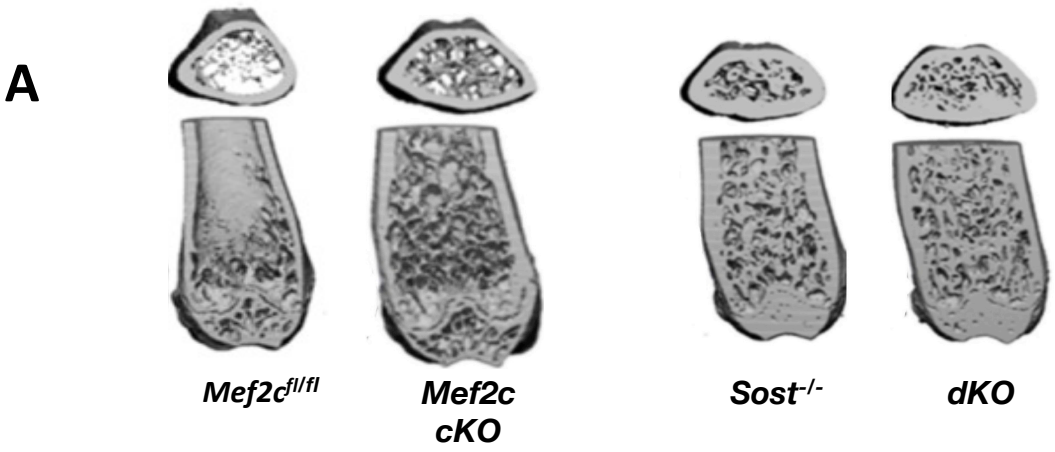
A
Mef2c^fl/fl
Mef2c cKO
Sost^-/-
dKO

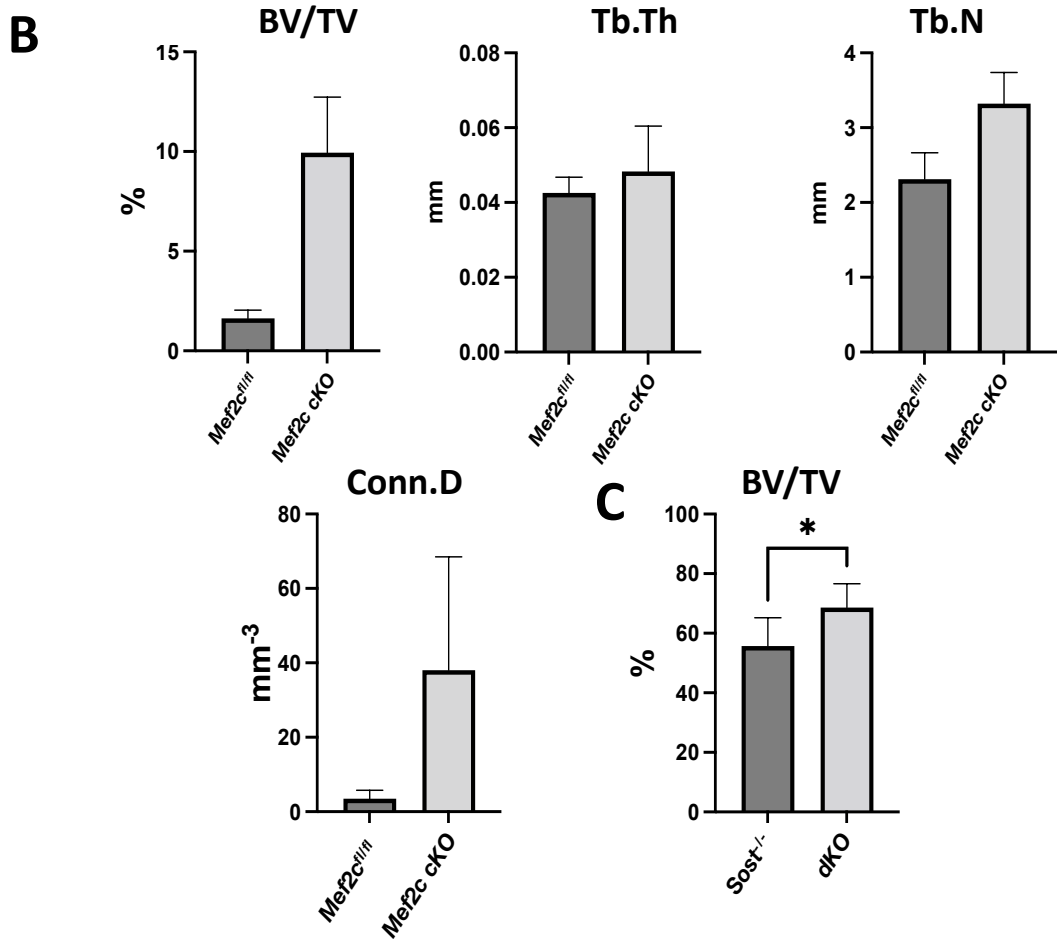
B
BV/TV
%
Tb.Th
mm
Tb.N
mm
Conn.D
mm^-3
C
BV/TV
%
*
Mef2c^fl/fl
Mef2c cKO
Sost^-/-
dKO

Figure 1. μCT analysis of femora comparing skeletal phenotypes of Mef2c$^{fl/fl;}$ Ctsk-Cre mice to Sost$^{-/-}$ and Mef2c$^{fl/fl}$; Ctsk-Cre, Sost$^{-/-}$ mice*. (A) 3D representation of Mef2c$^{fl/fl}$; Ctsk-Cre mice to Sost$^{-/-}$ and Mef2c$^{fl/fl}$; Ctsk-Cre, Sost$^{-/-}$ mice highlighting changes in bone mass amongst femora. Quantification of trabecular bone volume/total volume (BV/TV) in Mef2c$^{fl/fl}$; Ctsk-Cre, trabecular thickness (Tb.th), trabecular number (Tb. N) and connective density (Conn.D) in Mef2c$^{fl/fl}$; Ctsk-Cre mice mice (B). Quantification of trabecular bone volume/total volume (BV/TV) in Sost$^{-/-}$ and Mef2c$^{fl/fl}$; Ctsk-Cre, Sost$^{-/-}$ (dKO) mice. $p<0.05$, by t test compared to own Cre negative controls.*

Differentiation negatively impacted in Mef2c-deficient Osteoclasts

In order to study the effects of deleting *Mef2c* in OCL populations, we characterized OCLs from *Mef2c cKO* mice. To date, we are unaware of any successful reports of directly isolating OCL populations for use in cell culture studies as it is technically challenging to isolate mature osteoclasts. Therefore, CD11b$^+$ precursors from *Mef2c cKO* mice were isolated and differentiated into mature OCLs as has previously been conducted [162]. CD11b$^+$ precursors were differentiated by supplementing culture media with RANKL and M-CSF for 5-7 days. By day 5-7 mature OCLs are observed in culture well plates (Figure 2A). Mature OCLs are TRAP$^+$, contain an actin ring, and are multinuclear cell populations (number of nuclei ≥ 3) [268-270]. Differentiation of CD11b$^+$ precursors from *Mef2c cKO* mice is negatively impacted as mature OCLs are not generated compared to *cre negative* controls). After 5 days of differentiation, *Mef2c cKO* wells develop fewer multinuclear cell populations exhibiting minimal actin ring formation (Figure 2B). Additionally, *Mef2c cKO* populations exhibit less TRAP$^+$ populations where cells that were TRAP$^+$ are less intense while the *Mef2c$^{fl/fl}$* controls exhibit robust TRAP$^+$ cell populations

by day 5 and 7 (Figure 3A, B). Taken together, Mef2c deletion has a negative impact on OCL differentiation of myeloid CD11b^{+} precursors and is not clear what underlying molecular mechanisms are impacted as a result.

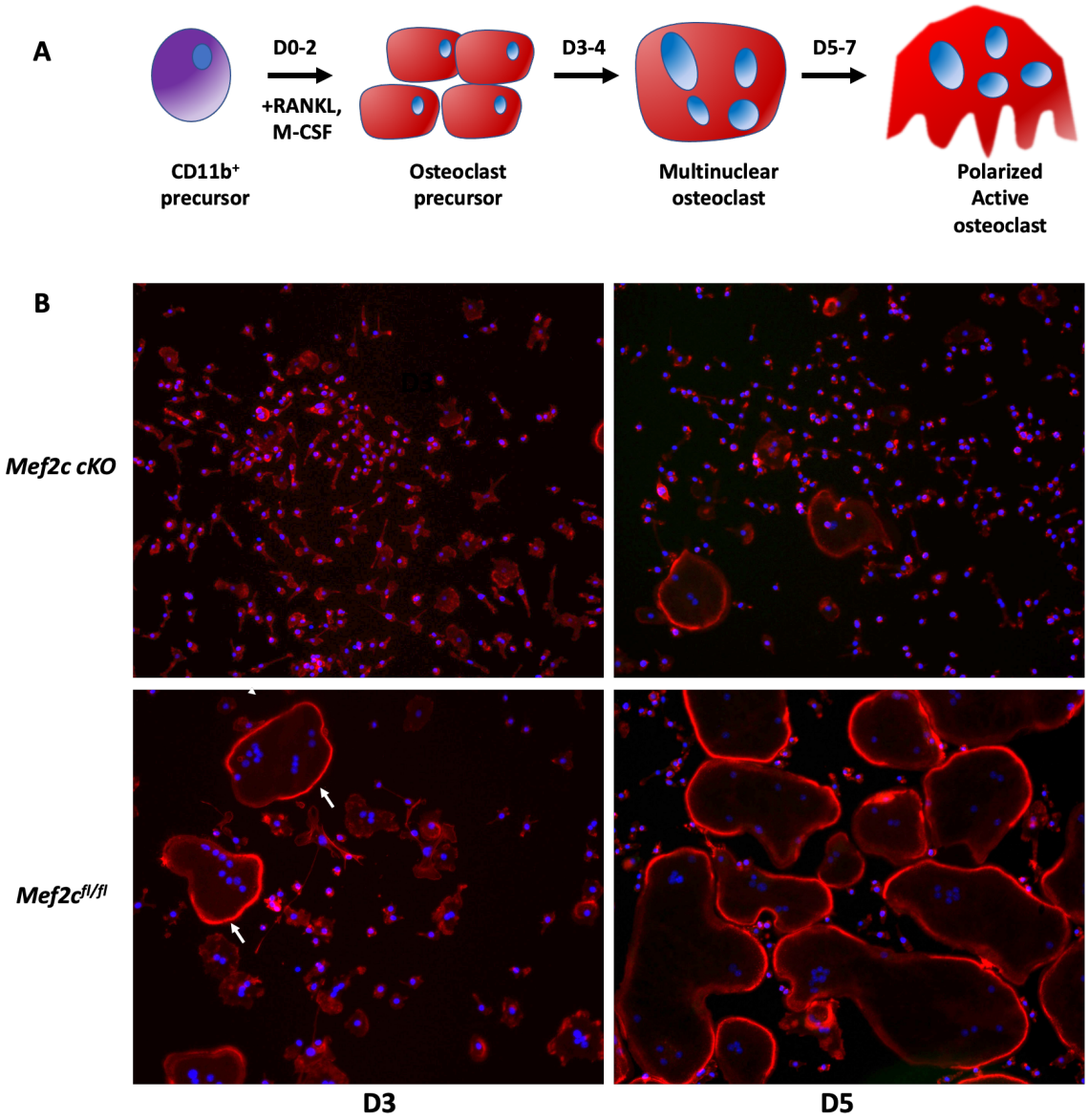

Figure 2. Osteoclast differentiation is less efficient in the absence of Mef2c. *(A) In vitro osteoclast differentiation experimental overview (B) Differentiation of* $Mef2c^{fl/fl}$ *and* $Mef2c^{fl/fl}$*; Ctsk-Cre* $Cd11b^{+}$ *bone marrow populations at days 1, 3 and 5. asterisks label mature osteoclasts (# of nuclei ≥ 3,* $actin\ ring^{+}$ *cells).*

scRNAseq of Mef2c cKO bone cells reveals changes amongst osteogenic populations

To examine the molecular mechanisms *Mef2c* mediates in osteoclast populations, primary bone cells were isolated from $Mef2c^{fl/fl}$ and *Mef2c cKO* hindlimbs (Femurs and tibias) at 16 weeks of age and analyzed using scRNAseq technology. A total of 6029 cells (*WT*: 4667 and *Mef2c cKO:* 1362) were used to identify bone cell subpopulations from murine hindlimbs. The approach identifyied clusters representing myeloid (clusters: 1-3, 5, 7, 9, 11, 15,16) and lymphoid (clusters: 8, 13, 14, 17) immune populations, adipocyte populations (clusters: 10), and osteogenic and chondrogenic populations (clusters: 4, 6, 12; Figure 4A, B). *Mef2c* expression is found in osteogenic and chondrogenic populations and a subset of immune populations including monocyte, macrophage, and B cells (Figure 3B). Interestingly, *Ctsk* is primarily expressed amongst the osteogenic (*Col1a1*) populations and not the immune populations (*Ptprc*; Figure 3C, D). The observation suggests that *Mef2c* deletion is also occurring amongst the osteogenic populations from cells isolated from *Mef2c cKO* mutants and is supported by previous reports showing *Ctsk* expression amongst osteogenic populations such as periosteal stem cells and osteolytic osteocytes [160, 271]. Additionally, $Ptprc^{+}$ populations lack expression of OCL markers (*Ctsk* and *Acp5*) suggesting that our scRNAseq analysis failed to capture mature osteoclasts. This data also suggests that the high bone mass phenotype observed in *Mef2c cKO* could at

least in part be driven by *Ctsk-cre* mediated deletion of *Mef2c* in osteogenic lineage cells. Additional studies should include OCL precursor populations post M-CSF and RANKL exposure, to examine the role of *Mef2c* in OCLs.

scRNAseq highlights Mef2c expression in early osteoclast precursors

A recent study highlighted the OCL differentiation program at the single cell level (GSE147174). In their approach, bone marrow cells were isolated and differentiated into mature osteoclasts. Examined timepoints included day RANKL induction of OCL differentiation (D0), 24 hours post induction (D1), and 72 hours post OCL induction (D3) [272]. Re-analysis of the publicly available dataset reveals that *Mef2c* expression is strongest at D0 while expression is largely absent by D1 and D3, timepoints at which *Ctsk* is expressed (Figure 5 B, E). The scRNAseq dataset also was informative on the effectiveness of targeting OCL populations using *Mef2c cKO* mice as the expression profile of *Ctsk* shows minimal overlap with *Mef2c* expression (Figure 5 C, F). These findings further suggests that the HBM phenotype observed in *Mef2c cKO* mice could be primarily mediated through the absence of *Mef2c* amongst osteogenic populations. To uncover additional mechanisms in OCL populations, an earlier marker would be better suited such as *Cx₃cr1*. Others have reported successful targeting of OCL populations using *Cx₃cr1* since its expression profile is also found early in precursors and in D0 populations (Figure 5 E, G). Targeting with *Cx₃cr-Cre* mice should minimize the number of bone cell populations affected by recombination and get achieve better deletion efficiency when *Mef2c* function is greatest.

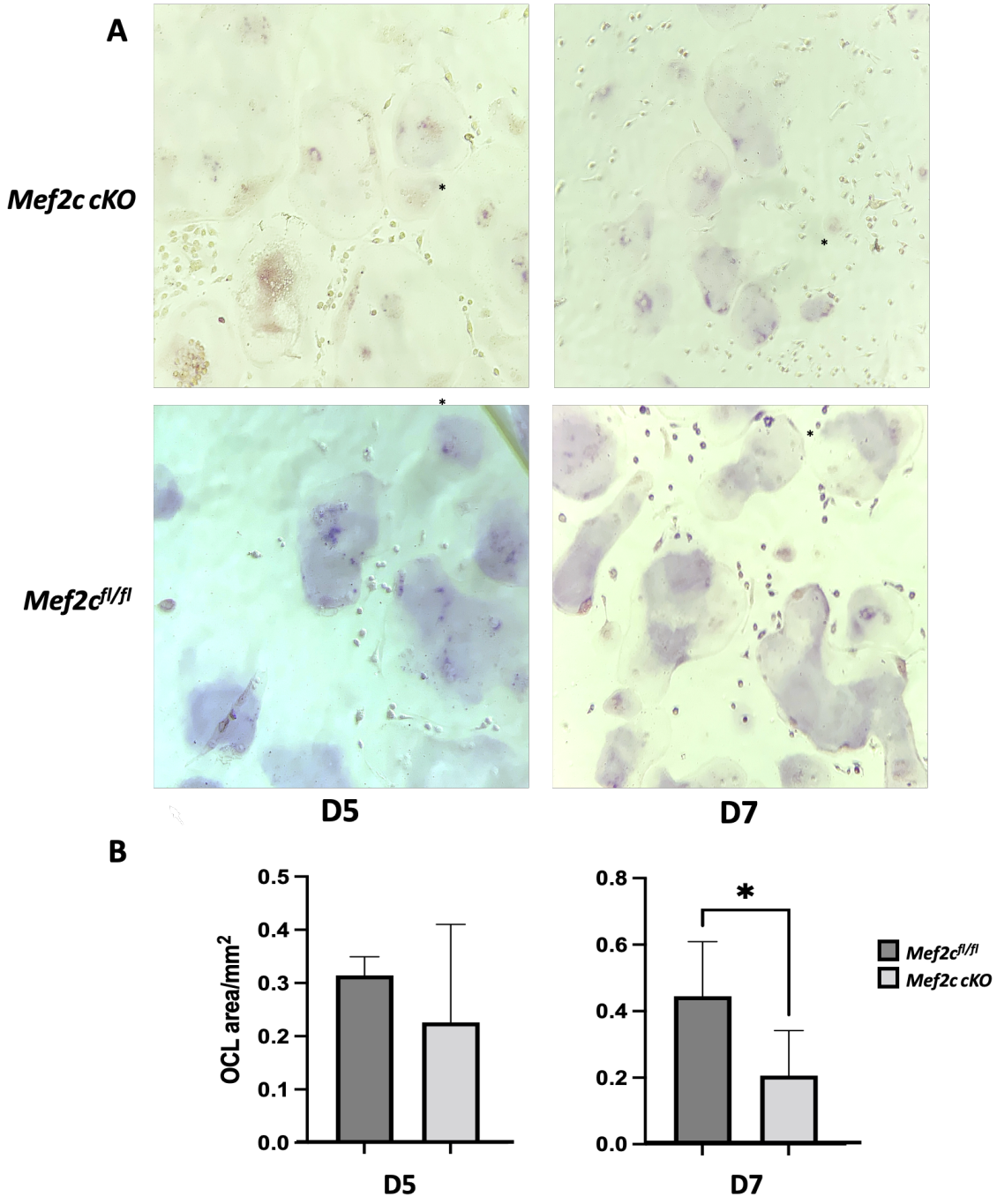
A
Mef2c cKO
Mef2c fl/fl
D5
D7
B
OCL area/mm2
0.5
0.4
0.3
0.2
0.1
0.0
D5
0.8
0.6
0.4
0.2
0.0
*
D7
Mef2c fl/fl
Mef2c cKO

Figure 3. Decreased number of TRAP+ Osteoclast cell populations from the absence of Mef2c. *(A) Differentiation of Mef2c$^{fl/fl}$ and Mef2c$^{fl/fl}$; Ctsk-Cre Cd11b^{+} bone marrow populations at days 1, 3, 5, and 7. asterisks label mature osteoclasts (TRAP+ cells). Surface area osteoclast per well at day 5 (B) and 7 (C). Scale bar = x, p<0.05, by ANOVA t test compared to Cre negative controls.*

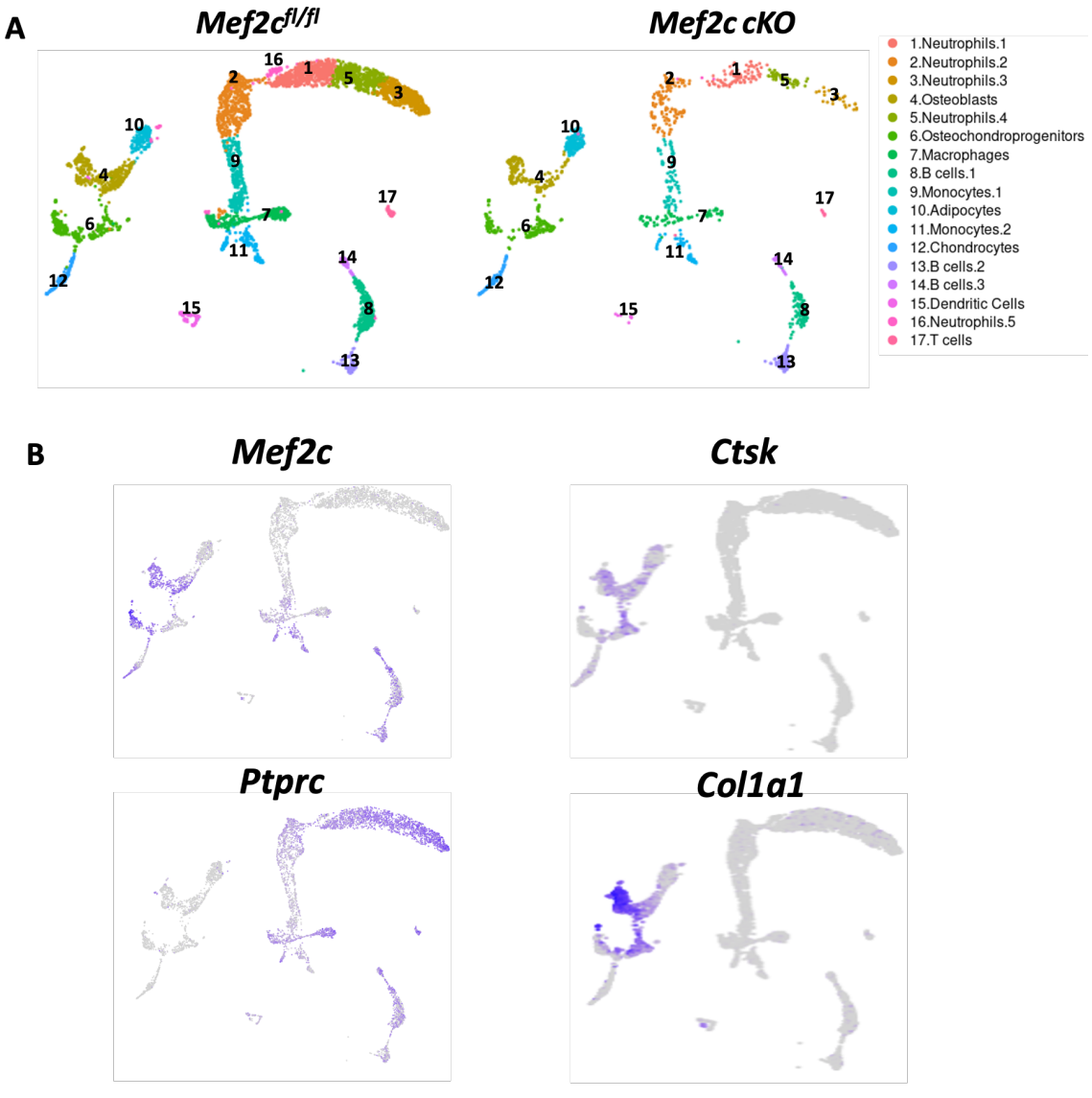

Figure 4. Single cell analysis of Mef2c cKO bone cells. *(A) Cell clusters from 10x Genomics scRNA-seq analysis visualized by Uniform Manifold Approximation and Projection (UMAP) in Mef2c$^{fl/fl}$ and Mef2c cKO. Colors indicated clusters of various cell types. (B) Feature plot of Mef2c and markers of immune and bone cell subtypes used to denote each subtype.*

Discussion

While there is a growing body of research reporting *Mef2c* function in maintaining bone homeostasis and strength, very little is known about the function amongst OCL populations. Previous work has shown how *Mef2c* can regulate bone development and metabolism. Knockout studies amongst early osteogenic progenitors and chondrocytes exhibited defects in hypertrophy and bone formation [139, 140]. In fact, modulating *Mef2c* levels in human mesenchymal progenitors affects their ability towards inducing an osteogenic cell fate [132] using mechanisms downstream of anabolic pathways such as Wnt and PTH. Previously, it was generally understood that the target gene *Sost,* an inhibitor of Wnt signaling pathway is the primary driver of modulating bone mass. scRNAseq amongst *Mef2c*-deficient osteogenic populations demonstrates that additional gene targets are associated with bone and energy metabolism (See chapter 3). Amongst OCL populations, a recent report identified *c-Fos* as a direct target gene but is the only known gene target described to date.

In the present study, we shed light on *Mef2c* function amongst OCL populations that appears to negatively impact differentiation. *Mef2c cKO* mice exhibit a HBM bone phenotype that was characteristic of other bone specific knockouts [135, 136]. In fact, *dKO* (*Sost$^{-/-}$; Mef2c$^{fl/fl}$ Ctsk-cre)* mutant mice exhibit a greater HBM phenotype compared to the individual Mef*2c cKO and*

Sost$^{-/-}$ mutants. The finding suggests that *Mef2c* function is independent of *Sost* and amongst OCL populations. Additionally, cell culture studies demonstrate how *Mef2c cKO* CD11b^{+} cells are less efficient at differentiating into mature OCLs compared to *wildtype* populations.

Unexpectedly, scRNAseq of primary bone cells from *Mef2c cKO* mice was not capable of capturing OCL populations. However, captured single cell transcriptional signatures reveal *Ctsk* expression amongst osteogenic populations indicating that the HBM phenotype found in *Mef2c cKO* mice could recapitulate the findings from previous *Mef2c* knockout studies. Given the results from the cell culture studies, we utilized publicly available single cell transcriptomic data (GSE147174) to determine the Mef2c expression profile in differentiating OCLs. Examination of the data revealed insights of using *Ctsk-Cre* mice to target OCLs as the expression profile of *Ctsk* only minimally overlaps with *Mef2c* expression and found at early points of differentiation. The publicly available data also point to an appropriate OCL-specific targeting promoter *Cx$_3$cr1* as expression more closely matches the expression profile of *Mef2c.*

With the aim of characterizing the OCL Mef2c-mediated transcriptome, utilizing *Cx$_3$cr1-Cre* mice should aid in shedding light to better understand novel gene regulatory mechanisms that possibly are involved in generating functional and mature OCLs. Such knowledge shows great potential in informing bone researchers on how to target the different cell types involved in bone remodeling by identifying common signaling pathways and possibly maintain the level of coordination required to maintain bone homeostasis and strength throughout adulthood.

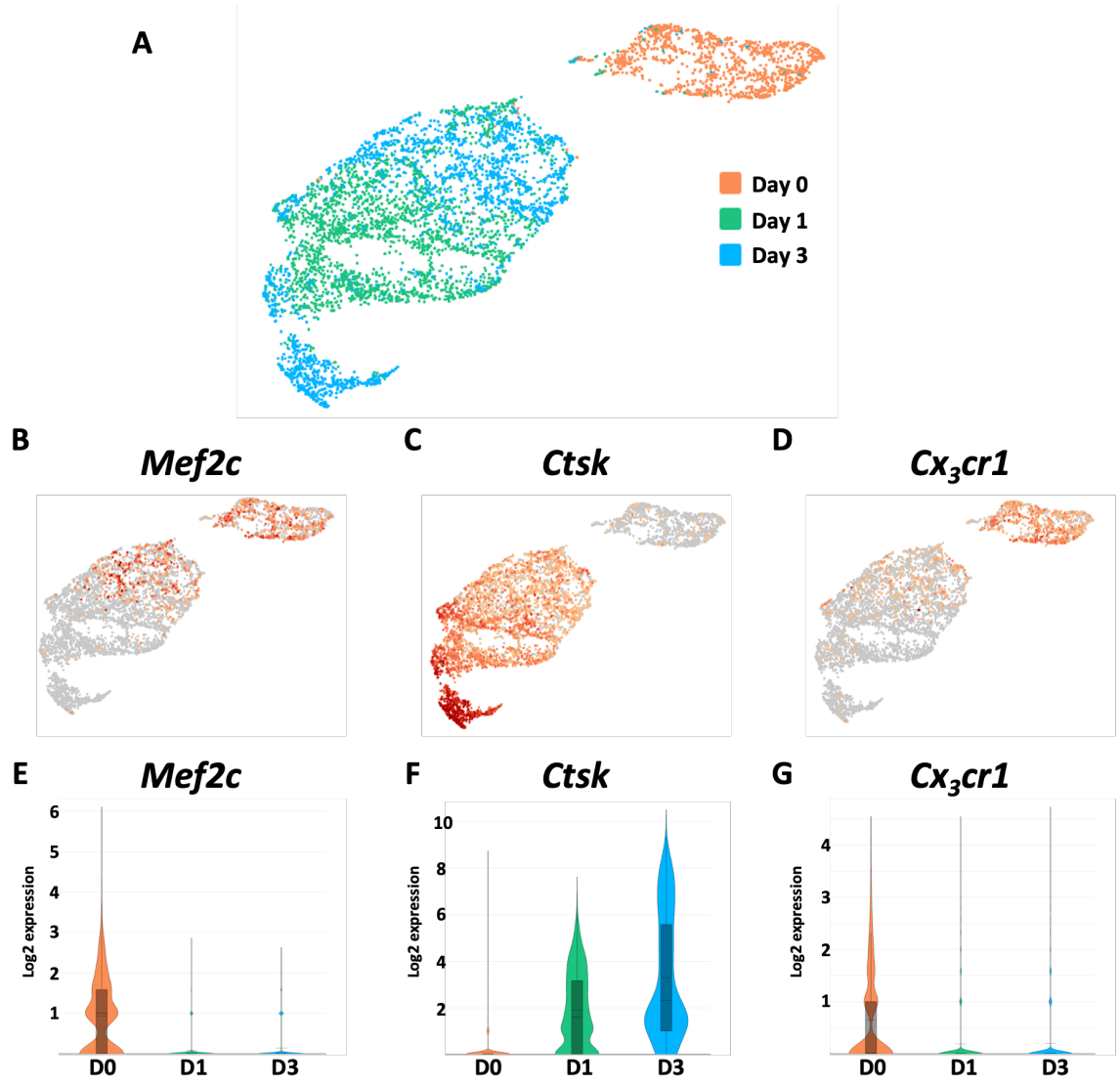

Figure 5. Single cell analysis of differentiating osteoclasts at days 0, 1, and 3. *Data was generated using publicly available data using isolated murine OCL precursors [272]. (A) Cell clusters from 10x Genomics scRNA-seq analysis visualized by Uniform Manifold Approximation and Projection (UMAP) of differentiating osteoclasts on days 0, 1, and 3. Colors indicated clusters of individual time points. Feature plot of Mef2c (B), Ctsk (C), and Cx$_3$cr1 (D).*

Violin plot of Mef2c (E), Ctsk (F), and Cx$_3$cr1 (G) expression at days 0, 1 and 3 of osteoclast differentiation.

Chapter 5. Conclusions and Future Directions

The studies mentioned in the present thesis has led to a better understanding of GRN associated with *Mef2c* amongst bone cell populations. Additionally, such knowledge highlights novel mechanisms involved in maintaining bone homeostasis. These experimental studies have led to the development of a bone cell isolation method that can obtain primary bone cell populations, including osteocytes, for use in single cell-based sequencing technologies. Additionally, the following conclusions were also made:

1. *Mef2c* mediates a cell-type specific transcriptome across various bone cell populations that could be coordinating the cellular behaviors of the osteogenic lineage.

2. A single cell analysis of the various bone cell populations supports the transdifferentiation theory as OS appear to arise from more than one bone cell type.

The present findings indicate that the *Mef2c* GRN amongst osteogenic populations mediate the production of suffecient cellular energy levels to meet the demands associated with bone formation. At earlier stages of the osteogenic lineage, such as in mesenchymal progenitors and osteochondral progenitors, *Mef2c* mediates energy production through regulating the expression of glycolytic pathways. Whereas in OBs and OS, *Mef2c* mediates the energy production through the oxidative phosphorylation pathway. The work also demonstrated how interconnected the energy metabolism genes are with bone metabolism genes as both gene programs harbored evidence of Mef2c binding. Taken together, these findings point to bone tissue homeostasis and strength

are promoted the coordinated expression of both sets of genes as part of the transcriptional activating function of *Mef2c*.

A key step in characterizing Mef2c function in bone was largely in part to the development of a bone cell isolation method for downstream scRNAseq. The accessibility of bone cell populations have been an ongoing issue for bone researchers but with the advent of single cell technologies will prove to successfully circumnavigate the problems associated with investigating mineralized tissues. The incorporation of the singe cell-based technologies will greatly aid in elucidating the complex cellular behaviors that function in maintaining bone tissues. This is accomplished by identifying novel subpopulations of major bone cell types and their functional contributions to tissue homeostasis. An exhaustive characterization of the osteogenic lineage will also provide novel bone cell markers that can accurately and sufficiently target discrete cell populations. The bone cell isolation method, found in chapter 2, captures mesenchymal progenitors, early (OBs) and late (OSs) cell populations of the osteogenic lineage provides an opportunity to fill the various gaps of knowledge of how bone tissues are maintained throughout adulthood. Such knowledge will greatly inform bone researchers and their approach to developed improved therapeutics to treat bone loss disorders such as osteoporosis.

Future studies should focus on further characterizing the role of *Mef2c* function in bone. At the tissue level, *Mef2c* deletion resulted in the characteristic HBM phenotype typically found amongst mouse mutants. An intriguing finding as the scRNAseq analysis revealed several key genes associated with the formation of bone were downregulated in the absence of *Mef2c*. The contradictory nature of these findings can be resolved by future studies that focus on characterizing the mineralization activity and function of

osteoblast populations. Such findings would provide a nuance understanding of the mineralization process and the organization of the ECM needed to provide sufficient bone strength as part of maintaining bone tissue homeostasis.

The currenting findings presented illustrate a partial view of how osteogenic cell populations are programmed to maintain bone tissues throughout adulthood. First, we presented a method to capture major bone cell populations that provides a tissue-wide snapshot of the functional impact of a given experimental condition. Here, this approach was taken to characterize the functional contributions of a ubiquitously expressed TF *Mef2c*. The isolation of *Mef2c*-defecient bone cell populations demonstrated how a commonly expressed TF could have a cell-type specific GRN that is potentially coordinating the complex cellular behaviors associated with the formation of bone tissues. The continued characterization of TF-mediated GRNs will lead to a greater understanding of how cellular behaviors are programmed and ultimately be utilized to dissect pathophysiology associated with osteoporosis and inform future regenerative approaches.

References

1. Breeland, G., M.A. Sinkler, and R.G. Menezes, *Embryology, Bone Ossification*, in *StatPearls*. 2022: Treasure Island (FL).
2. Chai, Y. and R.E. Maxson, Jr., *Recent advances in craniofacial morphogenesis.* Dev Dyn, 2006. **235**(9): p. 2353-75.
3. Doro, D., et al., *The Osteogenic Potential of the Neural Crest Lineage May Contribute to Craniosynostosis.* Mol Syndromol, 2019. **10**(1-2): p. 48-57.
4. Quarto, N., et al., *Origin matters: differences in embryonic tissue origin and Wnt signaling determine the osteogenic potential and healing capacity of frontal and parietal calvarial bones.* J Bone Miner Res, 2010. **25**(7): p. 1680-94.
5. Chan, W.C.W., et al., *Regulation and Role of Transcription Factors in Osteogenesis.* Int J Mol Sci, 2021. **22**(11).
6. Kobayashi, S., et al., *Trabecular minimodeling in human iliac bone.* Bone, 2003. **32**(2): p. 163-9.
7. Karsenty, G., H.M. Kronenberg, and C. Settembre, *Genetic control of bone formation.* Annu Rev Cell Dev Biol, 2009. **25**: p. 629-48.
8. Teitelbaum, S.L., *Osteoclasts: what do they do and how do they do it?* Am J Pathol, 2007. **170**(2): p. 427-35.
9. Bonewald, L.F., *Osteocytes as dynamic multifunctional cells.* Ann N Y Acad Sci, 2007. **1116**: p. 281-90.
10. Bonewald, L.F. and G.R. Mundy, *Role of transforming growth factor-beta in bone remodeling.* Clin Orthop Relat Res, 1990(250): p. 261-76.
11. Bonewald, L.F. and M.L. Johnson, *Osteocytes, mechanosensing and Wnt signaling.* Bone, 2008. **42**(4): p. 606-15.

12. Martin, T.J. and N.A. Sims, *Osteoclast-derived activity in the coupling of bone formation to resorption.* Trends Mol Med, 2005. **11**(2): p. 76-81.
13. Lind, M., et al., *Chemotaxis of human osteoblasts. Effects of osteotropic growth factors.* APMIS, 1995. **103**(2): p. 140-6.
14. Parfitt, A.M., *The mechanism of coupling: a role for the vasculature.* Bone, 2000. **26**(4): p. 319-23.
15. Cappariello, A., M. Ponzetti, and N. Rucci, *The "soft" side of the bone: unveiling its endocrine functions.* Horm Mol Biol Clin Investig, 2016. **28**(1): p. 5-20.
16. Lorentzon, M. and S.R. Cummings, *Osteoporosis: the evolution of a diagnosis.* J Intern Med, 2015. **277**(6): p. 650-61.
17. Hernlund, E., et al., *Osteoporosis in the European Union: medical management, epidemiology and economic burden. A report prepared in collaboration with the International Osteoporosis Foundation (IOF) and the European Federation of Pharmaceutical Industry Associations (EFPIA).* Arch Osteoporos, 2013. **8**: p. 136.
18. Tian, L., et al., *Prevalence of osteoporosis and related lifestyle and metabolic factors of postmenopausal women and elderly men: A cross-sectional study in Gansu province, Northwestern of China.* Medicine (Baltimore), 2017. **96**(43): p. e8294.
19. Ji, M.X. and Q. Yu, *Primary osteoporosis in postmenopausal women.* Chronic Dis Transl Med, 2015. **1**(1): p. 9-13.
20. Pisani, P., et al., *Major osteoporotic fragility fractures: Risk factor updates and societal impact.* World J Orthop, 2016. **7**(3): p. 171-81.
21. Sozen, T., L. Ozisik, and N.C. Basaran, *An overview and management of osteoporosis.* Eur J Rheumatol, 2017. **4**(1): p. 46-56.
22. Porter, J.L. and M. Varacallo, *Osteoporosis*, in *StatPearls*. 2022: Treasure Island (FL).

23. Curtis, E.M., et al., *Epidemiology of fractures in the United Kingdom 1988-2012: Variation with age, sex, geography, ethnicity and socioeconomic status.* Bone, 2016. **87**: p. 19-26.
24. Foger-Samwald, U., et al., *Age Related Osteoporosis: Targeting Cellular Senescence.* Int J Mol Sci, 2022. **23**(5).
25. Melton, L.J., 3rd, et al., *Bone density and fracture risk in men.* J Bone Miner Res, 1998. **13**(12): p. 1915-23.
26. LeBoff, M.S., et al., *Correction to: The clinician's guide to prevention and treatment of osteoporosis.* Osteoporos Int, 2022. **33**(10): p. 2243.
27. Bischoff, H.A., et al., *Identifying a cut-off point for normal mobility: a comparison of the timed 'up and go' test in community-dwelling and institutionalised elderly women.* Age Ageing, 2003. **32**(3): p. 315-20.
28. Seeman, E., *Age- and menopause-related bone loss compromise cortical and trabecular microstructure.* J Gerontol A Biol Sci Med Sci, 2013. **68**(10): p. 1218-25.
29. Schwartz, A.V., et al., *Vertebral bone marrow fat associated with lower trabecular BMD and prevalent vertebral fracture in older adults.* J Clin Endocrinol Metab, 2013. **98**(6): p. 2294-300.
30. Lips, P., P. Courpron, and P.J. Meunier, *Mean wall thickness of trabecular bone packets in the human iliac crest: changes with age.* Calcif Tissue Res, 1978. **26**(1): p. 13-7.
31. Burghardt, A.J., et al., *High-resolution peripheral quantitative computed tomographic imaging of cortical and trabecular bone microarchitecture in patients with type 2 diabetes mellitus.* J Clin Endocrinol Metab, 2010. **95**(11): p. 5045-55.
32. Van Staa, T.P., et al., *Bone density threshold and other predictors of vertebral fracture in patients receiving oral glucocorticoid therapy.* Arthritis Rheum, 2003. **48**(11): p. 3224-9.

33. Brent, M.B., *Abaloparatide: A review of preclinical and clinical studies.* Eur J Pharmacol, 2021. **909**: p. 174409.
34. Hodsman, A.B., et al., *Parathyroid hormone and teriparatide for the treatment of osteoporosis: a review of the evidence and suggested guidelines for its use.* Endocr Rev, 2005. **26**(5): p. 688-703.
35. Miller, P.D., et al., *Abaloparatide: an anabolic treatment to reduce fracture risk in postmenopausal women with osteoporosis.* Curr Med Res Opin, 2020. **36**(11): p. 1861-1872.
36. Minisola, S., et al., *Update on the safety and efficacy of teriparatide in the treatment of osteoporosis.* Ther Adv Musculoskelet Dis, 2019. **11**: p. 1759720X19877994.
37. Dempster, D.W., et al., *Early Effects of Abaloparatide on Bone Formation and Resorption Indices in Postmenopausal Women With Osteoporosis.* J Bone Miner Res, 2021. **36**(4): p. 644-653.
38. Dempster, D.W., et al., *Longitudinal Effects of Teriparatide or Zoledronic Acid on Bone Modeling- and Remodeling-Based Formation in the SHOTZ Study.* J Bone Miner Res, 2018. **33**(4): p. 627-633.
39. Li, X., et al., *Sclerostin binds to LRP5/6 and antagonizes canonical Wnt signaling.* J Biol Chem, 2005. **280**(20): p. 19883-7.
40. Ellies, D.L., et al., *Bone density ligand, Sclerostin, directly interacts with LRP5 but not LRP5G171V to modulate Wnt activity.* J Bone Miner Res, 2006. **21**(11): p. 1738-49.
41. McClung, M.R., *Clinical utility of anti-sclerostin antibodies.* Bone, 2017. **96**: p. 3-7.
42. Chavassieux, P., et al., *Bone-Forming and Antiresorptive Effects of Romosozumab in Postmenopausal Women With Osteoporosis: Bone Histomorphometry and Microcomputed Tomography Analysis After 2 and 12 Months of Treatment.* J Bone Miner Res, 2019. **34**(9): p. 1597-1608.

43. McClung, M.R., et al., *Romosozumab in postmenopausal women with low bone mineral density.* N Engl J Med, 2014. **370**(5): p. 412-20.
44. Russell, R.G., *Bisphosphonates: the first 40 years.* Bone, 2011. **49**(1): p. 2-19.
45. Reid, I.R., et al., *Fracture Prevention with Zoledronate in Older Women with Osteopenia.* N Engl J Med, 2018. **379**(25): p. 2407-2416.
46. Abrahamsen, B., et al., *Risk of hip, subtrochanteric, and femoral shaft fractures among mid and long term users of alendronate: nationwide cohort and nested case-control study.* BMJ, 2016. **353**: p. i3365.
47. Khan, A.A., et al., *Case-Based Review of Osteonecrosis of the Jaw (ONJ) and Application of the International Recommendations for Management From the International Task Force on ONJ.* J Clin Densitom, 2017. **20**(1): p. 8-24.
48. Shane, E., et al., *Atypical subtrochanteric and diaphyseal femoral fractures: report of a task force of the American Society for Bone and Mineral Research.* J Bone Miner Res, 2010. **25**(11): p. 2267-94.
49. Bone, H.G., et al., *10 years of denosumab treatment in postmenopausal women with osteoporosis: results from the phase 3 randomised FREEDOM trial and open-label extension.* Lancet Diabetes Endocrinol, 2017. **5**(7): p. 513-523.
50. Cummings, S.R., et al., *Vertebral Fractures After Discontinuation of Denosumab: A Post Hoc Analysis of the Randomized Placebo-Controlled FREEDOM Trial and Its Extension.* J Bone Miner Res, 2018. **33**(2): p. 190-198.
51. Miller, P.D., et al., *Effect of denosumab on bone density and turnover in postmenopausal women with low bone mass after long-term continued, discontinued, and restarting of therapy: a randomized blinded phase 2 clinical trial.* Bone, 2008. **43**(2): p. 222-229.

52. Stolzing, A., et al., *Age-related changes in human bone marrow-derived mesenchymal stem cells: consequences for cell therapies.* Mech Ageing Dev, 2008. **129**(3): p. 163-73.
53. Muschler, G.F., et al., *Age- and gender-related changes in the cellularity of human bone marrow and the prevalence of osteoblastic progenitors.* J Orthop Res, 2001. **19**(1): p. 117-25.
54. Halloran, B.P., et al., *Changes in bone structure and mass with advancing age in the male C57BL/6J mouse.* J Bone Miner Res, 2002. **17**(6): p. 1044-50.
55. Baxter, M.A., et al., *Study of telomere length reveals rapid aging of human marrow stromal cells following in vitro expansion.* Stem Cells, 2004. **22**(5): p. 675-82.
56. Brennan, T.A., et al., *Mouse models of telomere dysfunction phenocopy skeletal changes found in human age-related osteoporosis.* Dis Model Mech, 2014. **7**(5): p. 583-92.
57. Yu, Z., et al., *Improvement of intertrochanteric bone quality in osteoporotic female rats after injection of polylactic acid-polyglycolic acid copolymer/collagen type I microspheres combined with bone mesenchymal stem cells.* Int Orthop, 2012. **36**(10): p. 2163-71.
58. Uri, O., E. Behrbalk, and Y. Folman, *Local implantation of autologous adipose-derived stem cells increases femoral strength and bone density in osteoporotic rats: A randomized controlled animal study.* J Orthop Surg (Hong Kong), 2018. **26**(3): p. 2309499018799534.
59. Uejima, S., et al., *Bone marrow stromal cell therapy improves femoral bone mineral density and mechanical strength in ovariectomized rats.* Cytotherapy, 2008. **10**(5): p. 479-89.
60. Ocarino Nde, M., et al., *Intra-bone marrow injection of mesenchymal stem cells improves the femur bone mass of osteoporotic female rats.* Connect Tissue Res, 2010. **51**(6): p. 426-33.

61. Li, J.H., et al., *Effects of mesenchymal stem cells on solid tumor metastasis in experimental cancer models: a systematic review and meta-analysis.* J Transl Med, 2018. **16**(1): p. 113.
62. Alvaro-Gracia, J.M., et al., *Intravenous administration of expanded allogeneic adipose-derived mesenchymal stem cells in refractory rheumatoid arthritis (Cx611): results of a multicentre, dose escalation, randomised, single-blind, placebo-controlled phase Ib/IIa clinical trial.* Ann Rheum Dis, 2017. **76**(1): p. 196-202.
63. Ducy, P., et al., *Osf2/Cbfa1: a transcriptional activator of osteoblast differentiation.* Cell, 1997. **89**(5): p. 747-54.
64. Manolagas, S.C., *Birth and death of bone cells: basic regulatory mechanisms and implications for the pathogenesis and treatment of osteoporosis.* Endocr Rev, 2000. **21**(2): p. 115-37.
65. Martin, T.J. and E. Seeman, *Bone remodelling: its local regulation and the emergence of bone fragility.* Best Pract Res Clin Endocrinol Metab, 2008. **22**(5): p. 701-22.
66. Takayanagi, H., *Osteoimmunology: shared mechanisms and crosstalk between the immune and bone systems.* Nat Rev Immunol, 2007. **7**(4): p. 292-304.
67. Anderson, H.C., *Matrix vesicles and calcification.* Curr Rheumatol Rep, 2003. **5**(3): p. 222-6.
68. Burger, E.H., J. Klein-Nulend, and T.H. Smit, *Strain-derived canalicular fluid flow regulates osteoclast activity in a remodelling osteon--a proposal.* J Biomech, 2003. **36**(10): p. 1453-9.
69. Chen, H., T. Senda, and K.Y. Kubo, *The osteocyte plays multiple roles in bone remodeling and mineral homeostasis.* Med Mol Morphol, 2015. **48**(2): p. 61-8.

70. Rochefort, G.Y., S. Pallu, and C.L. Benhamou, *Osteocyte: the unrecognized side of bone tissue.* Osteoporos Int, 2010. **21**(9): p. 1457-69.
71. Dowthwaite, G.P., et al., *The surface of articular cartilage contains a progenitor cell population.* J Cell Sci, 2004. **117**(Pt 6): p. 889-97.
72. Friedenstein, A.J., R.K. Chailakhjan, and K.S. Lalykina, *The development of fibroblast colonies in monolayer cultures of guinea-pig bone marrow and spleen cells.* Cell Tissue Kinet, 1970. **3**(4): p. 393-403.
73. Friedenstein, A.J., et al., *Heterotopic of bone marrow. Analysis of precursor cells for osteogenic and hematopoietic tissues.* Transplantation, 1968. **6**(2): p. 230-47.
74. Lazzeri, D., et al., *Bone regeneration and periosteoplasty: a 250-year-long history.* Cleft Palate Craniofac J, 2009. **46**(6): p. 621-8.
75. Li, L., et al., *Superficial cells are self-renewing chondrocyte progenitors, which form the articular cartilage in juvenile mice.* FASEB J, 2017. **31**(3): p. 1067-1084.
76. Mizuhashi, K., et al., *Resting zone of the growth plate houses a unique class of skeletal stem cells.* Nature, 2018. **563**(7730): p. 254-258.
77. Nakahara, H., et al., *In vivo osteochondrogenic potential of cultured cells derived from the periosteum.* Clin Orthop Relat Res, 1990(259): p. 223-32.
78. Usami, Y., et al., *Possible Contribution of Wnt-Responsive Chondroprogenitors to the Postnatal Murine Growth Plate.* J Bone Miner Res, 2019. **34**(5): p. 964-974.
79. Zhou, B.O., et al., *Leptin-receptor-expressing mesenchymal stromal cells represent the main source of bone formed by adult bone marrow.* Cell Stem Cell, 2014. **15**(2): p. 154-68.
80. Su, P., et al., *Mesenchymal Stem Cell Migration during Bone Formation and Bone Diseases Therapy.* Int J Mol Sci, 2018. **19**(8).

81. Haudenschild, A.K., et al., *Pressure and distortion regulate human mesenchymal stem cell gene expression.* Ann Biomed Eng, 2009. **37**(3): p. 492-502.
82. Wagner, D.R., et al., *Hydrostatic pressure enhances chondrogenic differentiation of human bone marrow stromal cells in osteochondrogenic medium.* Ann Biomed Eng, 2008. **36**(5): p. 813-20.
83. Teitelbaum, S.L. and F.P. Ross, *Genetic regulation of osteoclast development and function.* Nat Rev Genet, 2003. **4**(8): p. 638-49.
84. Tsukasaki, M. and H. Takayanagi, *Osteoimmunology: evolving concepts in bone-immune interactions in health and disease.* Nat Rev Immunol, 2019. **19**(10): p. 626-642.
85. Okamoto, K., et al., *Osteoimmunology: The Conceptual Framework Unifying the Immune and Skeletal Systems.* Physiol Rev, 2017. **97**(4): p. 1295-1349.
86. Udagawa, N., et al., *Origin of osteoclasts: mature monocytes and macrophages are capable of differentiating into osteoclasts under a suitable microenvironment prepared by bone marrow-derived stromal cells.* Proc Natl Acad Sci U S A, 1990. **87**(18): p. 7260-4.
87. Takahashi, N., et al., *Postmitotic osteoclast precursors are mononuclear cells which express macrophage-associated phenotypes.* Dev Biol, 1994. **163**(1): p. 212-21.
88. Jacome-Galarza, C.E., et al., *Developmental origin, functional maintenance and genetic rescue of osteoclasts.* Nature, 2019. **568**(7753): p. 541-545.
89. Juppner, H., et al., *A G protein-linked receptor for parathyroid hormone and parathyroid hormone-related peptide.* Science, 1991. **254**(5034): p. 1024-6.
90. Ikeda, K. and S. Takeshita, *The role of osteoclast differentiation and function in skeletal homeostasis.* J Biochem, 2016. **159**(1): p. 1-8.

91. Nakashima, T., M. Hayashi, and H. Takayanagi, *New insights into osteoclastogenic signaling mechanisms.* Trends Endocrinol Metab, 2012. **23**(11): p. 582-90.

92. Yoshida, H., et al., *The murine mutation osteopetrosis is in the coding region of the macrophage colony stimulating factor gene.* Nature, 1990. **345**(6274): p. 442-4.

93. Yamaza, T., et al., *Study of immunoelectron microscopic localization of cathepsin K in osteoclasts and other bone cells in the mouse femur.* Bone, 1998. **23**(6): p. 499-509.

94. Cohn, D.V. and B.K. Forscher, *Aerobic metabolism of glucose by bone.* J Biol Chem, 1962. **237**: p. 615-8.

95. Borle, A.B., N. Nichols, and G. Nichols, Jr., *Metabolic studies of bone in vitro. II. The metabolic patterns of accretion and resorption.* J Biol Chem, 1960. **235**: p. 1211-4.

96. Gruneboom, A., et al., *A network of trans-cortical capillaries as mainstay for blood circulation in long bones.* Nat Metab, 2019. **1**(2): p. 236-250.

97. Smith, C.O. and R.A. Eliseev, *Energy Metabolism During Osteogenic Differentiation: The Role of Akt.* Stem Cells Dev, 2021. **30**(3): p. 149-162.

98. Shum, L.C., et al., *Energy Metabolism in Mesenchymal Stem Cells During Osteogenic Differentiation.* Stem Cells Dev, 2016. **25**(2): p. 114-22.

99. Shares, B.H., et al., *Active mitochondria support osteogenic differentiation by stimulating beta-catenin acetylation.* J Biol Chem, 2018. **293**(41): p. 16019-16027.

100. Chen, C.T., et al., *Coordinated changes of mitochondrial biogenesis and antioxidant enzymes during osteogenic differentiation of human mesenchymal stem cells.* Stem Cells, 2008. **26**(4): p. 960-8.

101. Ryall, J.G., et al., *Metabolic Reprogramming of Stem Cell Epigenetics.* Cell Stem Cell, 2015. **17**(6): p. 651-662.
102. Dahan, P., et al., *Metabolism in pluripotency: Both driver and passenger?* J Biol Chem, 2019. **294**(14): p. 5420-5429.
103. Viguet-Carrin, S., P. Garnero, and P.D. Delmas, *The role of collagen in bone strength.* Osteoporos Int, 2006. **17**(3): p. 319-36.
104. Singh, D., et al., *Overexpression of hypoxia-inducible factor and metabolic pathways: possible targets of cancer.* Cell Biosci, 2017. **7**: p. 62.
105. Alcorta-Sevillano, N., et al., *Deciphering the Relevance of Bone ECM Signaling.* Cells, 2020. **9**(12).
106. Osterhoff, G., et al., *Bone mechanical properties and changes with osteoporosis.* Injury, 2016. **47 Suppl 2**(Suppl 2): p. S11-20.
107. Folkestad, L., et al., *Bone geometry, density, and microarchitecture in the distal radius and tibia in adults with osteogenesis imperfecta type I assessed by high-resolution pQCT.* J Bone Miner Res, 2012. **27**(6): p. 1405-12.
108. Garnero, P., *The contribution of collagen crosslinks to bone strength.* Bonekey Rep, 2012. **1**: p. 182.
109. Bella, J. and D.J. Hulmes, *Fibrillar Collagens.* Subcell Biochem, 2017. **82**: p. 457-490.
110. Lambert, S.A., et al., *The Human Transcription Factors.* Cell, 2018. **172**(4): p. 650-665.
111. Kronenberg, H.M., *Developmental regulation of the growth plate.* Nature, 2003. **423**(6937): p. 332-6.
112. Wu, H., et al., *Genomic occupancy of Runx2 with global expression profiling identifies a novel dimension to control of osteoblastogenesis.* Genome Biol, 2014. **15**(3): p. R52.

113. Worthley, D.L., et al., *Gremlin 1 identifies a skeletal stem cell with bone, cartilage, and reticular stromal potential.* Cell, 2015. **160**(1-2): p. 269-84.
114. Suh, J.H., et al., *Hes1 stimulates transcriptional activity of Runx2 by increasing protein stabilization during osteoblast differentiation.* Biochem Biophys Res Commun, 2008. **367**(1): p. 97-102.
115. Carlone, D.L., et al., *Telomerase expression marks transitional growth-associated skeletal progenitor/stem cells.* Stem Cells, 2021. **39**(3): p. 296-305.
116. Qin, X., et al., *Runt-related transcription factor-2 (Runx2) is required for bone matrix protein gene expression in committed osteoblasts in mice.* J Bone Miner Res, 2021. **36**(10): p. 2081-2095.
117. Enomoto, H., et al., *Induction of osteoclast differentiation by Runx2 through receptor activator of nuclear factor-kappa B ligand (RANKL) and osteoprotegerin regulation and partial rescue of osteoclastogenesis in Runx2-/- mice by RANKL transgene.* J Biol Chem, 2003. **278**(26): p. 23971-7.
118. Takarada, T., et al., *An analysis of skeletal development in osteoblast-specific and chondrocyte-specific runt-related transcription factor-2 (Runx2) knockout mice.* J Bone Miner Res, 2013. **28**(10): p. 2064-9.
119. Chen, H., et al., *Runx2 regulates endochondral ossification through control of chondrocyte proliferation and differentiation.* J Bone Miner Res, 2014. **29**(12): p. 2653-65.
120. Melsen, F. and T. Steiniche, *Bone histomorphometry.* Osteoporos Int, 1993. **3 Suppl 1**: p. 98-9.
121. Florencio-Silva, R., et al., *Biology of Bone Tissue: Structure, Function, and Factors That Influence Bone Cells.* Biomed Res Int, 2015. **2015**: p. 421746.

122. Zhou, X., et al., *Chondrocytes transdifferentiate into osteoblasts in endochondral bone during development, postnatal growth and fracture healing in mice.* PLoS Genet, 2014. **10**(12): p. e1004820.

123. Yang, L., et al., *Hypertrophic chondrocytes can become osteoblasts and osteocytes in endochondral bone formation.* Proc Natl Acad Sci U S A, 2014. **111**(33): p. 12097-102.

124. Park, J., et al., *Dual pathways to endochondral osteoblasts: a novel chondrocyte-derived osteoprogenitor cell identified in hypertrophic cartilage.* Biol Open, 2015. **4**(5): p. 608-21.

125. Qin, X., et al., *Runx2 is essential for the transdifferentiation of chondrocytes into osteoblasts.* PLoS Genet, 2020. **16**(11): p. e1009169.

126. Nakashima, K., et al., *The novel zinc finger-containing transcription factor osterix is required for osteoblast differentiation and bone formation.* Cell, 2002. **108**(1): p. 17-29.

127. Zhou, X., et al., *Multiple functions of Osterix are required for bone growth and homeostasis in postnatal mice.* Proc Natl Acad Sci U S A, 2010. **107**(29): p. 12919-24.

128. Lin, Q., et al., *Control of mouse cardiac morphogenesis and myogenesis by transcription factor MEF2C.* Science, 1997. **276**(5317): p. 1404-7.

129. Li, H., et al., *Transcription factor MEF2C influences neural stem/progenitor cell differentiation and maturation in vivo.* Proc Natl Acad Sci U S A, 2008. **105**(27): p. 9397-402.

130. Edmondson, D.G., et al., *Mef2 gene expression marks the cardiac and skeletal muscle lineages during mouse embryogenesis.* Development, 1994. **120**(5): p. 1251-63.

131. Naya, F.J., et al., *Transcriptional activity of MEF2 during mouse embryogenesis monitored with a MEF2-dependent transgene.* Development, 1999. **126**(10): p. 2045-52.

132. Arnold, H.H. and B. Winter, *Muscle differentiation: more complexity to the network of myogenic regulators.* Curr Opin Genet Dev, 1998. **8**(5): p. 539-44.
133. Potthoff, M.J., et al., *Regulation of skeletal muscle sarcomere integrity and postnatal muscle function by Mef2c.* Mol Cell Biol, 2007. **27**(23): p. 8143-51.
134. Ieda, M., et al., *Direct reprogramming of fibroblasts into functional cardiomyocytes by defined factors.* Cell, 2010. **142**(3): p. 375-86.
135. Collette, N.M., et al., *Targeted deletion of Sost distal enhancer increases bone formation and bone mass.* Proc Natl Acad Sci U S A, 2012. **109**(35): p. 14092-7.
136. Kramer, I., et al., *Mef2c deletion in osteocytes results in increased bone mass.* J Bone Miner Res, 2012. **27**(2): p. 360-73.
137. Leupin, O., et al., *Control of the SOST bone enhancer by PTH using MEF2 transcription factors.* J Bone Miner Res, 2007. **22**(12): p. 1957-67.
138. Nakatani, T. and N.C. Partridge, *MEF2C Interacts With c-FOS in PTH-Stimulated Mmp13 Gene Expression in Osteoblastic Cells.* Endocrinology, 2017. **158**(11): p. 3778-3791.
139. Arnold, M.A., et al., *MEF2C transcription factor controls chondrocyte hypertrophy and bone development.* Dev Cell, 2007. **12**(3): p. 377-89.
140. Dreher, S.I., et al., *Significance of MEF2C and RUNX3 Regulation for Endochondral Differentiation of Human Mesenchymal Progenitor Cells.* Front Cell Dev Biol, 2020. **8**: p. 81.
141. Browe, D.C., et al., *Hypoxia Activates the PTHrP -MEF2C Pathway to Attenuate Hypertrophy in Mesenchymal Stem Cell Derived Cartilage.* Sci Rep, 2019. **9**(1): p. 13274.
142. Fujii, T., et al., *MEF2C regulates osteoclastogenesis and pathologic bone resorption via c-FOS.* Bone Res, 2021. **9**(1): p. 4.

143. Chang, M.K., et al., *Osteal tissue macrophages are intercalated throughout human and mouse bone lining tissues and regulate osteoblast function in vitro and in vivo.* J Immunol, 2008. **181**(2): p. 1232-44.

144. Suto, E.G., et al., *Advantage of fat-derived CD73 positive cells from multiple human tissues, prospective isolated mesenchymal stromal cells.* Sci Rep, 2020. **10**(1): p. 15073.

145. Yasui, T., et al., *Purified Human Dental Pulp Stem Cells Promote Osteogenic Regeneration.* J Dent Res, 2016. **95**(2): p. 206-14.

146. Ogata, Y., et al., *Purified Human Synovium Mesenchymal Stem Cells as a Good Resource for Cartilage Regeneration.* PLoS One, 2015. **10**(6): p. e0129096.

147. Dominici, M., et al., *Minimal criteria for defining multipotent mesenchymal stromal cells. The International Society for Cellular Therapy position statement.* Cytotherapy, 2006. **8**(4): p. 315-7.

148. Bianco, P., et al., *The meaning, the sense and the significance: translating the science of mesenchymal stem cells into medicine.* Nat Med, 2013. **19**(1): p. 35-42.

149. El Agha, E., et al., *Mesenchymal Stem Cells in Fibrotic Disease.* Cell Stem Cell, 2017. **21**(2): p. 166-177.

150. Jonsson, K.B., et al., *Three isolation techniques for primary culture of human osteoblast-like cells: a comparison.* Acta Orthop Scand, 1999. **70**(4): p. 365-73.

151. Orriss, I.R., et al., *Optimisation of the differing conditions required for bone formation in vitro by primary osteoblasts from mice and rats.* Int J Mol Med, 2014. **34**(5): p. 1201-8.

152. Mills, B.G., et al., *Long-term culture of cells from bone affected by Paget's disease.* Calcif Tissue Int, 1979. **29**(2): p. 79-87.

153. Declercq, H., et al., *Isolation, proliferation and differentiation of osteoblastic cells to study cell/biomaterial interactions: comparison of different isolation techniques and source.* Biomaterials, 2004. **25**(5): p. 757-68.

154. Taylor, S.E., M. Shah, and I.R. Orriss, *Generation of rodent and human osteoblasts.* Bonekey Rep, 2014. **3**: p. 585.

155. Marahleh, A., et al., *Obtaining Primary Osteocytes through Murine Calvarial Fractionation of GFP-Expressing Osteocytes.* J Vis Exp, 2020(160).

156. Kalajzic, I., et al., *Dentin matrix protein 1 expression during osteoblastic differentiation, generation of an osteocyte GFP-transgene.* Bone, 2004. **35**(1): p. 74-82.

157. Paic, F., et al., *Identification of differentially expressed genes between osteoblasts and osteocytes.* Bone, 2009. **45**(4): p. 682-92.

158. Nakashima, T., et al., *Evidence for osteocyte regulation of bone homeostasis through RANKL expression.* Nat Med, 2011. **17**(10): p. 1231-4.

159. Zhang, J. and D.C. Link, *Targeting of Mesenchymal Stromal Cells by Cre-Recombinase Transgenes Commonly Used to Target Osteoblast Lineage Cells.* J Bone Miner Res, 2016. **31**(11): p. 2001-2007.

160. Debnath, S., et al., *Discovery of a periosteal stem cell mediating intramembranous bone formation.* Nature, 2018. **562**(7725): p. 133-139.

161. Manolagas, S.C. and H.M. Kronenberg, *Reproducibility of results in preclinical studies: a perspective from the bone field.* J Bone Miner Res, 2014. **29**(10): p. 2131-40.

162. Ibanez, L., et al., *Inflammatory Osteoclasts Prime TNFalpha-Producing CD4(+) T Cells and Express CX(3) CR1.* J Bone Miner Res, 2016. **31**(10): p. 1899-1908.

163. Wakkach, A., et al., *Bone marrow microenvironment controls the in vivo differentiation of murine dendritic cells into osteoclasts.* Blood, 2008. **112**(13): p. 5074-83.
164. Marino, S., et al., *Generation and culture of osteoclasts.* Bonekey Rep, 2014. **3**: p. 570.
165. Boyle, W.J., W.S. Simonet, and D.L. Lacey, *Osteoclast differentiation and activation.* Nature, 2003. **423**(6937): p. 337-42.
166. Tikhonova, A.N., et al., *The bone marrow microenvironment at single-cell resolution.* Nature, 2019. **569**(7755): p. 222-228.
167. Shekhar, K., et al., *Comprehensive Classification of Retinal Bipolar Neurons by Single-Cell Transcriptomics.* Cell, 2016. **166**(5): p. 1308-1323 e30.
168. Macosko, E.Z., et al., *Highly Parallel Genome-wide Expression Profiling of Individual Cells Using Nanoliter Droplets.* Cell, 2015. **161**(5): p. 1202-1214.
169. Baryawno, N., et al., *A Cellular Taxonomy of the Bone Marrow Stroma in Homeostasis and Leukemia.* Cell, 2019. **177**(7): p. 1915-1932 e16.
170. Plasschaert, L.W., et al., *A single-cell atlas of the airway epithelium reveals the CFTR-rich pulmonary ionocyte.* Nature, 2018. **560**(7718): p. 377-381.
171. Pijuan-Sala, B., et al., *A single-cell molecular map of mouse gastrulation and early organogenesis.* Nature, 2019. **566**(7745): p. 490-495.
172. Kanton, S., et al., *Organoid single-cell genomic atlas uncovers human-specific features of brain development.* Nature, 2019. **574**(7778): p. 418-422.
173. Chan, M.M., et al., *Molecular recording of mammalian embryogenesis.* Nature, 2019. **570**(7759): p. 77-82.

174. Chan, C.K.F., et al., *Identification of the Human Skeletal Stem Cell.* Cell, 2018. **175**(1): p. 43-56 e21.

175. Chan, C.K., et al., *Identification and specification of the mouse skeletal stem cell.* Cell, 2015. **160**(1-2): p. 285-98.

176. Mizuhashi, K., et al., *Growth Plate Borderline Chondrocytes Behave as Transient Mesenchymal Precursor Cells.* J Bone Miner Res, 2019. **34**(8): p. 1387-1392.

177. Zhong, L., et al., *Single cell transcriptomics identifies a unique adipose lineage cell population that regulates bone marrow environment.* Elife, 2020. **9**.

178. Yoshioka, H., et al., *Single-Cell RNA-Sequencing Reveals the Breadth of Osteoblast Heterogeneity.* JBMR Plus, 2021. **5**(6): p. e10496.

179. Dasgupta, K., et al., *Sensitive detection of Cre-mediated recombination using droplet digital PCR reveals Tg(BGLAP-Cre) and Tg(DMP1-Cre) are active in multiple non-skeletal tissues.* Bone, 2021. **142**: p. 115674.

180. Yang, C., et al., *Mesenchymal Stem Cell-Specific and Preosteoblast-Specific Ablation of TSC1 in Mice Lead to Severe and Slight Spinal Dysplasia, Respectively.* Biomed Res Int, 2020. **2020**: p. 4572687.

181. Zhong, Z.A., et al., *Sex-Dependent, Osteoblast Stage-Specific Effects of Progesterone Receptor on Bone Acquisition.* J Bone Miner Res, 2017. **32**(9): p. 1841-1852.

182. Chiu, W.S., et al., *Transgenic mice that express Cre recombinase in osteoclasts.* Genesis, 2004. **39**(3): p. 178-85.

183. Das, B.K., et al., *Transferrin receptor 1-mediated iron uptake regulates bone mass in mice via osteoclast mitochondria and cytoskeleton.* Elife, 2022. **11**.

184. Chen, M., et al., *Generation of a transgenic mouse model with chondrocyte-specific and tamoxifen-inducible expression of Cre recombinase.* Genesis, 2007. **45**(1): p. 44-50.

185. Li, Y., S.T. Yang, and S. Yang, *Trp53 controls chondrogenesis and endochondral ossification by negative regulation of TAZ activity and stability via beta-TrCP-mediated ubiquitination.* Cell Death Discov, 2022. **8**(1): p. 317.

186. Madisen, L., et al., *A robust and high-throughput Cre reporting and characterization system for the whole mouse brain.* Nat Neurosci, 2010. **13**(1): p. 133-40.

187. Liu, F., et al., *Expression and activity of osteoblast-targeted Cre recombinase transgenes in murine skeletal tissues.* Int J Dev Biol, 2004. **48**(7): p. 645-53.

188. Nagao, M., C.W. Cheong, and B.R. Olsen, *Col2-Cre and tamoxifen-inducible Col2-CreER target different cell populations in the knee joint.* Osteoarthritis Cartilage, 2016. **24**(1): p. 188-91.

189. Wang, T., et al., *Effects of Leukaemia Inhibitory Factor Receptor on the Early Stage of Osteogenic Differentiation of Human Bone Marrow Mesenchymal Cells.* Folia Biol (Praha), 2018. **64**(5-6): p. 186-194.

190. Alekos, N.S., M.C. Moorer, and R.C. Riddle, *Dual Effects of Lipid Metabolism on Osteoblast Function.* Front Endocrinol (Lausanne), 2020. **11**: p. 578194.

191. Yao, Z., et al., *CCL2 is a critical mechano-responsive mediator in crosstalk between osteoblasts and bone mesenchymal stromal cells.* FASEB J, 2021. **35**(10): p. e21851.

192. Huang, E., et al., *Growth hormone synergizes with BMP9 in osteogenic differentiation by activating the JAK/STAT/IGF1 pathway in murine multilineage cells.* J Bone Miner Res, 2012. **27**(7): p. 1566-75.

193. Gazzerro, E., et al., *Conditional deletion of gremlin causes a transient increase in bone formation and bone mass.* J Biol Chem, 2007. **282**(43): p. 31549-57.

194. Ferretti, C., et al., *Role of IGF1 and IGF1/VEGF on human mesenchymal stromal cells in bone healing: two sources and two fates.* Tissue Eng Part A, 2014. **20**(17-18): p. 2473-82.

195. Bodine, P.V., et al., *A small molecule inhibitor of the Wnt antagonist secreted frizzled-related protein-1 stimulates bone formation.* Bone, 2009. **44**(6): p. 1063-8.

196. Joukov, V., et al., *Proteolytic processing regulates receptor specificity and activity of VEGF-C.* EMBO J, 1997. **16**(13): p. 3898-911.

197. Joukov, V., et al., *A novel vascular endothelial growth factor, VEGF-C, is a ligand for the Flt4 (VEGFR-3) and KDR (VEGFR-2) receptor tyrosine kinases.* EMBO J, 1996. **15**(7): p. 1751.

198. Scott, R.E., et al., *Cell cycle gene expression networks discovered using systems biology: Significance in carcinogenesis.* J Cell Physiol, 2015. **230**(10): p. 2533-42.

199. Staines, K.A., et al., *E11/Podoplanin Protein Stabilization Through Inhibition of the Proteasome Promotes Osteocyte Differentiation in Murine in Vitro Models.* J Cell Physiol, 2016. **231**(6): p. 1392-404.

200. Youlten, S.E., et al., *Osteocyte transcriptome mapping identifies a molecular landscape controlling skeletal homeostasis and susceptibility to skeletal disease.* Nat Commun, 2021. **12**(1): p. 2444.

201. Maurel, D.B., et al., *Characterization of a novel murine Sost ER(T2) Cre model targeting osteocytes.* Bone Res, 2019. **7**: p. 6.

202. Tam, C.S., et al., *Parathyroid hormone stimulates the bone apposition rate independently of its resorptive action: differential effects of intermittent and continuous administration.* Endocrinology, 1982. **110**(2): p. 506-12.

203. Neer, R.M., et al., *Effect of parathyroid hormone (1-34) on fractures and bone mineral density in postmenopausal women with osteoporosis.* N Engl J Med, 2001. **344**(19): p. 1434-41.

204. Miller, P.D., et al., *Effect of Abaloparatide vs Placebo on New Vertebral Fractures in Postmenopausal Women With Osteoporosis: A Randomized Clinical Trial.* JAMA, 2016. **316**(7): p. 722-33.

205. Jolette, J., et al., *Comparing the incidence of bone tumors in rats chronically exposed to the selective PTH type 1 receptor agonist abaloparatide or PTH(1-34).* Regul Toxicol Pharmacol, 2017. **86**: p. 356-365.

206. Padhi, D., et al., *Single-dose, placebo-controlled, randomized study of AMG 785, a sclerostin monoclonal antibody.* J Bone Miner Res, 2011. **26**(1): p. 19-26.

207. Lewiecki, E.M., et al., *A Phase III Randomized Placebo-Controlled Trial to Evaluate Efficacy and Safety of Romosozumab in Men With Osteoporosis.* J Clin Endocrinol Metab, 2018. **103**(9): p. 3183-3193.

208. Ordway, G.A. and D.J. Garry, *Myoglobin: an essential hemoprotein in striated muscle.* J Exp Biol, 2004. **207**(Pt 20): p. 3441-6.

209. Yoshida, T., *MCAT elements and the TEF-1 family of transcription factors in muscle development and disease.* Arterioscler Thromb Vasc Biol, 2008. **28**(1): p. 8-17.

210. Krainc, D., et al., *Synergistic activation of the N-methyl-D-aspartate receptor subunit 1 promoter by myocyte enhancer factor 2C and Sp1.* J Biol Chem, 1998. **273**(40): p. 26218-24.

211. Sun, L., et al., *Cabin 1, a negative regulator for calcineurin signaling in T lymphocytes.* Immunity, 1998. **8**(6): p. 703-11.

212. Hosking, B.M., et al., *SOX18 directly interacts with MEF2C in endothelial cells.* Biochem Biophys Res Commun, 2001. **287**(2): p. 493-500.

213. Cermenati, S., et al., *Sox18 and Sox7 play redundant roles in vascular development.* Blood, 2008. **111**(5): p. 2657-66.

214. Johnson, M.E., et al., *A ChIP-seq-defined genome-wide map of MEF2C binding reveals inflammatory pathways associated with its role in bone density determination.* Calcif Tissue Int, 2014. **94**(4): p. 396-402.

215. Velazquez-Cruz, R., et al., *Analysis of association of MEF2C, SOST and JAG1 genes with bone mineral density in Mexican-Mestizo postmenopausal women.* BMC Musculoskelet Disord, 2014. **15**: p. 400.

216. Kawane, T., et al., *Dlx5 and mef2 regulate a novel runx2 enhancer for osteoblast-specific expression.* J Bone Miner Res, 2014. **29**(9): p. 1960-9.

217. Sebastian, A., et al., *Global gene expression analysis identifies Mef2c as a potential player in Wnt16-mediated transcriptional regulation.* Gene, 2018. **675**: p. 312-321.

218. Li, X., et al., *Targeted deletion of the sclerostin gene in mice results in increased bone formation and bone strength.* J Bone Miner Res, 2008. **23**(6): p. 860-9.

219. Sebastian, A., et al., *Single-cell RNA-Seq reveals changes in immune landscape in post-traumatic osteoarthritis.* Front Immunol, 2022. **13**: p. 938075.

220. Sebastian, A., et al., *Single-Cell Transcriptomic Analysis of Tumor-Derived Fibroblasts and Normal Tissue-Resident Fibroblasts Reveals Fibroblast Heterogeneity in Breast Cancer.* Cancers (Basel), 2020. **12**(5).

221. Butler, A., et al., *Integrating single-cell transcriptomic data across different conditions, technologies, and species.* Nat Biotechnol, 2018. **36**(5): p. 411-420.

222. Love, M.I., W. Huber, and S. Anders, *Moderated estimation of fold change and dispersion for RNA-seq data with DESeq2.* Genome Biol, 2014. **15**(12): p. 550.

223. Kuleshov, M.V., et al., *Enrichr: a comprehensive gene set enrichment analysis web server 2016 update.* Nucleic Acids Res, 2016. **44**(W1): p. W90-7.

224. Durinck, S., et al., *Mapping identifiers for the integration of genomic datasets with the R/Bioconductor package biomaRt.* Nat Protoc, 2009. **4**(8): p. 1184-91.

225. Gearing, L.J., et al., *CiiiDER: A tool for predicting and analysing transcription factor binding sites.* PLoS One, 2019. **14**(9): p. e0215495.

226. Castro-Mondragon, J.A., et al., *JASPAR 2022: the 9th release of the open-access database of transcription factor binding profiles.* Nucleic Acids Res, 2022. **50**(D1): p. D165-D173.

227. Chang, J.C., et al., *Global molecular changes in a tibial compression induced ACL rupture model of post-traumatic osteoarthritis.* J Orthop Res, 2017. **35**(3): p. 474-485.

228. Lee, J.Y., et al., *Muscle-Derived Lumican Stimulates Bone Formation via Integrin alpha2beta1 and the Downstream ERK Signal.* Front Cell Dev Biol, 2020. **8**: p. 565826.

229. Raouf, A., et al., *Lumican is a major proteoglycan component of the bone matrix.* Matrix Biol, 2002. **21**(4): p. 361-7.

230. Xiao, D., et al., *Lumican promotes joint fibrosis through TGF-beta signaling.* FEBS Open Bio, 2020. **10**(11): p. 2478-2488.

231. Krishnan, A., et al., *Lumican, an extracellular matrix proteoglycan, is a novel requisite for hepatic fibrosis.* Lab Invest, 2012. **92**(12): p. 1712-25.

232. Sautchuk, R., Jr. and R.A. Eliseev, *Cell energy metabolism and bone formation.* Bone Rep, 2022. **16**: p. 101594.

233. van Gastel, N. and G. Carmeliet, *Metabolic regulation of skeletal cell fate and function in physiology and disease.* Nat Metab, 2021. **3**(1): p. 11-20.

234. Yu, Y., et al., *Glutamine Metabolism Regulates Proliferation and Lineage Allocation in Skeletal Stem Cells.* Cell Metab, 2019. **29**(4): p. 966-978 e4.

235. Schilling, K., E. Brown, and X. Zhang, *NAD(P)H autofluorescence lifetime imaging enables single cell analyses of cellular metabolism of osteoblasts in vitro and in vivo via two-photon microscopy.* Bone, 2022. **154**: p. 116257.

236. Lee, S.Y., E.D. Abel, and F. Long, *Glucose metabolism induced by Bmp signaling is essential for murine skeletal development.* Nat Commun, 2018. **9**(1): p. 4831.

237. Schmid, T.M. and T.F. Linsenmayer, *Immunohistochemical localization of short chain cartilage collagen (type X) in avian tissues.* J Cell Biol, 1985. **100**(2): p. 598-605.

238. Kwan, A.P., et al., *Comparative studies of type X collagen expression in normal and rachitic chicken epiphyseal cartilage.* J Cell Biol, 1989. **109**(4 Pt 1): p. 1849-56.

239. Chen, Q., et al., *Domains of type X collagen: alteration of cartilage matrix by fibril association and proteoglycan accumulation.* J Cell Biol, 1992. **117**(3): p. 687-94.

240. Schmid, T.M., R.G. Popp, and T.F. Linsenmayer, *Hypertrophic cartilage matrix. Type X collagen, supramolecular assembly, and calcification.* Ann N Y Acad Sci, 1990. **580**: p. 64-73.

241. Welgus, H.G., et al., *Differential susceptibility of type X collagen to cleavage by two mammalian interstitial collagenases and 72-kDa type IV collagenase.* J Biol Chem, 1990. **265**(23): p. 13521-7.

242. Shen, G., *The role of type X collagen in facilitating and regulating endochondral ossification of articular cartilage.* Orthod Craniofac Res, 2005. **8**(1): p. 11-7.

243. Habuchi, H., H.E. Conrad, and J.H. Glaser, *Coordinate regulation of collagen and alkaline phosphatase levels in chick embryo chondrocytes.* J Biol Chem, 1985. **260**(24): p. 13029-34.

244. Arias, J.L., et al., *Role of type X collagen on experimental mineralization of eggshell membranes.* Connect Tissue Res, 1997. **36**(1): p. 21-33.

245. Warman, M.L., et al., *A type X collagen mutation causes Schmid metaphyseal chondrodysplasia.* Nat Genet, 1993. **5**(1): p. 79-82.

246. Drissi, H., et al., *Transcriptional regulation of chondrocyte maturation: potential involvement of transcription factors in OA pathogenesis.* Mol Aspects Med, 2005. **26**(3): p. 169-79.

247. Dreier, R., *Hypertrophic differentiation of chondrocytes in osteoarthritis: the developmental aspect of degenerative joint disorders.* Arthritis Res Ther, 2010. **12**(5): p. 216.

248. Wallis, G.A., et al., *Amino acid substitutions of conserved residues in the carboxyl-terminal domain of the alpha 1(X) chain of type X collagen occur in two unrelated families with metaphyseal chondrodysplasia type Schmid.* Am J Hum Genet, 1994. **54**(2): p. 169-78.

249. Kwan, K.M., et al., *Abnormal compartmentalization of cartilage matrix components in mice lacking collagen X: implications for function.* J Cell Biol, 1997. **136**(2): p. 459-71.

250. Bouleftour, W., et al., *The role of the SIBLING, Bone Sialoprotein in skeletal biology - Contribution of mouse experimental genetics.* Matrix Biol, 2016. **52-54**: p. 60-77.

251. Gorski, J.P., et al., *Extracellular bone acidic glycoprotein-75 defines condensed mesenchyme regions to be mineralized and localizes with bone sialoprotein during intramembranous bone formation.* J Biol Chem, 2004. **279**(24): p. 25455-63.

252. Jani, P.H., et al., *Transgenic expression of Dspp partially rescued the long bone defects of Dmp1-null mice.* Matrix Biol, 2016. **52-54**: p. 95-112.
253. Maalouf, M., et al., *Deletion of osteopontin or bone sialoprotein induces opposite bone responses to mechanical stimulation in mice.* Bone Rep, 2022. **17**: p. 101621.
254. Lowell, B.B. and G.I. Shulman, *Mitochondrial dysfunction and type 2 diabetes.* Science, 2005. **307**(5708): p. 384-7.
255. Montgomery, M.K. and N. Turner, *Mitochondrial dysfunction and insulin resistance: an update.* Endocr Connect, 2015. **4**(1): p. R1-R15.
256. Rovira-Llopis, S., et al., *Mitochondrial dynamics in type 2 diabetes: Pathophysiological implications.* Redox Biol, 2017. **11**: p. 637-645.
257. Vestergaard, P., *Discrepancies in bone mineral density and fracture risk in patients with type 1 and type 2 diabetes--a meta-analysis.* Osteoporos Int, 2007. **18**(4): p. 427-44.
258. Hamann, C., et al., *Bone, sweet bone--osteoporotic fractures in diabetes mellitus.* Nat Rev Endocrinol, 2012. **8**(5): p. 297-305.
259. Bureau, U.S.C. *A Snapshot of the Fast-Growing U.S. Older Population.* 2019; Available from: www.census.gov/library/stories/2018/10/snapshot-fast-growing-us-older-population.html.
260. Borrelli, J., *Taking control: the osteoporosis epidemic.* Injury, 2012. **43**(8): p. 1235-6.
261. Lugtenberg, M., et al., *Current guidelines have limited applicability to patients with comorbid conditions: a systematic analysis of evidence-based guidelines.* PLoS One, 2011. **6**(10): p. e25987.
262. McClung, M.R., et al., *The role of osteoanabolic agents in the management of patients with osteoporosis.* Postgrad Med, 2022. **134**(6): p. 541-551.

263. Weivoda, M.M., et al., *Wnt Signaling Inhibits Osteoclast Differentiation by Activating Canonical and Noncanonical cAMP/PKA Pathways.* J Bone Miner Res, 2016. **31**(1): p. 65-75.
264. Panczel, A., et al., *Fluorescence-Based Real-Time Analysis of Osteoclast Development.* Front Cell Dev Biol, 2021. **9**: p. 657935.
265. Hassan, M.G., et al., *Altering osteoclast numbers using CTSK models in utero affects mice offspring craniofacial morphology.* Orthod Craniofac Res, 2022.
266. Vong, L.H., M.J. Ragusa, and J.J. Schwarz, *Generation of conditional Mef2cloxP/loxP mice for temporal- and tissue-specific analyses.* Genesis, 2005. **43**(1): p. 43-8.
267. Dobson, K.R., et al., *Centrifugal isolation of bone marrow from bone: an improved method for the recovery and quantitation of bone marrow osteoprogenitor cells from rat tibiae and femurae.* Calcif Tissue Int, 1999. **65**(5): p. 411-3.
268. Hall, T.J. and T.J. Chambers, *Molecular aspects of osteoclast function.* Inflamm Res, 1996. **45**(1): p. 1-9.
269. Vaananen, H.K., et al., *The cell biology of osteoclast function.* J Cell Sci, 2000. **113 (Pt 3)**: p. 377-81.
270. Bune, A.J., et al., *Mice lacking tartrate-resistant acid phosphatase (Acp 5) have disordered macrophage inflammatory responses and reduced clearance of the pathogen, Staphylococcus aureus.* Immunology, 2001. **102**(1): p. 103-13.
271. Ormsby, R.T., et al., *Osteocytes respond to particles of clinically-relevant conventional and cross-linked polyethylene and metal alloys by up-regulation of resorptive and inflammatory pathways.* Acta Biomater, 2019. **87**: p. 296-306.

272. Tsukasaki, M., et al., *Stepwise cell fate decision pathways during osteoclastogenesis at single-cell resolution.* Nat Metab, 2020. **2**(12): p. 1382-1390.